

# The physical interaction potential of gas atoms with single-crystal surfaces, determined from gas-surface diffraction experiments

H. Hoinkes

*Physikalisches Institut der Universität Erlangen-Nürnberg, Erwin-Rommel-Str. 1, D 8520 Erlangen, Germany*

A comprehensive survey and data collection of experimental results achieved from diffracting beams of light gases like H, D,  $^3\text{He}$ ,  $^4\text{He}$ , and  $\text{H}_2$  from single-crystal surfaces (alkali halides, oxides, and graphite) is given, and it is shown that gas-surface diffraction is a valuable tool to get detailed information on the physical gas-surface potential: (a) From comparison of diffracted beam intensities with calculations in a corrugated hard-wall approximation the periodic structure of the interaction potential is obtained together with information on the atomic structure at the surface. (b) From bound-state resonance investigations one gets information on the different terms of the gas-surface potential in Fourier expansion  $v(r) = \sum_G v_G(z) \exp(iG \cdot R)$ : the achieved spectrum of binding energies  $\{E_j\}$  can be used to construct the main term  $v_{00}(z)$ , whereas observed splitting of degenerate bound states allows evaluation of the strength of the periodic terms  $v_G(z)$ . (c) from  $E_j$  levels near the dissociation limit the constant  $C_3$  of gas-surface long-range dispersion attraction can be determined. Finally, regarding the experimental results on  $C_3$  and the potential well depth  $D$ , two semiempirical rules are established:  $C_3 = K_C \cdot \alpha(\epsilon - 1)/(\epsilon + 1)$  and  $D = K_D \cdot \alpha(\epsilon - 1)/(\epsilon + 1)$ . These rules allow the calculation of  $C_3$  and  $D$  from the static electric polarizability  $\alpha$  of the atom, the optical dielectric constant  $\epsilon$  of the solid, and the system-independent constants  $K_C, K_D$  given in the text. Calculated values of  $D$  for several gas-surface systems are given in a table.

## CONTENTS

I. Introduction	933	IV. Concluding Discussion	961
II. General Features of the Physical Gas-Surface Interaction Potential	935	Acknowledgments	962
A. The shape of the gas-surface potential	935	Appendix A: Some Special Results Concerning Gas-Surface Potential Curves Calculated from Summation of Pair Potentials	962
B. Theoretical results on the physical gas-surface interaction potential	936	1. Potential formulas obtained from summation or integration of pair potentials	962
1. First-principle calculations	936	2. Relations on the potential well depth extracted from pairwise potential summation	963
2. Pairwise summation calculations	936	Appendix B: Binding Energies from Experimental Resonance Investigations	963
3. Long-range asymptotic behavior of the gas-surface potential	938	Appendix C: Review of Model Potentials used to Fit Experimental Binding Energies $E_j$	963
III. The Gas-Surface Interaction Potential from Gas-Surface Diffraction Experiments	938	1. Morse potential	963
A. Survey on elastic gas-surface diffraction theory	938	2. (12-3) potential	966
B. Results with a hard corrugated wall	939	3. (9-3) potential	966
C. Results from resonance effects	941	4. Shifted Morse potential	966
1. General considerations on bound-state resonances	941	5. Shifted Morse hybrid potential	966
2. Determination of binding energies	942	6. Exponential-3 potential	966
3. Determination of $v_{00}(z)$ from binding energies $E_j$	945	7. Variable exponent potential	966
a. Experimental results on the long-range attractive part	946	8. Flat-bottom hard-wall potential	967
b. Semiempirical rule for the attraction constant $C_3$	947	9. Potential forms produced by pairwise summation	968
c. Construction of $v_{00}(z)$ with RKR method	949	Appendix D: Table with Potential Depths Calculated with the Semiempirical Rule Given in Sec. III.C.4	968
d. Model potentials used for $v_{00}(z)$	950	References	968
e. Potential parameters from fitting $\{E_j\}$ spectra	950		
4. Semiempirical rule for the potential well depth	951		
D. Results on the periodic potential terms from bound-state resonances	953		
1. Resonance splitting for degenerate bound states	953		
2. Results from comparison of calculated and experimental resonance structure in diffracted beams	957		
3. Relation between the periodic structure parameters $\xi_G$ and $\beta_G$	958		
E. Complex potential for describing inelastic effects in bound-state resonances	959		
		<b>I. INTRODUCTION</b>	
		In the early 1930s the first gas-surface diffraction experiments were carried out in order to verify the wave nature of atomic particles. And indeed the de Broglie relation was fully confirmed with He and $\text{H}_2$ beams diffracted from (001) surfaces of LiF, NaF, and NaCl (Stern, 1929; Estermann and Stern, 1930; Estermann, Frisch, and Stern, 1931) and with beams of atomic hydrogen diffracted from LiF (Johnson, 1930, 1931). A first review of these experiments was given by Frisch and Stern (1933a).	

Some of these first experiments showed also a minima structure in the diffracted intensities (Estermann and Stern, 1930; Frisch and Stern, 1932, 1933a, 1933b; Frisch 1933). This effect, called "selective adsorption," was explained a few years later by Lennard-Jones and Devonshire (1936, 1937; Devonshire, 1936) by transitions of incident particles into bound surface states. In more detail this special scattering process may be described in the following way. An incident atom is transferred to a bound surface state by diffraction; in this surface state the atom is bound normal to the surface in the gas-surface potential with a discrete binding energy  $E_j < 0$ , but moves parallel to the surface with an energy  $E_{||} = E_i + |E_j|$  which surmounts the incident energy  $E_i$  just by the gained binding energy  $|E_j|$ . After some time the atom may leave this bound state again by a second diffraction step leading to an outgoing diffracted beam. Since energy conservation and diffraction conditions have to hold simultaneously this process occurs only at certain conditions of incidence. But if these conditions are fulfilled the temporary bound states may act as intermediate states causing a resonance behavior in the elastic diffraction process. As a result strong changes in the diffracted beam intensities may occur under resonance condition (Garcia, Celli, and Goodman, 1979; Celli, Garcia, and Hutchison, 1979). The main effect observable at these bound-state resonances is minima in the specular beam intensity, but maxima may also appear in higher-order diffracted beams (Greiner *et al.*, 1980). From the conditions of incidence where the resonance minima are found the binding energies  $E_j$  can directly be calculated.

In their work in 1936 Lennard-Jones and Devonshire already pointed out the virtue of gas-surface diffraction in yielding information on the gas-surface interaction potential. Using the experimental data of Estermann, Frisch, and Stern they determined from the selective adsorption minima some energy levels of states bound in the gas-surface potential well and from these binding energies they also got the depth and the range of this potential well and deduced from observed diffracted beam intensities approximately the strength of the periodic variation of the potential well parallel to the surface.

After these first very promising results there was a rather long period with only little work in the field of gas-surface diffraction. But during the 1960s, when improved vacuum conditions and also improved methods of controlling surfaces were developed, the number of gas-surface interaction investigations increased rapidly, motivated also by the expected progress in technological problems like aerodynamics or heterogeneous catalysis. As mentioned above Lennard-Jones and Devonshire (1936, 1937) already have pointed out the virtue of diffraction experiments to elucidate gas-surface interaction. So one type of the experiments which started at the end of the 1960s was the diffraction of light atoms or molecules like H, D, H<sub>2</sub>, D<sub>2</sub>, <sup>3</sup>He, and <sup>4</sup>He with thermal energies from regularly ordered single-crystal surfaces. This seemed to be a promising way to advance in fundamental understanding of the physical gas-surface interaction. Here physical interaction means that the interaction between a gas atom and the surface

arises only from van der Waals forces causing binding energies for the light atoms mentioned above smaller than 100 meV. In the past ten years extensive diffraction experiments with these light particles have been carried out and their results have also stimulated a lot of theoretical work. And both experiments and theory together led to considerable progress in the understanding of gas-surface diffraction and from this also of physical gas-surface interaction. A series of review papers (Stickney, 1967; Beder, 1967; Goodman, 1971; Logan, 1973; Smith, 1973; Steele, 1974; Toennies, 1974; Somorjai and Brumbach, 1974; Goodman and Wachman, 1976; Goodman, 1977a; Cole and Frankl, 1978; Wilsch, 1978) which appeared in the past ten years reflects the increasing interest and successful development in this field.

As the method of determining gas-surface interaction potentials by gas-surface diffraction is now well established and has been successfully applied to several gas-surface systems, it is worthwhile to give a comprehensive review of the method and the results achieved. This will be done in the following sections.

Section II first gives a description of the general features and the shape of the physical gas-surface interaction potential (Sec. II.A) and then it deals with the state of theoretical methods for calculating potential curves (Sec. II.B). In this section results from first-principle calculations are discussed, concerning complete potential curves and also the long-range asymptotic behavior. Also considered here are potential curves which may be achieved by the approximative method of summation of pairwise potentials between the gas atom and the atoms or ions of the solid.

Section III deals with the different kinds of information on the gas-surface potential that may be extracted from gas-surface diffraction experiments. After a short survey on elastic gas-surface diffraction theory (Sec. III.A) results obtained within the corrugated hard-wall model are discussed (Sec. III.B), and then the main topics of this chapter are described in detail. These are bound-state resonances and the experimental results on the interaction potential obtained from investigating the resonance structure in diffracted beams (Sec. III.C). These results concern binding energies in the potential well, the strength of the long-range attractive part, and the shape of the potential well averaged parallel to the surface. It is also shown that semiempirical rules for the coefficient  $C_3$  of the long-range attractive part as well as for the potential well depth  $D$  can be established from these experimental results (Sec. III.C. 3 and 4). It is further demonstrated that experimentally observed resonance splitting of degenerate bound states may well be used for getting information on the strength of the periodic potential terms and the results achieved in this way are compared to results on the periodic terms in the hard-corrugated-wall model (Sec. III.D). Finally it is shown that the increase of inelastic effects at resonances can be described by using an additional imaginary part in the potential.

The article ends with a concluding discussion in Sec. IV which also points out the potential of thermal energy atom diffraction (TEAD) to become also a valuable technique of surface structure analysis.

Four appendixes present some supplementary results and collections of experimental data. Appendix A gives some special results concerning gas-surface potential curves calculated from summation of pair potentials. In Appendix B all the binding energies  $E_j$  obtained from experimental resonance investigations are collected in a table and in Appendix C all the model potentials used to fit these experimental binding energies  $E_j$  are discussed. Finally, Appendix D presents in a table potential well depths calculated for several gas-surface systems with the semiempirical rule established in Sec. III.C.4.

## II. GENERAL FEATURES OF THE PHYSICAL GAS-SURFACE INTERACTION POTENTIAL

Before discussing detailed features of the gas-surface interaction it should be stated here that we are dealing in the following with atoms or molecules of thermal energies. This means the particles being incident to the crystal surface have energies in the region from 10 to 100 meV, the consequence of which is that the incident particles can approach the atoms or ions forming the solid surface only up to a distance given by the corresponding van der Waals radii, and have no chance to penetrate the topmost monolayer at the solid surface.

A second aspect which should also be pointed out here is that we are dealing with van der Waals interactions, and that the attractive interaction between the gas atom and the solid is given by the polarization energy only, and that all kinds of charge exchange attraction will be excluded. From this we see that the well depth  $D$  of the potential for the light gases H, H<sub>2</sub>, or He has to be expected to be  $D \leq 100$  meV, which is comparable to the incident energy.

And a third aspect which should be mentioned in advance is that we will discuss only purely elastic diffraction effects so that we have to regard here only a time-independent potential which is averaged over the thermal vibrations of the solid atoms.

### A. The shape of the gas-surface potential

From the conditions given above we can state first that the potential function has a strong repulsive part in front of the solid. The reason for this repulsion is the overlapping of the wave functions of the electrons of the gas atom and of the electrons at the surface of the solid. In the case of inert gas crystals or ionic crystals the electrons are well localized at the positions of the atoms or ions forming the crystal surface so that the strength of the repulsion will change relatively strongly parallel to the surface at fixed gas atom-surface plane distance. The situation is quite different with metal surfaces where the electron distribution at the surface can be assumed to be smeared out much more, leading to a relatively small variation of the strength of repulsion when the position of the gas atom is varied parallel to the surface.

At longer distances the gas-surface potential is dominated by an attractive van der Waals interaction given by the distance-dependent polarization energy between a gas atom and the solid. This attractive part of the

potential is caused by the interaction of the gas atom with a relatively large number of crystal atoms or in good approximation with the crystal as a continuum characterized by a certain dielectric function, so that the attractive part of the potential function can be assumed to be practically constant parallel to the surface.

The weak periodic variation of the repulsion in the case of metals manifests itself also in the diffraction behavior. Only rather weak diffracted beams of first order have been observed with He on metal surfaces like W (211) (Tendulkar and Stickney, 1971; Stoll and Merrill, 1973; Stoll, Ehrhardt, and Merrill, 1976), Ag (111) (Boato, Cantini, and Tatarek, 1976; Horne and Miller, 1977), Cu (001) (Mason and Williams, 1978), Ni (110) (Rieder and Engel, 1979). Only by using stepped surfaces like Cu (117) (Lapujoulade and Lejay, 1977) or Pt (997) (Comsa *et al.* 1979) has more pronounced diffraction appeared, and there is only one very recent experiment, again with Cu (117) (Lapujoulade, Lejay, and Papanicolaou, 1979), where transitions to bound states could be observed. The consequence of these facts is that we will deal in the following mainly with insulating or semiconducting solid surfaces for which strong enough selective adsorption effects have been observed until now.

An example of the potential function  $v(z)$  with its steep repulsion which depends on the position in the unit cell and its constant long-range attractive part is given in Fig. 1. A quite general representation of this potential function reflecting the periodicity of the surface lattice is the following Fourier series:

$$v(\mathbf{r}) = \sum_{\mathbf{G}} v_{\mathbf{G}}(z) \exp(i\mathbf{G} \cdot \mathbf{R}). \quad (2.1)$$

Here, and in the following, the notation of Cabrera *et al.* (1970) is used, where the vector components parallel to the surface are denoted by capital letters and the  $z$  direction is the outward normal to the surface plane. Then the position vector of the gas atom

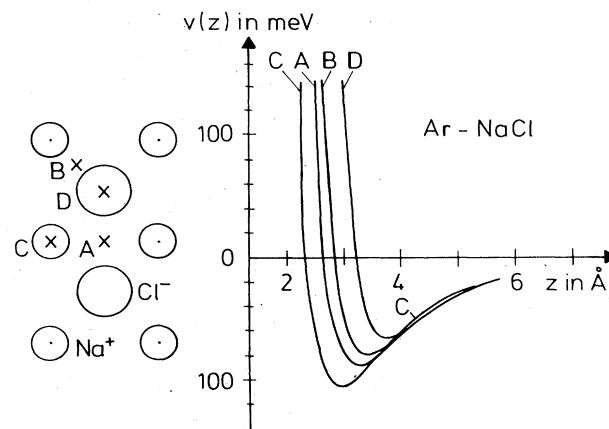


FIG. 1. Example of the physical gas-surface interaction energy as function of the distance  $z$  of the gas atom from the surface plane. The curves represent energy functions for Ar above four different sites (A, B, C, and D) of the (001) surface of a NaCl crystal as calculated from pairwise summation by Rogowska (1978).

is written as  $\mathbf{r} = (x, y, z) = (\mathbf{R}, z)$ , and  $\mathbf{G}$  represents a two-dimensional reciprocal surface lattice vector. For a square array with lattice constant  $l$ ,  $\mathbf{G}$  can be represented by  $\mathbf{G} = g(m, n)$ , with  $g = 2\pi/l$  and  $m, n$  integers.

The main term of the Fourier series  $v_{00}(z)$  represents the lateral average of the gas-surface interaction. A qualitative picture of it is given by the mean of the four curves shown in Fig. 1. Since the periodic surface structure appears only in the short-range repulsion the higher potential terms can be assumed to be repulsive only. Their strength decreases rapidly with increasing order  $m+n$  of  $\mathbf{G}$  as discussed, for instance, by Goodman (1967, 1973).

## B. Theoretical results on the physical gas-surface interaction potential

### 1. First-principle calculations

There have been only a relatively small number of attempts to calculate the physical gas-surface interaction potential from first principles, starting, say, with the electronic structure of the solid surface and of the gas atom. Recent calculations for He on metals have been done by Kleinman and Landman (1973, 1974; Landman and Kleinman, 1975) and by Zaremba and Kohn (1976, 1977). They calculate the attractive van der Waals interaction at large distances and the repulsive interaction energy at small distances and construct from these two parts a complete potential as a function of the distance  $z$  of the gas atom from the surface but without periodic structure parallel to the surface. An essential parameter in this procedure is the definition of the reference plane  $z = z_0$  from which the distance of the gas atom should be measured in the attractive part of the potential. Values of  $z_0$  relative to the first atom layer of the solid are given by Zaremba and Kohn (1976) for metals as well as for dielectric solids. The interaction of rare gas atoms with graphite surfaces has been calculated by Freeman (1975) using density functional techniques of Gordon and Kim (GK) (1972), but the results are rather qualitative due to the approximations in the graphite density function and due to the incorrect treatment of the dispersion energy by the GK method. Another *ab initio* calculation of physisorption was given recently by Wood (1978) for He on LiH. Using the molecular orbital approach of floating spherical Gaussian orbitals (FSGO) he gets potential functions which depend on the position over the lattice cell showing no minimum for the (100) LiH face and only a small minimum with a depth of 0.02 meV for the (110) face. Bruch and Ruijgrok (1979) studied also very recently the physical adsorption of atomic hydrogen within an approximative model where a hydrogen atom interacts with a perfectly imaging substrate bounded by a sharp planar surface and where the repulsion is introduced by a bounding condition which excludes the atomic electron from the substrate.

Because of the more or less severe approximations still used in these first-principle calculations the achieved results are in most cases only of qualitative character.

### 2. Pairwise summation calculations

An approximation frequently used that allows calculating physisorption potential energies of several gas-surface systems is based on the additivity assumption. In this case the potential function is achieved by summing or integrating over all binary interactions between the gas atom and the lattice atoms or ions. A discussion of this method together with a survey of results is given for instance by Beder (1967) or recently in more detail by Steele (1973, 1974).

With the pairwise gas atom-solid atom potential function  $U_{gs}(\rho_i)$ , where  $\rho_i = |\mathbf{r} - \mathbf{r}_i|$  denotes the distance between the gas atom at  $\mathbf{r}$  and the  $i$ th solid atom at  $\mathbf{r}_i$ , the total gas atom-solid surface potential is given by the sum

$$v(\mathbf{r}) = \sum_i U_{gs}(\rho_i). \quad (2.2)$$

This method avoids the difficulties arising in calculations which start with the electronic structure of the solid and the gas atom, but here some other problems and approximations have to be accepted.

First the distribution of the atoms in the solid must be known. In most cases this problem is overcome by assuming the same configuration in the surface region as in the bulk of the solid; relaxations at the surface are neglected or might be used as a fitting parameter in comparison with experiments.

A second and much more severe problem is connected with the deficient knowledge of the parameters of the pair potential curves. As the atoms or ions forming the solid are often in an electronic state not found in the gas phase, these parameters cannot be determined from independent experimental measurements and have to be evaluated by theoretical estimates. Frequently used in this context are combination rules; that means the gas atom-solid atom parameters (gs) are determined by combining the corresponding solid atom-solid atom (ss) and gas atom-gas atom (gg) parameters.

For instance, the geometrical mean is commonly used for the potential well depth

$$\varepsilon_{gs} = (\varepsilon_{gg} \cdot \varepsilon_{ss})^{1/2}, \quad (2.3)$$

and the arithmetic mean is used for the appropriate range parameter

$$\sigma_{gs} = (\sigma_{ss} + \sigma_{gg})/2. \quad (2.4)$$

A further shortcoming of this summation method arises from neglecting many-body effects in the interactions. For instance, the interaction of a pair of atoms may be changed by a solid nearby. The effect of each of these approximations on the potential parameters may be appreciably larger than 10% even in the case of rare gases interacting with rare gas crystals. A more detailed discussion of these problems, which become important for ionic crystals and even more for graphite, can be found, for instance, in Steele (1974) and references given there. Approximative procedures achieved by replacing the summation over the solid atoms by an integration are also discussed by Steele (1974). An essential result in this context is that gas-surface potentials of the form  $v(z) = Az^{-9} - Bz^{-3}$  are obtained from

integrating a (12-6) Lennard-Jones pair potential over the solid. (The detailed formulas achieved by Steele are given in Appendix A.)

Concerning gas-surface diffraction investigations, most of the pairwise summation calculations have been done for the system He-LiF (001) (Goodman, 1967, 1973, 1976; Tsuchida, 1969, 1974; Cabrera and Goodman, 1972; Davies and Ullermayer, 1973; Chow and Thompson, 1976) but also for atomic hydrogen on LiF (Finzel *et al.*, 1975). Very recent calculations of the interaction potential of rare gas atoms with alkali halide crystals have been done by Rogowska (1978) and by Hall and Rose (1978). In these cases the interaction between the gas atom and one of the lattice ions may be divided into three parts [see, for instance, Davies and Ullermayer (1973)]:

- (a) long-range attractive, nonpolar van der Waals dispersion interaction
- (b) short-range exchange repulsion and additionally
- (c) forces arising from the interaction of the Coulomb field of the lattice ions with the electron cloud of the gas atom, which is an induced dipole interaction.

The parts (a) and (b) are usually represented by the second and first term, respectively, of the modified Buckingham potential

$$U_{gs}(\rho) = A \exp(-\delta\rho) - C\rho^{-6}, \quad (2.5)$$

or the Lennard-Jones (12-6) potential

$$U_{gs}(\rho) = B\rho^{-12} - C\rho^{-6}, \quad (2.6)$$

where  $A$ ,  $B$ ,  $C$ , and  $\delta$  are constants depending on the interacting particles.

In terms of the equilibrium separation  $\rho_0$ , the potential well depth  $\varepsilon_{gs}$ , and the reciprocal repulsion range parameter  $\tau$ , these equations can be represented by

$$U_{gs}(\rho) = \frac{\tau\varepsilon_{gs}}{\tau-6} \left\{ \frac{6}{\tau} \exp\left[\tau\left(1 - \frac{\rho}{\rho_0}\right)\right] - \left(\frac{\rho_0}{\rho}\right)^6 \right\}, \quad (2.7)$$

or

$$U_{gs}(\rho) = \varepsilon_{gs} \left[ (\rho_0/\rho)^{12} - 2(\rho_0/\rho)^6 \right]. \quad (2.8)$$

The part (c) is proportional to the square of the electric field intensity  $\mathbf{E}(\mathbf{r})$  at the position  $\mathbf{r}$  of the gas atom,

$$U_{id}(\mathbf{r}) = -\frac{1}{2}\alpha |\mathbf{E}(\mathbf{r})|^2, \quad (2.9)$$

where  $\alpha$  is the polarizability of the gas atom. After summing the contributions of part (c) over the solid ions it turns out that the resulting attractive potential terms are very short ranged and in most cases negligible as compared to contributions of the dispersion interaction (Tsuchida, 1969; Davies and Ullermayer, 1973) (see also Fig. 2).

Further types of pair potentials used in gas-surface potential calculations are the Yukawa form (Cabrera and Goodman, 1972):

$$U_{gs}(\rho) = \beta\rho^{-1} \exp(-\delta\rho), \quad (2.10)$$

or Yukawa-6 form [see Appendix C, Eq. (C18)] and the Morse form (Goodman, 1976)

$$U_{gs}(\rho) = \varepsilon_{gs} \{ \exp[2a(\rho_0 - \rho)] - 2 \exp[a(\rho_0 - \rho)] \}. \quad (2.11)$$

In order to get the parameters in the Lennard-Jones

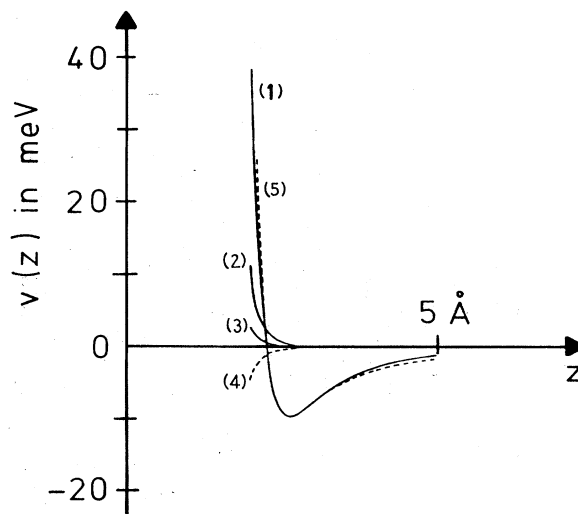


FIG. 2. Fourier components of the interaction potential between He and LiF (001) as calculated by Tsuchida (1969) from pairwise summation: (1)  $v_{00}(z)$ ; (2)  $v_{10}(z)$  or  $v_{1,1}(z)$ ; (3)  $v_{2,0}(z)$ . The dotted line (4) gives the (0,0) term of interaction energy caused by the electric field of the charges of Li and F ions (higher terms too small to be shown here) and the dashed line (5) shows the approximations of  $v_{00}(z)$  by a 12-3 potential.

12-6 pair potential between the gas atom and the alkali halide ions, combination rules of the form (2.3) and (2.4) were used together with the assumption of representing the ions by the corresponding rare gas atom (Tsuchida, 1969, 1974; Davies and Ullermayer, 1973). For the Buckingham pair potential the parameters of the exponential repulsion term were also calculated by corresponding combination rules (Finzel *et al.*, 1975; Rogowska, 1978), whereas the coefficient  $C$  in the attractive dispersion term was calculated by using the London formula (Finzel *et al.*, 1975)

$$C = \frac{3}{2} \alpha_g \alpha_s \frac{U_g U_s}{U_g + U_s}, \quad (2.12)$$

or by using the Kirkwood-Müller formula (Rogowska, 1978)

$$C = 6m_e c^2 \alpha_g \cdot \alpha_s / \left( \frac{\alpha_g}{\kappa_g} + \frac{\alpha_s}{\kappa_s} \right), \quad (2.13)$$

where  $\alpha_{g,s}$ ,  $U_{g,s}$ , and  $\kappa_{g,s}$  are the electric polarizability, the ionization potential [corrected following Pitzer (1959)], and the diamagnetic susceptibility for the gas atom and the solid ion, respectively,  $m_e$  is the mass of the electron, and  $c$  is the velocity of light.

In some of the pairwise summation investigations formulas were developed which allow analytical evaluation of the Fourier components  $v_G(z)$  [see Eq. (2.1)] from the pair potential parameters (Steele, 1973, 1974; Cabrera and Goodman, 1972; Tsuchida, 1970).

Figure 2 shows the Fourier components for He on LiF as they were derived by Tsuchida (1969) with a Lennard-Jones 12-6 pairwise potential, replacing Li<sup>+</sup> by He and F<sup>-</sup> by Ne and using the combination rules given above with the parameters

$$\varepsilon_{\text{He-He}} = 0.93 \text{ meV} \quad \varepsilon_{\text{Ne-Ne}} = 3.08 \text{ meV}$$

$$\rho_{0\text{He-He}} = 2.88 \text{ \AA} \quad \rho_{0\text{Ne-Ne}} = 3.09 \text{ \AA}.$$

The dashed line shows that the (0, 0) component can be well approximated by a function of the form

$$v_{00}(z) = (D/3)[(z_0/z)^{12} - 4(z_0/z)^3], \quad (2.14)$$

with well depth  $D = 10.4$  meV and  $z_0 = 2.65$  \AA. The higher terms are well approximated by

$$v_{mn}(z) = \varepsilon_{mn}(z_0/z)^{14}, \quad (2.15)$$

with  $\varepsilon_{10} = 0.26$  meV,  $\varepsilon_{11} = 0.22$  meV, and  $\varepsilon_{20} = 0.04$  meV.

A comparison with potential parameters ( $D = 8.7$  meV,  $z_0 = 2.8$  \AA) estimated from experimentally determined binding energies (see later) shows the approximative character of the results achieved by pairwise summation. The lack in precision was similar in the case of atomic hydrogen on LiF (Finzel *et al.*, 1975) with a well depth of  $D = 13.4$  meV calculated from pairwise summation as compared to  $D = 17.8$  meV determined from experimental binding energies. To get a more quantitative description of the strength of the periodic potential terms here the dispersion parameter  $C$  for H-F<sup>-</sup> was changed (from  $5.6 \text{ eV \AA}^6$  to  $7.0 \text{ eV \AA}^6$ ) so that the experimental well depth was reproduced by the calculation. Variations of the H-Li<sup>+</sup> parameter were ineffective since the contribution of the Li<sup>+</sup> ions to the total interactions amounts to about 10% only. A similar fitting procedure was used by Chow and Thompson (1976) for constructing a gas-surface potential for He-LiF atom-surface scattering calculations (for form and parameters used, see Sec. III.C.3 and Appendix C).

### 3. Long-range asymptotic behavior of the gas-surface potential

From pairwise potential integration in the continuum approximation of the solid we have already seen that a  $z^{-3}$  dependence results from the  $\rho^{-6}$  term of the dispersion energy in the pair interaction. But this result for the main contribution to the interaction energy at large gas-surface separations ( $z > l = \text{lattice constant}$ ) in physically interacting gas-solid systems can be deduced quite generally; see, for instance, Lifshitz (1956) or Zaremba and Kohn (1976). They showed that this polarization energy is given by

$$v_p(z) = -C_3 z^{-3}, \quad (2.16)$$

where the constant  $C_3$  can be expressed by optical properties of the atom and the solid. At very large distances ( $z > 10$  nm) retardation effects change the asymptotic behavior to  $v_p \propto z^{-4}$ , but the interaction at these distances is not relevant in the gas surface diffraction experiments discussed in the following.

For an isotropic atom and an isotropic solid,  $C_3$  is given by

$$C_3 = \frac{\hbar}{4\pi} \int_0^\infty \alpha(iw) \frac{\varepsilon(iw) - 1}{\varepsilon(iw) + 1} dw, \quad (2.17)$$

where  $\alpha(iw)$  is the electric dipole polarizability of the gas atom and  $\varepsilon(iw)$  is the dielectric function of the solid, both at pure imaginary frequencies. Some approximative forms of this expression have been discussed by Steele (1974).

Recently Bruch and Watanabe (1977) used formula (2.17) in order to calculate the coefficient  $C_3$  for H, He, and H<sub>2</sub> interacting with LiF and NaF. Their results will be compared with experimental results later. To conclude, we see that neither calculations from first principles nor pairwise summation can deliver physical potential energies which do not contain more or less severe approximations. Note that in a pairwise summation the problem is only shifted to the determination of the correct pair potential parameters. Thus it is indeed necessary to test the validity of the results of the different theoretical calculations by experimental investigations, and an appropriate method for measuring the physical interaction potential is the diffraction of light atoms from single-crystal surfaces. This method, together with its results on well depth, range, and strength of periodic terms of the interaction potential, will be discussed in the following chapter.

## III. THE GAS-SURFACE INTERACTION POTENTIAL FROM GAS-SURFACE DIFFRACTION EXPERIMENTS

### A. Survey on elastic gas-surface diffraction theory

As a consequence of the periodicity of the gas-surface potential the wave function of a gas atom incident on the surface with a wave vector  $\mathbf{k}_i = (\mathbf{K}, k_{iz})$  can be expressed by

$$\psi(\mathbf{r}) = \sum_{\mathbf{G}} \psi_{\mathbf{G}}(z) \exp[i(\mathbf{K} + \mathbf{G}) \cdot \mathbf{R}], \quad (3.1)$$

where the partial wave

$$\varphi_{\mathbf{G}}(\mathbf{r}) = \psi_{\mathbf{G}}(z) \exp[i(\mathbf{K} + \mathbf{G}) \cdot \mathbf{R}] \quad (3.2)$$

corresponds to:

(a) a diffracted beam of the order  $\mathbf{G} = (m, n)$  for

$$k_{Gz}^2 = k_i^2 - (\mathbf{K} + \mathbf{G})^2 > 0; \quad (3.3)$$

(b) a closed channel (waves decaying exponentially normal to the surface) for

$$k_{Gz}^2 < 0; \quad (3.4)$$

(c) a bound-state resonance channel for

$$k_{Gz}^2 = (2m_g/\hbar^2)E_j < 0, \quad (3.5)$$

where  $E_j$  is the binding energy of an atom bound normal to the surface in the gas surface potential well  $v_{00}(z)$  and  $m_g$  is the mass of the gas atom. If relation (3.5) holds for some special  $\mathbf{G}$  vector the incident atom may be transferred by diffraction to a state where it is bound normal to the surface with the binding energy  $E_j$  but moves parallel to the surface with the energy  $(\mathbf{K} + \mathbf{G})^2 \hbar^2 / 2m_g$  which surpasses the incident energy just by the gained binding energy  $|E_j|$ . Such intermediate diffraction states result in resonances in the elastically diffracted beams and may cause strong changes in the intensity of these beams (for a more detailed discussion of bound state resonances see Sec. III.C.1).

If condition (3.3) is fulfilled for some reciprocal lattice vectors other than the specular beam ( $\mathbf{G} = 0, 0$ ) the corresponding higher diffracted beams may appear. The distribution of the scattered intensity to these different allowed outgoing beams is then determined by the periodic structure of the gas-surface interaction potential.

In order to extract information on the gas-surface potential from observed diffracted beam intensities the dependence of the amplitudes of the partial waves  $\psi_{\mathbf{G}}(z)$  on the strength of the periodic potential terms  $v_{\mathbf{G}}(z)$  must be known, but this in general implies solving the Schrödinger equation with the gas-surface interaction potential  $v(\mathbf{r})$

$$[-(\hbar^2/2m_g)\nabla^2 + v(\mathbf{r}) - \hbar^2 k_i^2/2m_g] \psi(\mathbf{r}) = 0. \quad (3.6)$$

With the expansions for  $v(\mathbf{r})$  and  $\psi(\mathbf{r})$  given in Eqs. (2.1) and (3.1), the following infinite system of coupled differential equations for  $\psi_{\mathbf{G}}(z)$  is achieved (Goodman, 1977a; Cabrera *et al.*, 1970):

$$\left[ \frac{d^2}{dz^2} + k_{Gz}^2 \right] \psi_{\mathbf{G}}(z) - \left( \frac{2m_g}{\hbar^2} \right) \sum_{\mathbf{G}'} v_{\mathbf{G}-\mathbf{G}'}(z) \psi_{\mathbf{G}'}(z) = 0. \quad (3.7)$$

For comparison with experiment the asymptotic form  $\psi_{\mathbf{G}}(z \rightarrow \infty)$  has to be regarded. For the diffracted beams this can be represented by

$$\psi_{\mathbf{G}}(z \rightarrow \infty) = L^{-1/2} [\delta(\mathbf{G}, \mathbf{0}) \exp(-ik_{iz}z) + S_{\mathbf{G}} \exp(ik_{Gz}z)], \quad (3.8)$$

where  $\delta(\mathbf{G}, \mathbf{G}')$  is the Kronecker delta function, and  $L$  is a normalization length. The interesting quantity is the amplitude  $S_{\mathbf{G}}$  which is related to the observable diffraction probability  $P_{\mathbf{G}}$  by

$$P_{\mathbf{G}} = (k_{Gz}/k_{iz}) |S_{\mathbf{G}}|^2. \quad (3.9)$$

In purely elastic scattering particle conservation requires the sum over all allowed diffracted beams to be unity:

$$\sum_{\mathbf{G}} P_{\mathbf{G}} = 1. \quad (3.10)$$

So any reliable elastic theory should give results which satisfy this unitarity condition. There have been a number of attempts to solve Eq. (3.7) within several approximative methods. A detailed discussion of the different approaches is, for instance, given by Goodman and Wachman (1976) or by Goodman (1977a). Concerning the form of the potential used in the calculations two essentially different types have to be mentioned: (i) the hard corrugated wall with sometimes an attractive square well in front of it, and (ii) potentials with weaker repulsive and attractive forms like Morse potentials, 9-3 Lennard-Jones form, or similar forms.

It should be mentioned here that also semiclassical trajectory calculations have been shown to work quite well for describing He scattering from periodic solid surfaces at least if  $k_i$  is not too small ( $k_i l \gtrsim 20$ , where  $l$  is the lattice constant). A detailed discussion of different semiclassical calculations may be found, for instance, in a review paper by Goodman (1977a) and a comparison of semiclassical theory to approximations for solving Eq. (3.7) in the case of a corrugated hard-wall potential is given by Hill and Celli (1978).

## B. Results with a hard corrugated wall

In the method of calculating diffracted beam intensities discussed here the gas-surface interaction is approximated by a periodic hard corrugated wall. That means

the gas-surface potential is given by

$$\begin{aligned} v(\mathbf{r}) &= 0, & z > \xi(\mathbf{R}) \\ v(\mathbf{r}) &= \infty, & z \leq \xi(\mathbf{R}), \end{aligned} \quad (3.11)$$

where the surface is defined by the shape function

$$z = \xi(\mathbf{R}) = \sum_{\mathbf{G}} \xi_{\mathbf{G}} \exp(i\mathbf{G} \cdot \mathbf{R}). \quad (3.12)$$

With this form of the potential, of course, all effects caused by resonance channels mentioned above are neglected, and the calculated diffracted beam intensities are valid only if the conditions of incidence are so that no resonance may occur.

The corrugated hard-wall model was proposed for gas-surface scattering by Garibaldi *et al.* (1975) using the so-called "Rayleigh hypothesis," which allows determination of the scattering amplitudes for sufficiently small corrugation. Rigorous treatments were given later by Masel, Merrill, and Miller (1975) and by Goodman (1977b) and in a recent paper Garcia and Cabrera (1978) presented a formalism which is more suited for numerical evaluation of the scattered beam intensities, especially at strong corrugations. Garcia and Cabrera gave also a detailed discussion comparing the different methods mentioned above. Very recently also Armand and Manson (1978) gave an exact solution of the scattering by a hard corrugated wall.

For comparison with experiment two different methods of calculating should be mentioned, both based on the Rayleigh hypothesis. The first method introduced by Garibaldi *et al.* (1975) uses the eikonal approximation together with the simplest form of the shape function

$$\xi(\mathbf{R}) = \frac{1}{2} \xi_0 [\cos(2\pi x/a) + \cos(2\pi y/a)], \quad (3.13)$$

corresponding to a corrugation period of length  $a$ ,

$$\xi_{1,0} = \xi_{0,1} = \xi_{-1,0} = \xi_{0,-1} = \frac{1}{4} \xi_0$$

and the other  $\xi_{\mathbf{G}}$ 's all zero.

This method leads to a rather simple form of the diffracted intensities  $P_{\mathbf{G}}$ :

$$P_{\mathbf{G}} = \frac{k_{Gz}}{k_{iz}} J_{|m|}^2(C) J_{|n|}^2(C), \quad (3.14)$$

where  $J_{|m|}, J_{|n|}$  are the Bessel function of integral order  $|m|, |n|$  and the argument  $C$  is given by

$$C = \frac{1}{2} \xi_0 k_i (\cos\theta_i + \cos\theta_G). \quad (3.15)$$

It should be mentioned here that unitarity [Eq. (3.10)] does not hold for the intensities  $P_{\mathbf{G}}$  calculated by the approximative formula (3.14) [see also Chiroli and Levi (1976)].

Sometimes an attractive potential well of depth  $D$  in front of the wall is included in the calculations with the only effect of replacing the  $z$  component of the wave vector  $k_i \cos\theta_G$  by effective values of

$$(k_i^2 \cos^2\theta_G + 2m_g D/\hbar^2)^{1/2}$$

and changing  $C$  to

$$C' = \frac{1}{2} \xi_0 [(k_i^2 \cos^2\theta_i + 2m_g D/\hbar^2)^{1/2} + (k_i^2 \cos^2\theta_G + 2m_g D/\hbar^2)^{1/2}]. \quad (3.16)$$

In order to fit the calculated and experimental intensi-

ties the parameter  $\xi_0$  and sometimes also  $D$  were varied. The agreement achieved by such fitting is rather good; see, for instance, Boato, Cantini, and Mattera (1976). Values of  $\xi_0$  and  $D$  resulting from such fitting for several systems are given in Table I. Of course, this method is not well suited for determining the potential well depth  $D$  because of the approximative character of the model used and also because of the fact that the well depth is only small compared to the incident energy in many cases.

The second method to be mentioned here is the GR method proposed by Garcia (1977a), which is suited to achieve quite exact results for the diffracted beam intensities within the Rayleigh model. This method was used by Garcia (1976, 1977b) for comparing calculated intensities with experimental ones for He on LiF given by Boato, Cantini, and Mattera (1976). The shape function used by Garcia had the form

$$\begin{aligned} \xi(\mathbf{R}) = & \frac{1}{2} \xi_{10} [\cos(2\pi/a)x + \cos(2\pi/a)y] \\ & + \frac{1}{2} \xi_{11} [\cos(2\pi/a)(x+y) + \cos(2\pi/a)(x-y)] \\ & + \frac{1}{2} \xi_{20} [\cos(4\pi/a)x + \cos(4\pi/a)y], \end{aligned} \quad (3.17)$$

and the resulting set of best coefficients was:

$$\begin{aligned} \xi_{10} &= (0.0307 \pm 0.0003) \text{ nm}; \\ \xi_{11} &= (0.0017 \pm 0.0003) \text{ nm}; \quad \xi_{20} = 0. \end{aligned}$$

To give an impression of the quality of the fit, Fig. 3 shows a comparison of experimental and calculated intensities of some diffracted beams. A further attempt at determining corrugation parameters using the GR method was made by Garcia, Armand, and Lapujoulade (1977) with the following shape function

$$\xi(\mathbf{R}) = \frac{1}{2} \xi_{10} [\cos(2\pi/a)x + \cos(2\pi/a)y]. \quad (3.18)$$

Fitting experimental results for He on LiF(001) (Boato,

Cantini, and Mattera, 1976; Bledsoe and Fisher, 1976), and NaCl(001) (Bledsoe and Fisher, 1976), they found:

$$\xi_{10}[\text{He-LiF}(001)] = 0.030 \text{ nm},$$

$$\xi_{10}[\text{He-NaCl}(001)] \approx 0.034 \text{ nm},$$

and estimated from the specular beam intensity of He on Cu(001) (Armand, Lapujoulade, and Lejay, 1976, 1977) (no higher-order beams could be observed) an upper limit of the corrugation to be

$$\xi_{10}[\text{He-Cu}(001)] \leq 0.0025 \text{ nm}.$$

They achieved also a tentative value for the corrugation of the system He on W(112) by reexamination of the experiments by Tendulkar and Stickney (1971) and by Stoll and Merrill (1973):

$$\xi_{10}[\text{He-W}(112)] \approx 0.027 \text{ nm},$$

The He-W(112) data by Tendulkar and Stickney were also interpreted within a sinusoidal hard-wall model by Goodman (1978) with

$$\xi(\mathbf{R}) = 2\xi_x \cos(2\pi/a_x)x \quad (3.19)$$

and  $\xi_y = 0$  since the W(112) surface is corrugated only in  $x$  direction normal to the close packed rows of atoms.

The adjustable parameter in this model  $\xi_x$  and an effective Debye temperature were estimated to be

$$\xi_x[\text{He-W}(112)] = 0.004 \text{ nm}; \quad \theta_{\text{eff}} = 385 \text{ K}.$$

A successful application of the hard-wall model was also given by Armand and Manson (1978) using a triangular corrugation to reproduce the data of He scattered from a stepped Cu(117) surface by Lapujoulade and Lejay (1977). These He-Cu(117) data were also interpreted with hard-wall calculations by Garcia and Cabrera (1977). Regarding the results discussed above the hard-wall model seems to be a good approximation for

TABLE I. Corrugation parameter  $\xi_0$  and well depth  $D$  giving best agreement between experiment and calculations in eikonal approximation.

Gas-surface system	$\xi_0/\text{nm}$	$D/\text{meV}$	Ref.	Comment
He-LiF	0.0301	0	a	} $D$ fixed independently
He-LiF	0.0289	5	a	
Ne-LiF	0.0273	11 ± 2	a	
He-NiO	0.0135	10	b	
He-NiO	0.0139	0	c	Higher terms included $\xi_{11} \approx \xi_{20} \approx \xi_{21} \approx 0.001 \text{ nm}$
H <sub>2</sub> -NiO	0.025	50 <sup>f</sup>	b	$\xi(\mathbf{R}) = \frac{\xi_0}{2} (\cos \frac{2\pi}{a}x + \cos \frac{2\pi}{a}y + \alpha \cos \frac{2\pi}{a}x \cos \frac{2\pi}{a}y)$ ; $\alpha = 0.7$
He-graphite	0.0023	15 <sup>f</sup>	d	$\xi(\mathbf{R}) = 2\xi_0 [\cos \frac{2\pi}{a}x + \cos \frac{2\pi}{a}y + \cos \frac{2\pi}{a}(x-y)]$
H-KCl(H <sub>2</sub> O)	0.076	0	e	$\xi_0$ too high for eikon. approx., see also Garcia (1977a)

<sup>a</sup> Boato, Cantini, and Mattera (1976).

<sup>b</sup> Cantini, Felcher, and Tatarek (1977).

<sup>c</sup> Cantini, Tatarek, and Felcher (1979).

<sup>d</sup> Boato, Cantini, and Tatarek (1978).

<sup>e</sup> Frank, Hoinkes, and Wilsch (1977).

<sup>f</sup>  $D$  values from bound state resonances.

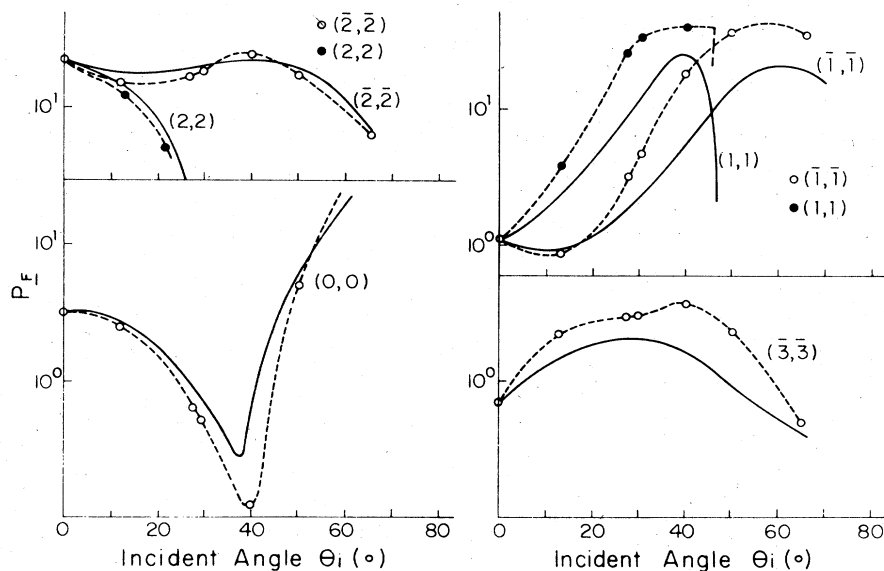


FIG. 3. Logarithmic plots of diffracted beam intensities as function of angle of incidence  $\theta_i$  ( $\langle 100 \rangle$  direction in the plane of incidence): Dashed lines are experimentally observed intensities [from Boato, Cantini, Mattera (1976)]; Full lines represent calculated diffraction probabilities normalized to the experimental curves at  $\theta_i = 0^\circ$  (parameters used:  $\xi_{10} = 0.0307$  nm,  $\xi_{11} = 0.0017$  nm,  $k_i = 110$  nm $^{-1}$ ) [from Garcia (1976, 1977b)].

describing diffracted beam intensities at least in the case of thermal He beams scattered from alkali halide or metal surfaces. But the question arises of how physically meaningful the corrugation parameters derived here are. If the corrugated wall is not really hard, the resulting corrugation could depend on the energy of the incident beam. Until now this effect has not been investigated in detail. But since this possible variation of the corrugation should appear mainly with respect to the energy normal to the surface it can be mentioned that in the case of He on LiF (Garcia, 1977b) one set of corrugation parameters worked well to describe the intensity distribution to different diffracted beams over a relatively wide range of angles of incidence ( $0 \leq \theta_i \leq 65^\circ$ ). With an incident wave vector of  $k_i = 110$  nm $^{-1}$  the energy normal to the surface  $E_{i,n} = \hbar^2 k_i^2 \cos^2 \theta_i / 2m_g$  varies in this range from 62 to 11 meV. It should also be mentioned in this context that for He on LiF the corrugation parameters extracted by Garcia (1977b) from experiments with relatively high incident energy ( $k_i = 110$  nm $^{-1}$ ) could also be used to reproduce well the detailed resonance structure observed by Frankl *et al.* (1978) at relatively low incident energy ( $k_i = 60$  nm $^{-1}$ ). This was shown by Garcia, Celli, and Goodman (1979) using a potential form where a long-range attractive part was added to the hard corrugated repulsive wall.

A problem not solved until now appears when the corrugation parameters resulting from a hard-wall analysis for He and for H on LiF(001) are compared. With similar conditions of incidence a much stronger specular beam is observed with atomic hydrogen as compared to He and this yields a corrugation parameter  $\xi_{10}$  [see Eq. (3.17)] with a value of

$$\xi_{10}[\text{H-LiF}(001)] = 0.009 \text{ nm},$$

(Greiner *et al.*, 1980) which is about one third of the value for He.

An answer to this problem could perhaps come from calculations of the type recently performed by Armand and Manson (1979) and Armand (1980). Using for the repulsion an exponential corrugated potential of the form

$$v(\mathbf{r}) = C \exp\{-\kappa[z - \xi(\mathbf{R})]\}, \quad (3.20)$$

they found an enhancement of the specular beam intensity when the repulsion becomes softer by decreasing  $\kappa$  ( $\kappa \rightarrow \infty$  gives the hard corrugated wall), and a softer repulsion for atomic hydrogen as compared to the harder closed-shell atom He is well conceivable.

We will come back to the corrugation parameters later in Sec. III.D when the hard-wall results are compared to the strength of periodic potential terms determined from band structure effects in bound-state resonances.

### C. Results from resonance effects

#### 1. General considerations on bound-state resonances

We include now in our considerations the attractive well in front of the surface and especially the states in which an atom is bound normal to the surface in the potential well  $v_{00}(z)$  with a discrete binding energy  $E_j$ . If then at certain conditions of incidence the following resonance condition is fulfilled:

$$\hbar^2 k_i^2 / 2m_g - E_j'(\mathbf{K} + \mathbf{G}) = E_j < 0, \quad (3.21)$$

an additional intermediate channel of diffraction opens for the incident atoms. In Eq. (3.21)  $E_j'(\mathbf{K} + \mathbf{G})$  is the energy of an atom moving parallel to the surface in the periodic gas-surface potential with the wave vector  $\mathbf{K}_G = \mathbf{K} + \mathbf{G}$  when the atom is bound normal to the surface in the state with quantum number  $j$ . This energy  $E_j'(\mathbf{K} + \mathbf{G})$  surmounts the incident energy just by the binding energy  $|E_j|$ . In other words this condition says that the incident beam is energetically in resonance with a closed channel in which the atom is bound normal to the surface with

binding energy  $-|E_j|$  and moves parallel to the surface with the corresponding higher energy  $E_j''(\mathbf{K} + \mathbf{G})$ .

The effect of such resonances on the experimentally observable diffracted beams is as follows:

The diffracted beams are coupled to the incident beam and also to each other by the periodic terms  $v_G(z)$  of the gas-surface interaction potential, and from this relatively strong coupling there results a certain distribution of the incident intensity to the different allowed diffracted beams. Theoretically this coupling is described by the system of coupled differential Eqs. (3.7). At resonance an additional intermediate channel opens into which the atom may be diffracted first and from which it may then in a second diffraction step be transferred to an outgoing diffracted beam again, with the consequence that the distribution of the scattered intensity to the observed beams may be strongly changed. The minima or maxima appearing at resonance in the diffracted beam intensities are easily observed in experiment and can be used to get information on the binding energies  $E_j$  and on the strength of the periodic potential terms. A relatively simple model, which gives a clear description of the intensity behavior at resonance, was developed recently by Celli, Garcia, and Hutchison (1979). Assuming that the particles bound normal to the surface are moving freely parallel to the surface (a good approximation in most cases; for essential deviations see later) we get for the resonance condition the form

$$(\mathbf{K} + \mathbf{G})^2 = (2m_g/\hbar^2)(E_i + |E_j|). \quad (3.22)$$

This form allows a simple geometrical representation of the resonance condition in  $\mathbf{K}$  space as shown in Fig. 4: to the surface component  $K = k_i \sin\theta_i$  lying in the plane of incidence a reciprocal lattice vector  $\mathbf{G}$  has to be added so that the resultant wave vector  $\mathbf{K}_G = \mathbf{K} + \mathbf{G}$  lies on the resonance circle with radius

$$K_{res,j} = [(2m_g/\hbar^2)(E_i + |E_j|)]^{1/2}$$

centered at the origin of  $\mathbf{K}$ . From Fig. 4 it is clear that this resonance constellation can be reached only at cer-

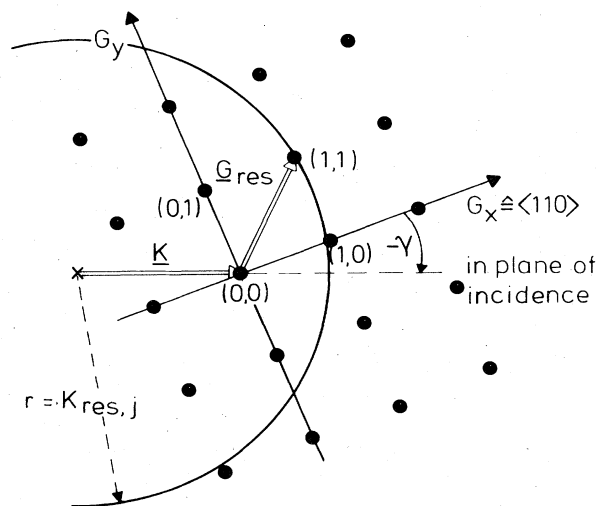


FIG. 4. Geometrical representation of resonance condition in  $\mathbf{K}$  space with  $K_{res,j} = [(2m_g/\hbar^2)(E_i + |E_j|)]^{1/2}$ .

tain conditions of incidence since  $\mathbf{G}$  and  $E_j$  can take only discrete values.

Regarding Fig. 4 and the usual scattering geometry as given in Fig. 5 the experimental variation of the following parameters seems to be adequate for investigating resonance effects:

(a) Variation of the azimuthal angle  $\gamma$  at fixed  $\theta_i$  and  $E_i$  by rotating the crystal around its surface normal. This corresponds in Fig. 4 to rotating the reciprocal lattice around its origin (0.0) at the end of  $\mathbf{K}$  and leads to a resonance when at a certain value of  $\gamma = \gamma_{res}$  a  $\mathbf{G}$  vector meets a resonance circle.

(b) Variation of the angle of incidence  $\theta_i$  changes the length of  $K = k_i \sin\theta_i$ , thus shifting the origin of the reciprocal lattice relative to the resonance circle so that at certain values of  $\theta_i$  a  $\mathbf{G}$  vector coincides with a resonance circle.

(c) Variation of the incident energy  $E_i$  has a similar effect as case (b) but changes also the radius of the resonance circle so that the situation becomes less easy to survey.

## 2. Determination of binding energies

The determination of binding energies  $E_j$  in the mean attractive potential well  $v_{00}(z)$  is mainly based on the minima appearing at resonance in the specular beam intensity. This effect, called "selective adsorption," has been known since the first diffraction experiments by Frisch and Stern (1933b) and has been used in the past for several gas-surface systems. The experimental method most frequently used corresponds to the case (a) mentioned above that is measuring the specular intensity  $I_{sp}$  as function of the azimuthal angle  $\gamma$  with the parameters  $E_i, \theta_i$  kept constant. From the resonance angles  $\gamma_{res}$  at which minima are observed the binding energies can be determined unequivocally using only the kinematic resonance condition without any assumption about the form of the gas-surface potential.

In order to get the correct labeling of the reciprocal lattice vector involved in the resonance the curves  $I_{spec} = f(\gamma)$  have to be measured with different parameters  $\theta_i$  or  $E_i$ . Then from the shift of  $\gamma_{res}$  from curve to curve the  $\mathbf{G}$  vector can be determined.

Figures 6-8 show typical experimental results: Figure 6 represents the quite simple structure observed with atomic hydrogen on NaF(001) (Finzel *et al.*, 1975).

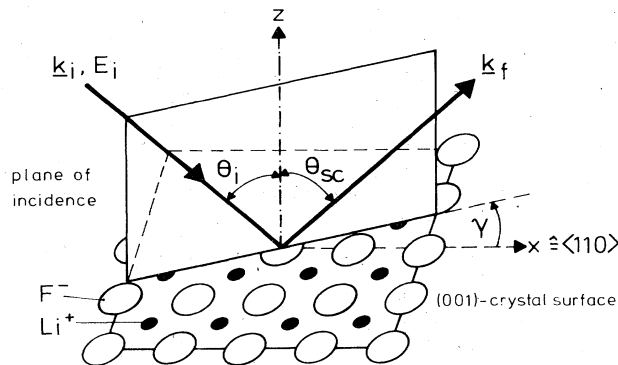


FIG. 5. Scattering geometry.

In this case only a  $\mathbf{G}$  vector of type  $(0, 1)$  is involved and only two bound-state levels are contributing, so that the labeling of  $\mathbf{G}$  and the determination of the  $E_j$  values is easy. Somewhat more complicated is the structure found with atomic deuterium diffracted from NaF(001) (Finzel *et al.*, 1975), since  $\mathbf{G}$  vectors of different type and more bound states are contributing (see Fig. 7). But the determination of the  $E_j$  values is still not very complicated. A borderline case for finding the correct labeling of the  $\mathbf{G}$  vectors is given in Fig. 8 with the system D on KCl(001) (Frank, Hoinkes, and Wilsch, 1977) where many overlapping minima are observed.

A good test of the correct labeling of the observed

minima may be derived from the resonance condition written in the form

$$(\mathbf{K}_i + \mathbf{G})^2 = (2m_g/\hbar^2)(E_i + |E_j|), \tag{3.23}$$

which obviously shows that for a certain resonance characterized by  $\mathbf{G}_{res}$  and  $E_{j,res}$ , which is observed by varying the azimuthal angle  $\gamma$  and the angle of incidence  $\theta_i$  but keeping the incident energy  $E_i$  constant, the surface component of the incident wave vector  $\mathbf{K}_i$  must always end on a circle with radius

$$K_{res} = [(2m_g/\hbar^2)(E_i + |E_j|)]^{1/2}$$

which is centered at  $-\mathbf{G}_{res}$ . An example of experimental

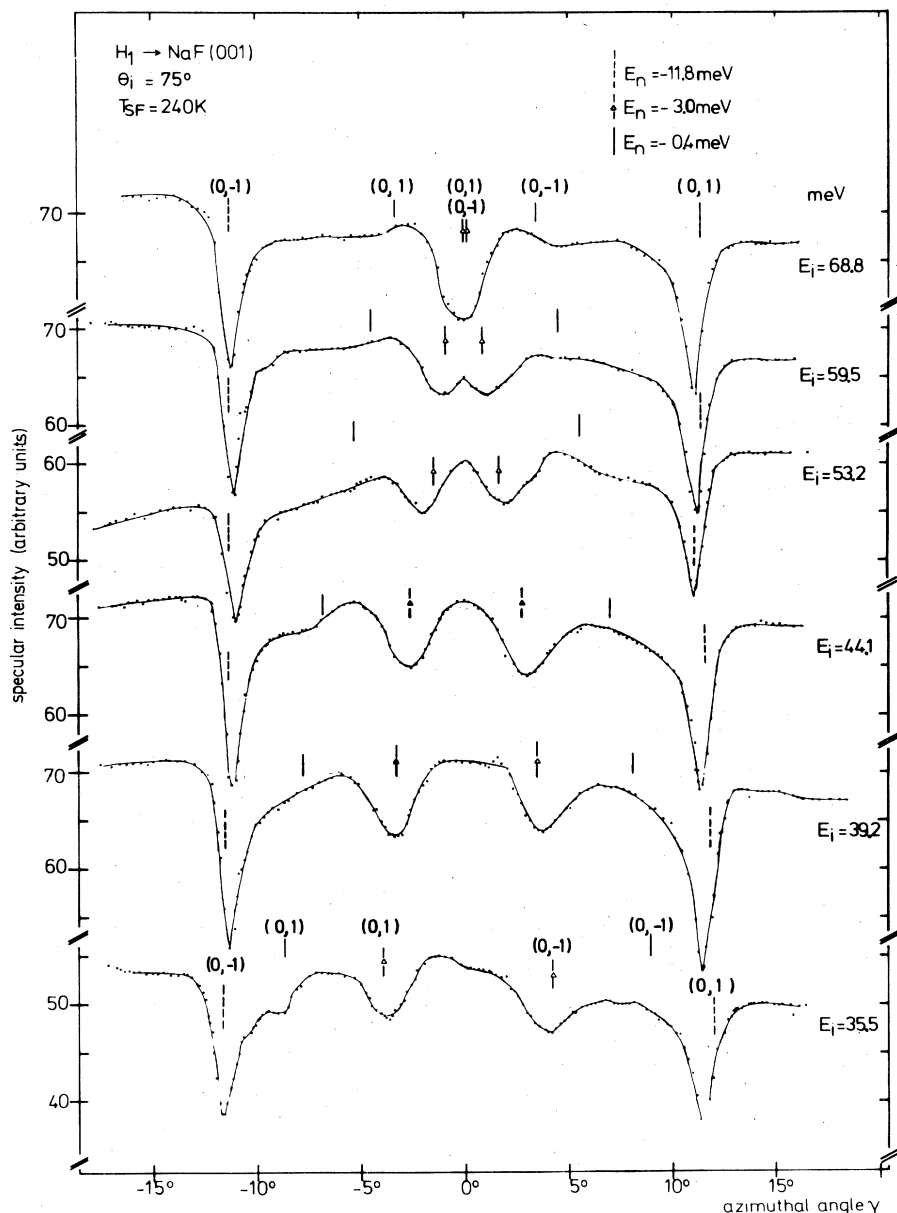


FIG. 6. Atomic hydrogen diffracted from NaF(001); resonance structure in the specular intensity as function of azimuthal angle  $\gamma$  measured at different incident energies  $E_i$  with a beam of  $(\Delta v/v) = 12\%$  FWHM. Bound-state resonances by  $G = (0, \pm 1)$  to bound-state levels  $E_j$  are indicated [from Finzel *et al.* (1975)].

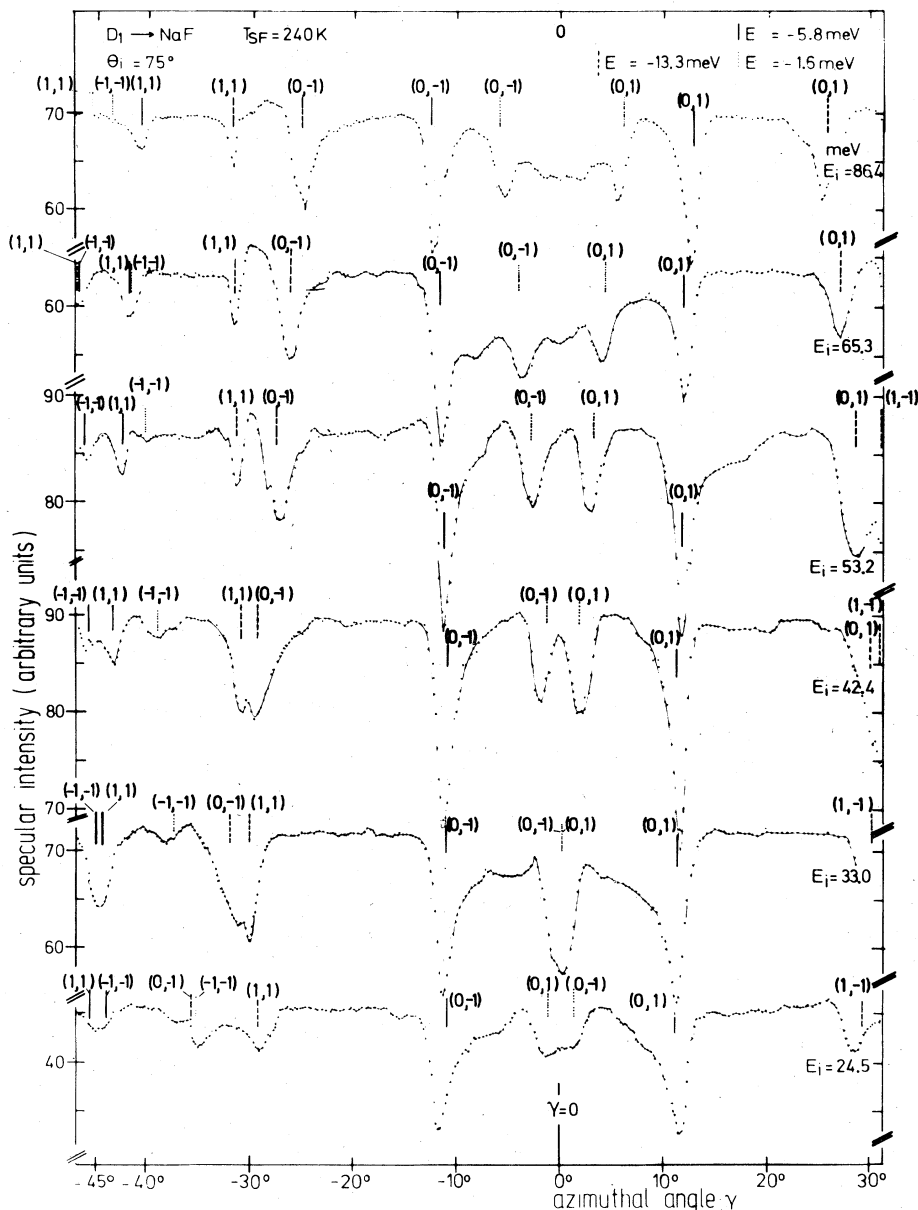


FIG. 7. Atomic deuterium diffracted from NaF(001); resonance structure in the specular intensity as function of azimuthal angle  $\gamma$  measured at different incident energies  $E_i$ . Bound-state resonances by reciprocal lattice vectors  $(m, n)$  to bound-state levels  $E_j$  are indicated [from Finzel *et al.* (1975)].

results plotted in the appropriate way is shown in Fig. 9 for the system  $^4\text{He-LiF}(001)$  investigated by Meyers and Frankl (1975). Some typical binding energy spectra resulting from resonance investigations are shown in Table II. A more detailed table with all the binding energies known to the author is given in Appendix B.

Any two isotopes like H and D or  $^3\text{He}$  and  $^4\text{He}$  with the same electronic shell but different mass should give different series of levels which fit to the same gas-surface interaction potential. Consequently this isotopic effect was used to confirm the labeling of the quantum number  $j$  of the observed levels. Especially the question of whether the deepest observed level is indeed the deepest level of the investigated system can be answered more

definitely if the  $j$  labeling is confirmed by a second set of levels given by an additional isotope. This isotopic effect was first applied by Hoinkes, Nahr, and Wilsch (1972b) and Finzel *et al.* (1975) in investigating the interaction of atomic hydrogen on LiF and NaF using H and D and was also used by Derry *et al.* (1977, 1978, 1979) for He on LiF, NaF, and graphite using  $^3\text{He}$  and  $^4\text{He}$ .

In some previous publications on bound-state resonances on LiF(001) [see, for instance, O'Keefe *et al.* (1970)] it was proposed that there is at least one monolayer of regularly adsorbed water on the surface. But in recent investigations we could show by secondary ion mass spectroscopy (SIMS) [Estel *et al.* (1976)] that there

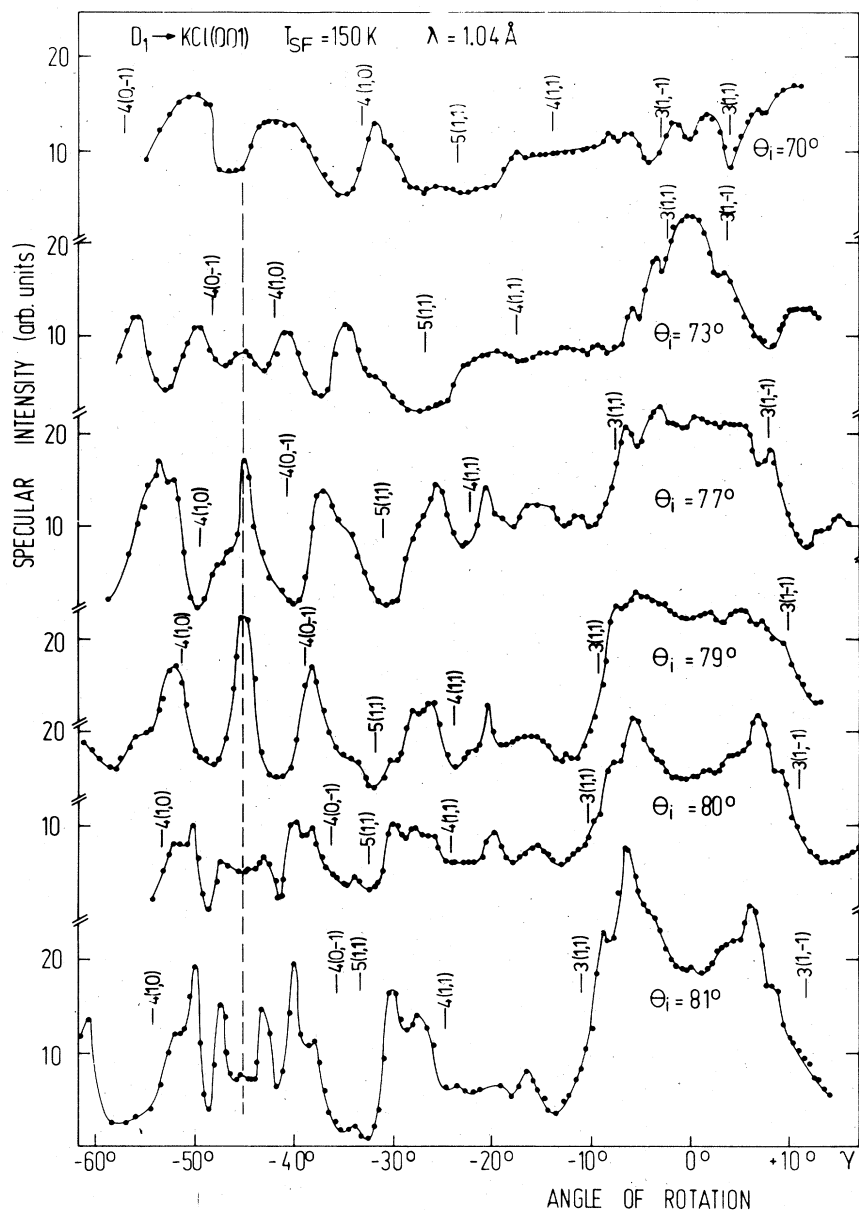


FIG. 8. Atomic deuterium diffracted from water-covered KCl(001); resonance structure in the specular intensity as function of azimuthal angle  $\gamma$  measured at different angles of incidence  $\theta_i$  with constant incident wavelength  $\lambda_i = 1.04$  Å. The resonance labeling has to be regarded as a tentative one [from Frank, Hoinkes, and Wilsch (1977)].

is definitely no water on the LiF(001) and NaF(001) surface at the conditions of the gas-surface diffraction experiments discussed here.

### 3. Determination of $v_{00}(z)$ from binding energies $E_j$

Knowing the spectrum of binding energies  $\{E_j\}$  the problem is now to determine a corresponding potential energy curve. The question of the uniqueness of the potential curve obtainable from  $\{E_j\}$  was discussed recently by Le Roy (1976). He pointed out that the inversion of a set of vibrational energy levels to determine a potential curve is a problem which has been extensively studied in diatomic molecular spectroscopy, where it was

shown that the  $\{E_j\}$  spectrum may be used to get the width of the potential as function of the depth of the potential. Regarding Fig. 10, this means the distance  $z_2 - z_1$  at a certain energy  $E$  is determined by  $\{E_j\}$  but there is no way of determining the individual values of  $z_1$  and  $z_2$  from the  $\{E_j\}$  spectrum only. This is demonstrated clearly by the Rydberg-Klein-Rees (RKR) method of molecular physics for calculating the width of the potential. This method recently was used by Schwartz, Cole, and Pliva (1978) and Cole and Frankl (1978) to develop a procedure of constructing gas-surface potential curves from  $\{E_j\}$ .

The RKR method is based on the Bohr-Sommerfeld quantization condition for the phase integral between the

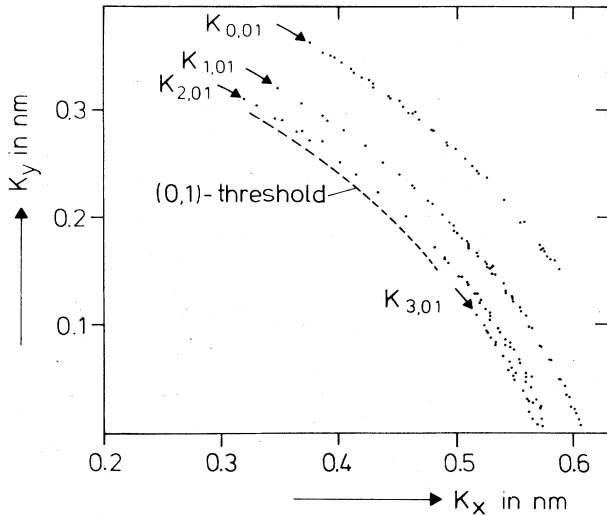


FIG. 9. Incident surface wave vectors in  $K_x, K_y$  plane at experimentally observed resonances for He-LiF (001). The points achieved from azimuthal scans at different angles of incidence but constant  $\lambda_i = 0.103$  nm fit well to resonance circles  $K_{j,0}$  with radii  $K_j = [(2m/\hbar^2)(E_i + |E_j|)]^{1/2}$  and centered at  $(0, -g)$  [from Meyers and Frankl (1975)].

classical turning points  $z_1$  and  $z_2$  at energy  $E$  (see Fig. 10)

$$(j + 1/2)h = 2 \int_{z_1}^{z_2} p \, dz, \quad (3.24)$$

where the momentum  $p$  as a function of  $z$  is given by the kinetic energy  $E_{\text{kin}}$  of a particle with total energy  $E$  moving in the potential well  $v_{00}(z)$ . Thus one gets the relation

$$(j + 1/2) = [2(2m_g)^{1/2}/h] \int_{z_1}^{z_2} [E - v_{00}(z)]^{1/2} dz, \quad (3.25)$$

where  $h =$  Planck's constant, and the quantum number  $j = j(E)$  becomes an integer when  $E$  equals an eigenvalue  $E_j$ . Differentiation of (3.25) with respect to  $E$  yields

$$\frac{dj(E)}{dE} = \frac{2(2m_g)^{1/2}}{h} \int_{z_1}^{z_2} \frac{dz}{[E - v_{00}(z)]^{1/2}}, \quad (3.26)$$

and this equation can be inverted to the relation for the

width of the potential ( $z_2 - z_1$ )

$$z_2(E) - z_1(E) = \hbar(2/m_H)^{1/2} \int_{-D}^B dE' (E - E')^{-1/2} d\eta/dE', \quad (3.27)$$

where, in addition, a mass reduced quantum number

$$\eta(E) = \frac{j(E) + 1/2}{(m_g/m_H)^{1/2}}, \quad (3.28)$$

where  $m_H =$  mass of H atom, has been introduced. The function  $\eta(E)$  may be constructed by interpolating between the experimental data points  $E_j$  at which  $j(E_j) = 0, 1, 2, \dots$ . So we have a formula for the distance between the classical turning points, but to fix these points at certain  $z$  values in order to get a unique potential curve we need additional information on the interaction. In diatomic molecular spectroscopy, in addition to the vibrational levels, the rotational levels contribute information on the potential so that in this case the turning points may be evaluated independently. But there is no equivalent quantity here in the case of linear vibration in  $v_{00}(z)$  normal to the surface.

#### a. Experimental results on the long-range attractive part

One kind of information on the gas-surface potential curve which can be introduced additionally to proceed in constructing  $v_{00}(z)$  is the asymptotic behavior already discussed

$$v_{00}(z) \rightarrow -C_3 z^{-3}. \quad (3.29)$$

With this behavior at the outer turning point Le Roy (1976) achieved a formula for the energy levels near the dissociation limit

$$|E_\eta|^{1/6} = b C_3^{-1/3} (\eta_D - \eta), \quad (3.30)$$

where  $b = 0.2027$  (meV) $^{1/2}$  nm and  $\eta, \eta_D =$  mass reduced quantum numbers defined in Eq. (3.28), where  $j_D =$  effective quantum number of the dissociation limit.

Formula (3.30) shows that for levels near the dissociation limit a plot of the one-sixth power of the binding energies versus  $\eta$  should be linear; the slope and the intercept with the  $\eta$  axis will give  $C_3$  and  $\eta_D$ , respectively. Corresponding plots of the experimental binding energies of H, D on LiF and NaF are given in Fig. 11a, b. They show that the measured  $E_j$  values fit quite

TABLE II. Examples of binding energies in the gas-surface potential well  $v_{00}(z)$  as determined from experimental resonance investigations.

Gas	Surface	Binding energies (meV)					Ref.
		$E_0$	$E_1$	$E_2$	$E_3$	$E_4$	
H	LiF(001)	$-12.2 \pm 0.2$	$-3.5 \pm 0.3$	$-0.5 \pm 0.3$			a
D		$-13.7 \pm 0.2$	$-6.7 \pm 0.2$	$-2.3 \pm 0.2$	$\pm 0.5 \pm 0.3$		a
$^3\text{He}$	LiF(001)	$-5.59 \pm 0.1$	$-2.0 \pm 0.1$				b
$^4\text{He}$		$-5.9 \pm 0.1$	$-2.46 \pm 0.1$	$-0.78 \pm 0.1$	$-0.21 \pm 0.1$		b
$^3\text{He}$	Graphite	$-11.62 \pm 0.12$	$-5.38 \pm 0.12$	$-1.78 \pm 0.12$			c
$^4\text{He}$		$-12.02 \pm 0.1$	$-6.34 \pm 0.1$	$-2.85 \pm 0.06$	$-1.00 \pm 0.06$	$-0.17 \pm 0.06$	c, d

<sup>a</sup> Finzel *et al.* (1975).

<sup>b</sup> Derry *et al.* (1978).

<sup>c</sup> Derry *et al.* (1979).

<sup>d</sup> Boato *et al.* (1979b).

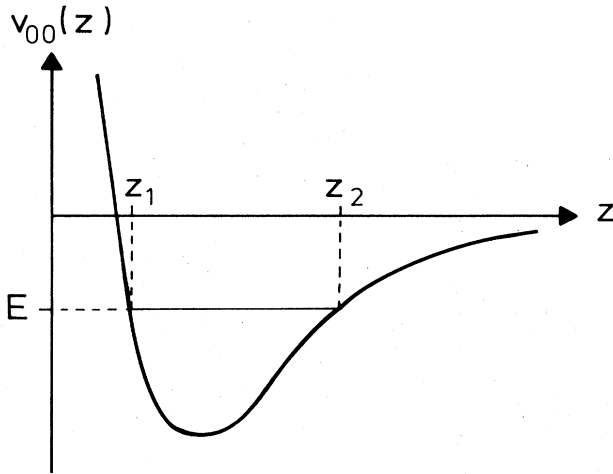


FIG. 10. Classical turning points  $z_1$  and  $z_2$  of a particle with total energy  $E$  in the potential well  $v_{00}(z)$

well to a straight line, but they also show that there should be some additional bound states between the highest observed level and the dissociation limit. The values of  $C_3$  and  $\eta_D$  determined from plots like those shown in Fig. 11 are given in Table III for those gas-surface systems for which reliable binding energies exist. Also shown in this table are the values of  $C_3$  calculated by Bruch and Watanabe (1977) and a comparison of the total number of levels  $N_{\text{tot}}$  calculated from  $\eta_D$  by

$$N_{\text{tot}} = \text{next larger integer to } j_D = \eta_D (m_g/m_H)^{1/2} - 1/2, \quad (3.31)$$

with the number of observed levels  $N_{\text{obs}}$ . In the last column the values of the potential well depth  $D$  are given, which were obtained from extrapolating the  $E(\eta)^{1/6}$  curve to  $\eta=0$  or  $j=-1/2$ . Of course, this value of the potential well depth achieved from extending the  $z^{-3}$  behavior to the potential minimum is only an approximative one. This should be compared with values of  $D$  achieved by other methods discussed later.

### b. Semiempirical rule for the attraction constant $C_3$

Bruch and Watanabe calculated the values of  $C_3$  for some gas-surface systems using the general formula for the polarization energy [Eq. (2.17)]. Since these are relatively complicated calculations which require the knowledge of the electric dipole polarizability of the atom and of the dielectric function of the solid both as function of imaginary frequencies, it will be shown in the following how a simpler procedure can be used to get rather reliable values of  $C_3$  for systems not investigated until now.

With the systems for which  $C_3$  is known from experiment (see Table III) we have checked the following relation:

$$C_3 = K_c \alpha (\epsilon - 1) / (\epsilon + 1), \quad (3.32)$$

where  $\alpha$  is the static electric polarizability of the gas atom,  $\epsilon$  is the optical dielectric constant of the solid, and  $K_c$  is a factor of proportionality which should be constant for all gas-surface systems. The result of this

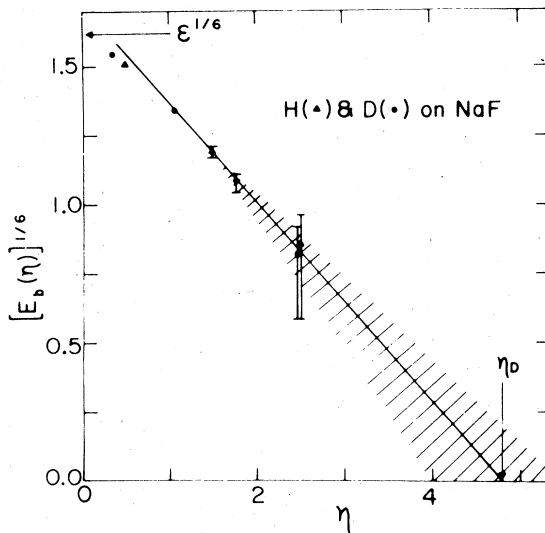
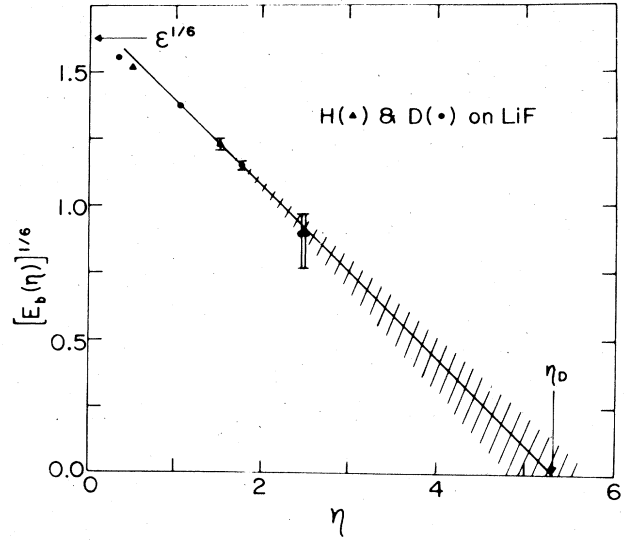


FIG. 11. Experimental binding energies  $E_b$  [from Finzel *et al.* (1975)] plotted as function of mass-reduced quantum number  $\eta$  according to Eq. (3.30) [after Le Roy (1976)]. (a) H, D on LiF (001); (b) H, D on NaF (001).

check is shown in Fig. 12 where the experimental values of  $C_3$  (Column 2 of Table III) are plotted as function of  $\alpha(\epsilon - 1)/(\epsilon + 1)$ . The values of  $\alpha$  and  $\epsilon$  used for these calculations are given in Table IV together with the resultant values of  $\alpha(\epsilon - 1)/(\epsilon + 1)$ . Indeed the functional dependence of the experimental points in Fig. 12 can be fitted quite well by a straight line, the slope of which gives a mean value of

$$K_c^{\text{exp}} = (0.141 \pm 0.010) \frac{\text{meV nm}^3}{10^{-25} \text{ cm}^3}.$$

Figure 13 shows a plot similar to Fig. 12, but here the values calculated by Bruch and Watanabe (Column 3 of Table III) were used. Again the functional dependence is rather well approximated by a straight line, but the resultant value of

$$K_c^{\text{calc}} = (0.108 \pm 0.003) \frac{\text{meV nm}^3}{10^{-25} \text{ cm}^3}$$

TABLE III. Values of attraction constant  $C_3^{\text{exp}}$ , the effective mass reduced quantum number of the dissociation limit  $\eta_D$  with the corresponding total number of bound-state levels  $N_{\text{tot}}$ , and the potential well depth  $D_{z-3}$  as obtained from plots of  $E_j^{1/6} = f(\eta)$  ( $E_j$  values from Table VIII) according to the method proposed by LeRoy (1976) are compared with values  $C_3^{\text{calc}}$  by Bruch and Watanabe (1977) and the number of experimentally observed levels  $N_{\text{obs}}$ .

System	$C_3^{\text{exp}}/\text{meV nm}^3$	$C_3^{\text{calc}}/\text{meV nm}^3$	$\eta_D$	$N_{\text{tot}}$	$N_{\text{obs}}$	$D_{z-3}/\text{meV}$
H D-LiF	$0.25 \pm 0.09^a$	0.194	$5.3 \pm 0.5^a$	5-6 <sup>a</sup> 7-8 <sup>a</sup>	3 4	$25.6 \pm 3.1$
H D-NaF	$0.18 \pm 0.11^a$	0.154	$4.8 \pm 0.8^a$	4-6 <sup>a</sup> 6-8 <sup>a</sup>	3 4	$27.5 \pm 3.5$
<sup>3</sup> He <sup>4</sup> He-LiF	$0.12 \pm 0.03$	0.093	$3.6 \pm 0.2$	6-7 7-8	2 4	$9.3 \pm 0.8$
<sup>3</sup> He <sup>4</sup> He-NaF	$0.12 \pm 0.044$	0.073	$3.4 \pm 0.3$	5-6 7-8	2 3	$8.8 \pm 1.3$
<sup>4</sup> He-NiO	$0.22 \pm 0.11$	...	$4.4 \pm 0.6$	8-10	3	$12.8 \pm 2.3$
H <sub>2</sub> -LiF D <sub>2</sub>	...	0.27	...	...	...	...
H <sub>2</sub> -NiO	$0.80 \pm 0.14$	...	$9.5 \pm 0.5$	13-14	5	$85 \pm 6$
<sup>3</sup> He <sup>4</sup> He-graph.	$0.11 \pm 0.03$	0.173 <sup>b</sup>	$4.0 \pm 0.3$	6-7 7-9	3 5	$25 \pm 6$
H D-graph.	$0.54 \pm 0.05$	...	$7.85 \pm 0.2$	8 11	2 4	$57 \pm 2$
H <sub>2</sub> -graph. D <sub>2</sub>	$0.67 \pm 0.08$	...	$8.6 \pm 0.3$	12-13 17-18	6 8	$63 \pm 4$
Kr-graph.	...	1.74	...	...	...	...
Xe-graph.	...	2.47	...	...	...	...

<sup>a</sup> Values determined by Le Roy (1976).

<sup>b</sup> Calculated by Bruch and Watanabe as cited by Derry *et al.* (1979).

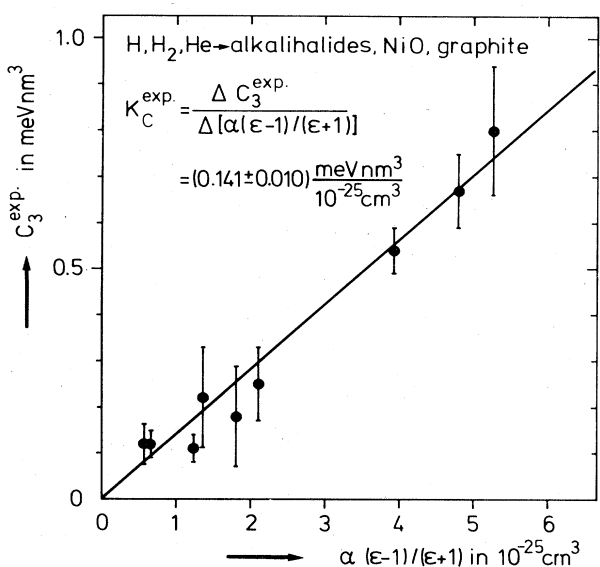


FIG. 12. Constant of attractive dispersion interaction  $C_3$  determined from experimental binding energies  $E_j$  plotted as function of  $\alpha(\epsilon - 1)/(\epsilon + 1)$  with  $\alpha$  = static electric polarizability of the atom and  $\epsilon$  = optical dielectric constant of the solid. An approximative linear dependence with the constant of proportionality  $K_C^{\text{exp}}$  is clearly demonstrated.

is somewhat smaller as could be expected from comparing the experimental and theoretical values of  $C_3$  in Table III. So taking one of these two mean values,  $K_C^{\text{exp}}$  or  $K_C^{\text{calc}}$ , an approximative value of the polarization energy coefficient  $C_3$  of an unknown system may be evaluated with the values of  $\alpha(\epsilon - 1)/(\epsilon + 1)$  as given in Table IV or calculated from static dipole polarizability  $\alpha$  and optical dielectric constant  $\epsilon$  tabulated elsewhere. Regarding the deviations of the known values of  $C_3$  from the straight line in Fig. 12, the error in a  $C_3$  coefficient calculated in this way can be assumed not to be larger than 30%, which was the deviation in the worst cases.

The situation is still better with the calculated  $C_3$  values. There the deviations from the straight line are in general much smaller than 30%. The good agreement is also demonstrated by  $C_3$  values recently calculated by Vidali, Cole, and Schwartz (1979). With the general formula [Eq. (2.17)] they get for atomic and molecular hydrogen on graphite:

$$C_3^{\text{vid}}(\text{H-gr}) = (0.397 \pm 0.006) \text{ meV nm}^3;$$

$$C_3^{\text{vid}}(\text{H}_2\text{-gr}) = (0.55 \pm 0.03) \text{ meV nm}^3,$$

whereas from our rule one has

$$C_3^{\text{rule}}(\text{H-gr}) = (0.43 \pm 0.01) \text{ meV nm}^3;$$

$$C_3^{\text{rule}}(\text{H}_2\text{-gr}) = (0.52 \pm 0.02) \text{ meV nm}^3.$$

TABLE IV. Static electric polarizabilities  $\alpha$  and optical dielectric constants  $\epsilon$  together with the values of  $\alpha(\epsilon-1)/(\epsilon+1)$  calculated with these  $\alpha$  and  $\epsilon$  for different gas-surface systems.

Crystal ↓	Gas → $\epsilon$	H	He	H <sub>2</sub>	Ne	Ar	Kr	Xe
		$\alpha^a/10^{-25} \text{ cm}^3$ 6.7 <sup>b</sup>	2.1 <sup>b</sup>	8.1 <sup>c</sup>	3.96 <sup>b</sup>	16.5 <sup>b</sup>	24.9 <sup>b</sup>	40.6 <sup>b</sup>
LiF	1.92 <sup>d</sup>	2.11	0.66	2.55	1.25	5.20	7.85	12.79
NaF	1.74 <sup>d</sup>	1.81	0.57	2.19	1.07	4.46	6.72	10.96
NaCl	2.25 <sup>d</sup>	2.58	0.81	3.12	1.52	6.35	9.58	15.62
KCl	2.13 <sup>d</sup>	2.42	0.76	2.92	1.43	5.96	8.99	14.66
RbCl	2.19 <sup>d</sup>	2.50	0.78	3.02	1.48	6.16	9.29	15.15
NiO	4.7 <sup>e</sup>	4.35	1.36	5.26	2.57	10.71	16.16	26.35
MnO	4.7 <sup>e</sup>	4.35	1.36	5.26	2.57	10.71	16.16	26.35
MgO	2.95 <sup>f</sup>	3.31	1.04	4.00	1.95	8.15	12.29	20.04
Graphite	3.9 <sup>g</sup>	3.97	1.24	4.79	2.34	9.77	14.74	24.03

<sup>a</sup> The electric polarizabilities here and in the following are given in cgs units, since these units are used in most tables,  $\alpha$  in SI units is achieved by multiplying the values given here by  $1.11 \times 10^{-16}$  As  $\text{m}^2/\text{V cm}^3$ .  
<sup>b</sup> Static electric polarizabilities  $\alpha$  from Tang, Norbeck, and Certain (1976) and references given there.  
<sup>c</sup> Average polarizability  $\alpha = (1/3)(\alpha_{\parallel} + 2\alpha_{\perp})$  from Landolt-Börnstein (1951a).  
<sup>d</sup> Optical dielectric constants  $\epsilon(\lambda \approx 500 \text{ nm})$  from Landolt-Börnstein (1951b)  
<sup>e</sup>  $\epsilon$  from *CRC Handbook of Chemistry and Physics* (Weast, 1974).  
<sup>f</sup>  $\epsilon$  from Kittel (1969).  
<sup>g</sup> Effective dielectric constant for graphite constructed somewhat arbitrarily by  $\epsilon_{\text{eff}} = (\text{Re } \epsilon_x + \epsilon_z)/2$  proved to be working well for representing graphite in the  $C_3$  or  $D$  rule [ $\epsilon_x = 5.6 + i 7.0$  and  $\epsilon_z = 2.25$  calculated from optical constants at 2.5 eV given by Greenaway *et al.* (1969)].

This shows that the values from our rule and those calculated by Vidali *et al.* differ by a few percent only. The reason for the difference between the experimental and theoretical values of  $C_3$  may be caused by the fact that even with the weakest bound levels observed in selective adsorption, still a region of the attractive potential is probed which is too near to the potential minimum to be well described by the asymptotic long-range behavior of pure polarization attraction. A more decisive answer to the question of whether there is some fundamental effect causing the observed difference could

be given by confirming or rejecting the existence of the additional levels expected from theory near the dissociation limit. If these levels could be observed in experiments with higher resolution the uncertainty in the experimental values of  $C_3$  could be diminished, for until now in most cases the theoretical values lie within relatively large experimental error bars.

c. Construction of  $v_{00}(z)$  with RKR method

Assuming the asymptotic form of the potential to be known by  $v_{00}^{\text{as}}(z) = -C_3/z^3$ , Schwartz, Cole, and Pliva (1978) proposed a procedure based on RKR method of constructing  $v_{00}(z)$  from the spectrum  $\{E_j\}$ . The first step is getting the function  $\eta(E)$  defined in Eq. (3.28) by interpolating between the experimental values of  $E_j$  at which  $j(E_j)$  takes the values  $j = 0, 1, 2, \dots$ . In doing this interpolation account is also taken of the fact that the potential is nearly harmonic at the bottom of the well so that  $\eta(E)$  should vary with  $E$  linearly there. The second step is calculating the width of the potential well as a function of energy  $E$  from Eq. (3.27). The third step is combining the well width with the known asymptotic form; that means setting in the asymptotic region the outer turning point  $z_2$  to

$$z_2 = (C_3/|E|)^{1/3},$$

where Schartz, Cole, and Pliva (1978) used the values of  $C_3$ <sup>1</sup> calculated by Bruch and Watanabe (1977). For the construction of the complete potential curve a graphical procedure is applied which uses again the fact that  $v_{00}(z)$  is harmonic near the equilibrium position  $z_e$ . But there remains a small ambiguity in the shape resulting from

<sup>1</sup>The values of  $C_3$  for H-LiF, H-NaF, and He-LiF used by Schwartz *et al.* deviate somewhat from those given by Bruch and Watanabe:  $C_3$  (Schwartz)  $\approx (3,5/4)C_3$  (Bruch, Watanabe); only the value for He-NaF is the same in both papers.

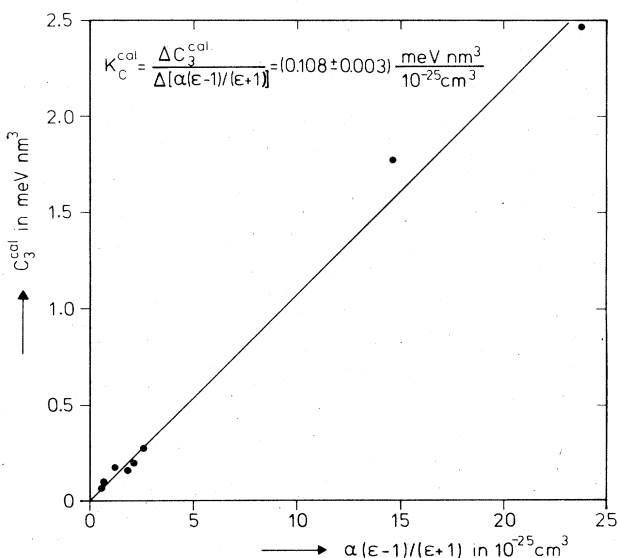


FIG. 13. Constant of attractive dispersion interaction  $C_3$  as calculated by Bruch and Watanabe (1977) plotted in the same manner as Fig. 12.

different ways of connecting the repulsive and the attractive part of the potential in this graphical interpolation. The resulting form of the potential curves for H, D-LiF and H, D-NaF are shown in Figs. 14 and 15, respectively, together with (9-3) and shifted Morse hybrid potential curves determined from fitting binding energies (see next section and Appendix C).

#### d. Model potentials used for $v_{00}(z)$

The method most frequently used to overcome the inversion problem in determining  $v_{00}(z)$  from the spectrum of binding energies  $\{E_j\}$  is to choose some appropriate model potential with two or more free parameters, and to determine these parameters by fitting the energy levels of the assumed potential to the experimental  $\{E_j\}$  spectrum. A review of the different types of model potentials used in this connection is given in Appendix C.

A form frequently used since the first calculations by Lennard-Jones and Devonshire (1937) is the Morse potential (Appendix C.1). Although it does not have the correct long-range asymptotic form, it works well for describing the experimental values of  $E_j$ , at least for the stronger bound levels. This is clearly demonstrated in Fig. 16 for H, D on LiF and NaF (Finzel *et al.*,

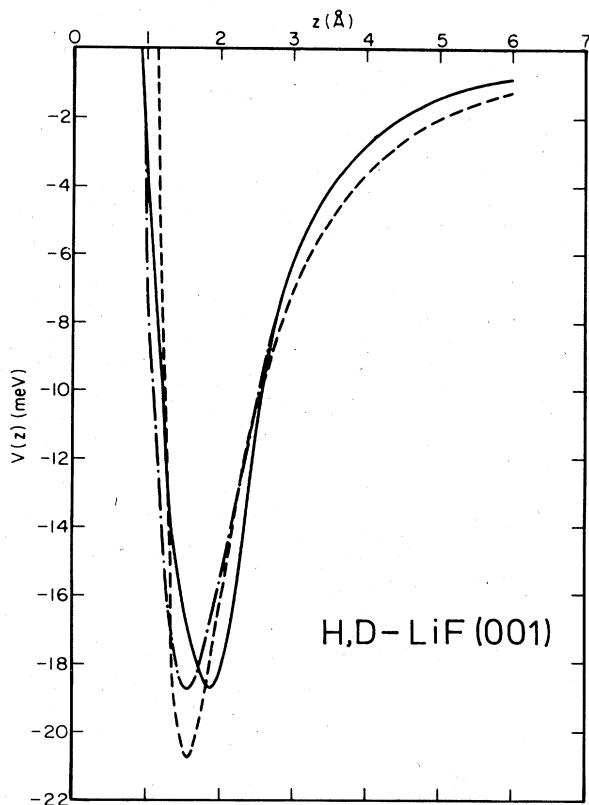


FIG. 14. Interaction potential curves  $v_{00}(z)$  for H or D on LiF (001) constructed from experimental binding energies (Finzel *et al.*, 1975) by: RKR procedure (full curve); fitting a (9-3) model potential (---); and fitting a shifted Morse hybrid model potential (-.-) [after Schwartz, Cole, and Pliva (1978)].

1975). Two other examples of potential forms which were also used in order to fit experimental binding energies are the (9-3) and the "shifted Morse hybrid potential" (Appendix C.3 and 5). In Figs. 14 and 15 the potential curves for H, D on LiF and NaF resulting from these model potentials are compared to the potential curves constructed with the RKR method by Schwartz, Cole, and Pliva (1978).

#### e. Potential parameters from fitting $\{E_j\}$ spectra

A detailed survey of the potential parameters obtained for the different potential forms from fitting experimental binding energies  $\{E_j\}$  is given in Appendix C in Table IX. An essential aspect which can be seen from this table is that the resultant parameters vary appreciably with the model potential used, especially the highest and lowest values obtained for the potential well depth  $D$ , which differ by up to 20%. But this is not surprising considering the arguments given above about the uniqueness of a potential curve as determined from  $\{E_j\}$ . Very different potential forms chosen from different points of view may force certain parameters to rather different values. The (9-3) potential, for instance, with steep sides and a strong curvature near the minimum, becomes relatively deep and narrow, whereas the more moderate curved Morse potential gets a much smaller depth.

The values of  $C_3$  in Table IX determined from  $D$  and  $\sigma$  of the (9-3) potential, are appreciably larger than

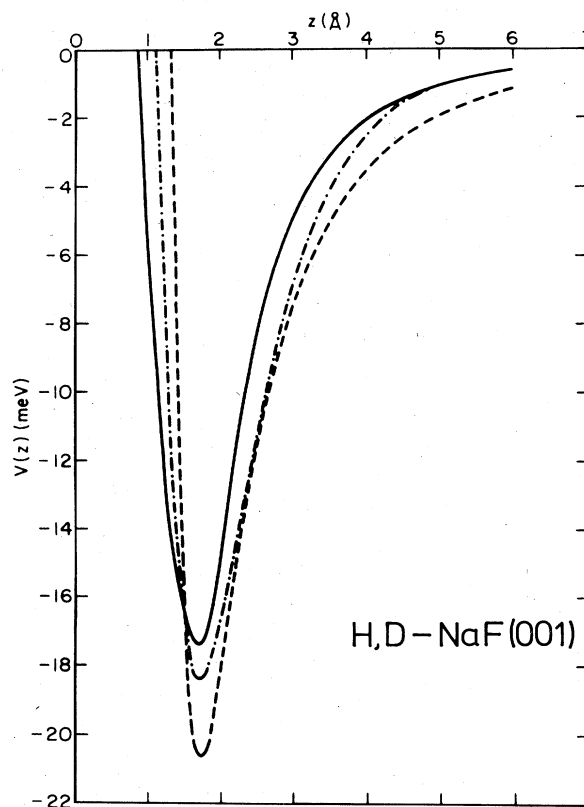


FIG. 15. The same as Fig. 14 but for H, D on NaF (001).

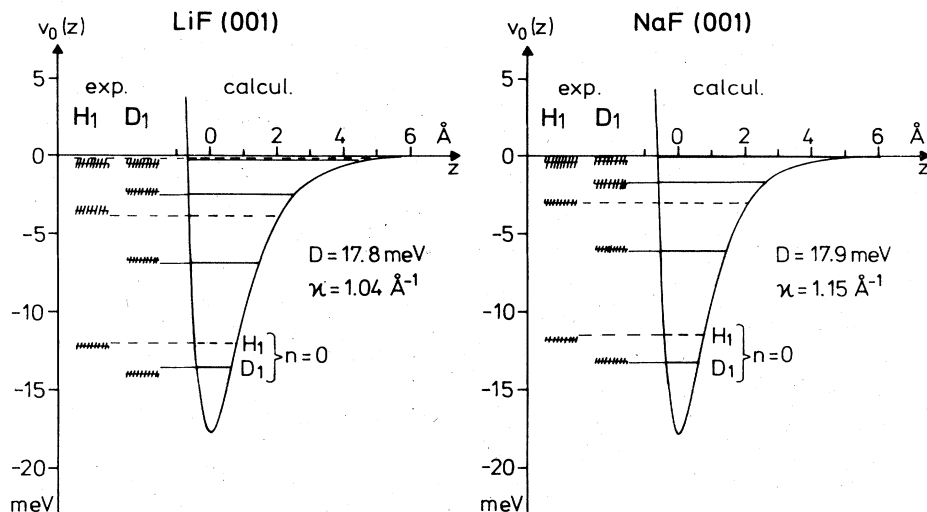


FIG. 16. Gas-surface Morse potentials ( $D$  = well depth and  $\kappa$  = reciprocal range parameter) for the systems H, D-LiF(001) and H, D-NaF(001); experimental and calculated binding energies are compared [from Finzel *et al.* (1975)].

those calculated by Bruch and Watanabe (1977) and those evaluated according to the method of Le Roy (1976) (see Table III). The reason for this is that  $D$  and  $\sigma$  are determined mainly in order to fit  $E_j$  values of states deep in the potential well and it cannot be expected that they then reproduce the correct asymptotic behavior of the potential too. Comparisons of different potential forms have been also given by Tsuchida (1975) and by Schartz, Cole, and Pliva (1978). Tsuchida compared the applicability of Morse, (12-3), and zeta potentials for He-LiF (001). Schwartz *et al.* constructed and discussed potentials from the RKR method and of the shifted Morse hybrid and (9-3) form for H, D on LiF and NaF and for  $^3\text{He}$ ,  $^4\text{He}$  on LiF, and NaF. Very recently Goodman, Garcia, and Celli (1979) gave a comparison of the shifted Morse hybrid and the flat-bottom hard-wall potential and discussed also the values of  $C_3$  determined by different methods. Comparing the quality of the fit to binding energies within the different model potentials, the "shifted Morse hybrid potential" (SMH, see Appendix C.5) turns out to be one of the most appropriate ones. It also has a realistic form with the correct asymptotic behavior and fits well to the potential curve constructed with the RKR method. So the SMH form and the curve constructed with the RKR method may be regarded as giving the best representation of the potential well  $v_{00}(z)$ .

4. Semiempirical rule for the potential well depth

In the following a rule will be established, which allows us to get approximative values of the potential well depth  $D$  in physical gas-surface interaction. This rule is an extension of an empirical rule proposed previously (Hoinkes, Nahr, and Wilsch, 1972b) which related the well depth of an arbitrary gas atom interacting with LiF (001) to the electric polarizability of the atom. Now various crystals characterized by the optical dielectric constant  $\epsilon$  will be included in the new rule.

A qualitative derivation of a potential well depth rule

can be given by starting with the rule for  $C_3$  developed above. Approximating the gas-surface interaction by a hard repulsive wall at  $z_w$  and an attractive part of  $v_a(z) = -C_3(z - z_0)^{-3}$  we get a potential of the form as shown in Fig. 17. The gas atom approaches the crystal surface up to the hard wall at a distance  $z_w$  measured from the first surface layer, and this distance of closest approach is given by the sum of the radii of the surface particle  $r_s$  and the gas atom  $r_g$ . Since we are dealing with the lateral average of the gas-surface interaction we may use an average value for the radius of the surface particles given by half the layer distance  $d/2$ . So we get for  $z_w$

$$z_w = r_s + r_g = d/2 + r_g. \tag{3.33}$$

Putting this value of closest approach into the attractive potential  $v_a(z)$  one gets for the well depth in our model

$$D = C_3(d/2 + r_g - z_0)^{-3}. \tag{3.34}$$

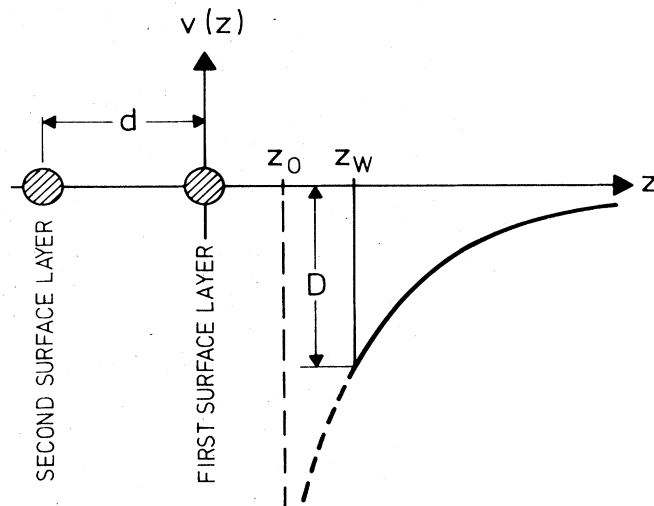


FIG. 17. Approximative representation of the gas-surface interaction potential by a repulsive hard wall at  $z_w$  and a  $z^{-3}$ -attractive term counted from  $z_0$ .

We now need the value of  $z_0$ , the coordinate of the plane parallel to the surface from which the attraction has to be counted. This problem was recently discussed by Zaremba and Kohn (1976), with the result that for dielectric solids as regarded here  $z_0$  is well approximated by half a lattice distance

$$z_0 = d/2. \tag{3.35}$$

So we finally get for the well depth

$$D = C_3 r_g^{-3}. \tag{3.36}$$

This means as long as the radius of the gas particles  $r_g$  can be assumed to differ only weakly for different particles, and this is the case at least for H, He, and  $H_2$ , we get

$$D \propto C_3. \tag{3.37}$$

So we finally have for  $D$  a rule corresponding to that for  $C_3$  [see Eq. (3.32)]:

$$D = K_D \alpha(\epsilon - 1)/(\epsilon + 1). \tag{3.38}$$

This relation developed here resembles approximately one of the relations recently discussed by Rogowska (1978) for potentials achieved from pairwise summation (see Appendix A.2).

In order to test this  $D$  rule given above, the well depths  $D$  of all the systems investigated experimentally by selective adsorption are plotted as a function of  $\alpha(\epsilon - 1)/(\epsilon + 1)$  in Fig. 18. Since the value of  $D$  evaluated from the  $\{E_j\}$  spectrum depends on the model potential used, in Fig. 18 two  $D$  values, determined from two extreme models, the Morse and the (9-3) form, are shown. In both cases  $D$  was evaluated from the two deepest energy levels  $E_0$  and  $E_1$  using the corresponding formulas (C2) and (C6). The resultant values  $D^M$  and  $D^{9-3}$  are summarized in Table V.

Figure 19 demonstrates indeed in good approximation a linear relation between the well depth  $D$  and  $\alpha(\epsilon - 1)/(\epsilon + 1)$ . Using the data plotted in Fig. 19 a least squares fit for the constant of proportionality  $K_D$  results in a mean value of

$$\bar{K}_D = (11.2 \pm 0.4) \text{ meV}/10^{-25} \text{ cm}^3.$$

In a second attempt, where only rare gases were considered and where the range of  $D$  values was expanded by also taking into account heats of adsorption for He to Kr as compiled in Table VI, the linear relation be-

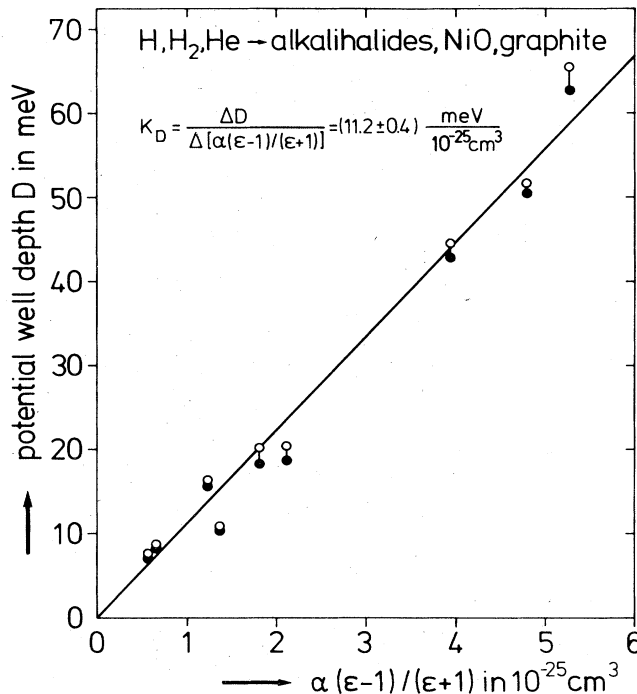


FIG. 18. Potential well depth  $D$  determined from experimental binding energies  $E_j$  as function of  $\alpha(\epsilon - 1)/(\epsilon + 1)$  with  $\alpha$  = static electric polarizability of the atom and  $\epsilon$  = optical dielectric constant of the solid. An approximative linear dependence with the constant of proportionality  $K_D$  is clearly demonstrated.

tween  $D$  and  $\alpha(\epsilon - 1)/(\epsilon + 1)$  turned out to be comparably good (see Fig. 19) with a mean value of  $K_D$

$$\bar{K}_D^{RG} = (12.6 \pm 0.5) \text{ meV}/10^{-25} \text{ cm}^3.$$

The deviations of the actual values of  $D$  from those calculated by  $D_K = \bar{K}_D \alpha(\epsilon - 1)/(\epsilon + 1)$  are in both cases for almost all systems smaller than 20% (the main deviation appears in the system He-NiO with 30%) as shown in the last columns of Tables V and VI, respectively. The mean value of these relative deviations is also quite similar in both cases with

$$\frac{1}{n} \sum_n \frac{|D_n - D_{K,n}|}{D_{K,n}} \approx 0.10.$$

So we can finally state here that for a gas-surface sys-

TABLE V. Values of the well depth  $D$  as used for plotting Fig. 18.  $D^M$  and  $D^{9-3}$  are calculated with Eqs. (C2) or (C6) with the two deepest levels  $E_0$  and  $E_1$  and then averaged over isotopes.  $D_K = K_D \alpha(\epsilon - 1)/(\epsilon + 1)$  with  $K_D = 11.2 \text{ meV}/10^{-25} \text{ cm}^3$ .

Gas	Surface	$D^M/\text{meV}$	$D^{9-3}/\text{meV}$	$\bar{D} = \frac{D^M + D^{9-3}}{2} / \text{meV}$	$D_K/\text{meV}$	$\frac{\bar{D} - D_K}{D_K} \times 100$
He	NaF (001)	6.86	7.55	7.21	6.4	13.0
He	LiF (001)	8.10	8.70	8.40	7.4	13.6
He	Graphite	15.55	16.3	15.9	13.8	15.4
He	NiO (001)	10.34	10.81	10.6	15.2	30.4
H	NaF (001)	18.3	20.2	19.3	20.3	4.8
H	LiF (001)	18.6	20.4	19.5	23.6	17.5
H	Graphite	42.9	44.5	43.7	44.0	0.7
$H_2$	Graphite	50.5	51.6	51.0	53.7	4.9
$H_2$	NiO (001)	62.7	65.5	64.1	58.9	8.8

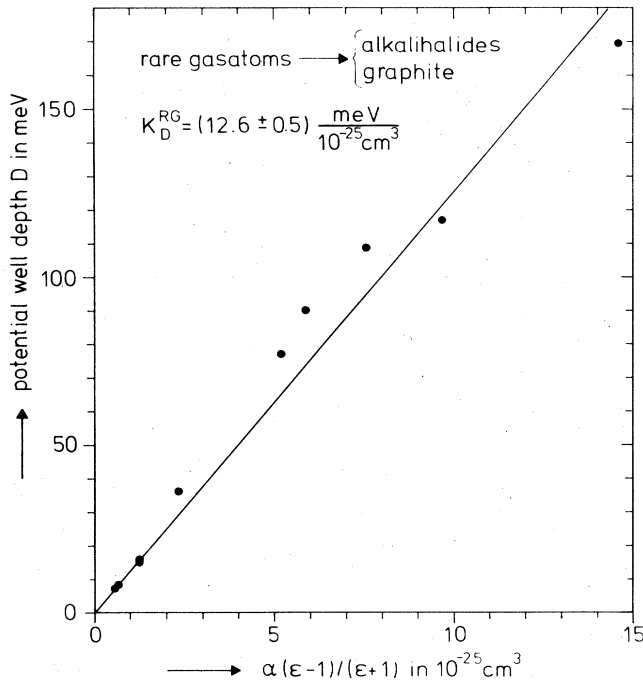


FIG. 19. The same as Fig. 18 but extended to heavier rare gases with  $D$  taken from heats of adsorption (see Table VI).

tem with van der Waals interaction the potential well depth  $D$  may be estimated from the static electric polarizability  $\alpha$  of the gas atom and the optical dielectric constant  $\epsilon$  of the solid by the  $D$  rule:

$$D = \bar{K}_D \alpha (\epsilon - 1) / (\epsilon + 1), \tag{3.39}$$

and taking an averaged value of  $\bar{K}_D = 12 \text{ meV}/10^{-25} \text{ cm}^3$  the error in the achieved value of  $D$  can be assumed to be smaller than 25%. A table with potential well depths calculated with this rule for several gas-surface systems is given in Appendix D.

TABLE VI. Potential well depths and heats of adsorption together with the values of  $\alpha(\epsilon - 1)/(\epsilon + 1)$  used for plotting Fig. 19.  $D_K$  calculated with  $K_D = 12.6 \text{ meV}/10^{-25} \text{ cm}^3$ .

Gas	Surface	$D/\text{meV}$	$\alpha \frac{\epsilon - 1}{\epsilon + 1} / 10^{-25} \text{ cm}^3$	$D_K = K_D \alpha \frac{\epsilon - 1}{\epsilon + 1}$	$\frac{ D - D_K }{D_K} \times 100$
Select. ads.					
He	NaF (001)	7.21	0.57	7.18	0.4
He	LiF (001)	8.40	0.66	8.32	1.0
He	Graphite	15.9	1.23	15.5	2.6
Heats of adsorp. (Beder, 1967)					
He	Graphite	14.8	1.23	15.5	4.5
Ne	Graphite	36.0	2.32	29.2	23.2
Ar	LiF (001)	77	5.20	65.5	17.5
Ar	KCl (001)	90	5.87	74.0	21.7
Ar	KJ (001)	109	7.56	95.3	14.4
Ar	Graphite	117	9.68	122.0	4.1
Kr	Graphite	169	14.6	184.0	8.1

<sup>a</sup> From Table IV.

### D. Results on the periodic potential terms from bound-state resonances

In Sec. III.A it was discussed that the strength of the periodic variation of the gas-surface interaction determines the distribution of the elastically scattered intensity to the different diffracted beams, and in Sec. III.B it was also shown that corrugation parameters may be extracted from the observed diffracted beam intensities within the corrugated hard-wall model. In the following a second way of getting information on the periodic structure of the gas-surface interaction will be discussed. It will be shown that the strength of the periodic terms  $v_G$  of the general expansion of the potential [see Eq. (2.1)] may be determined from bound-state resonance investigations.

#### 1. Resonance splitting for degenerate bound states

The method of determining the strength of the periodic terms discussed here is based on an effect pointed out recently by Chow and Thompson (1976). As we have seen above, at certain conditions of incidence an atom may be diffracted by a certain  $G$  vector to a bound surface state. In this state the atom is bound normal to the surface with a discrete binding energy  $E_j$  and moves parallel to the surface with a wave vector  $K_G = K + G$ . Since this two-dimensional motion parallel to the surface takes place in a periodic potential, band structure effects may occur in the energy  $E_j'$  of this motion as a function of the two-dimensional wave vector  $K_G$ . In most cases the band structure  $E_j''(K_G)$  is well approximated by the free-particle relation

$$E_j''(K_G) = (\hbar^2/2m_e)(K + G)^2. \tag{3.40}$$

Measurable deviations from this free-particle relation may occur if two bound states with  $K_{G_1}$  and  $K_{G_2}$  are energetically degenerate but differ from one another in  $K_G$  by a vector  $G_d = K_{G_1} - K_{G_2}$  which belongs to a relatively strong periodic potential term  $v_{G_d}$ . Since the two degenerate states can be bound normal to the surface in two different levels  $E_j$  and  $E_{j'}$ , in general the de-

generacy is described by the following condition

$$(\hbar^2/2m_g)(\mathbf{K} + \mathbf{G}_1)^2 - |E_j| = (\hbar^2/2m_g)(\mathbf{K} + \mathbf{G}_2)^2 - |E_{j'}| \quad (3.41)$$

The degeneracy of these two states  $\varphi_1 = \varphi(j; \mathbf{G}_1)$  and  $\varphi_2 = \varphi(j'; \mathbf{G}_2)$  is lifted because of the coupling by the periodic component  $v_{G_d}(z)$ , and two new admixed states  $\varphi_{a,b}$  are created with new energy eigenvalues  $E_{a,b} = E_{1,2} \pm \Delta E$ . The energy splitting  $2\Delta E$  of the new states depends on the strength of the periodic potential term  $v_{G_d}$ .

Now the conditions of incidence in a diffraction experiment may be chosen so that the incident beam is in resonance with such degenerate bound states as indicated by the following resonance condition:

$$E_i = (\hbar^2/2m)(\mathbf{K} + \mathbf{G}_1)^2 - |E_j| = (\hbar^2/2m_g)(\mathbf{K} + \mathbf{G}_2)^2 - |E_{j'}| \quad (3.42)$$

If in addition  $\mathbf{G}_d = \mathbf{G}_1 - \mathbf{G}_2$  belongs to a strong  $v_G$  term [terms of the type (1, 0) or (1, 1) in most gas-surface systems], the resonance minimum in the specular beam is not observed for the incidence condition determined by Eq. (3.42), but a splitting of the resonance minimum may be found. The resonance now occurs with the shifted energy eigenvalues  $E_1 + \Delta E$  and  $E_1 - \Delta E$  of the admixed states.

Minimum splitting of this kind in azimuthal plots of the specular intensity was observed first with atomic deuterium on LiF and NaF by the Erlangen group (Frank, 1973; Wonka, 1973; Hoinkes, Greiner, and Wilsch, 1977) and with He on NaF by the Pennsylvania State University group (Liva, Derry, and Frankl, 1976). An example of experimentally observed splitting for D-NaF (001) is shown in Fig. 20. There the specular intensity was measured as a function of the azimuthal angle  $\gamma$  at different incident energies  $E_i$  and the constant angle of incidence  $\theta_i = 75^\circ$ . At the point of degeneracy of the resonant bound states  $\varphi(0; 0, -1)$  and  $\varphi(0; -1, -2)$  two minima shifted from the undisturbed position are observed.

Following the ideas of Chow and Thompson (1976) we have calculated the energy of the admixed bound states and succeeded in determining the strength of the periodic coupling term  $v_{11}$  from the observed splitting (Hoinkes, Greiner, and Wilsch, 1977). From perturbation theory the energy eigenvalues of the admixed states are known to be

$$E_{a,b} = 1/2 \{ E(0; 0, -1) + E(0; -1, -2) \pm [(E(0; 0, -1) - E(0; -1, -2))^2 + 4H_{12}^2]^{1/2} \} \quad (3.43)$$

showing that at the point of degeneracy where  $E(0; 0, -1) = E(0; -1, -2)$  the energy splitting between the mixed states is given by

$$\Delta E_{a,b} = E_a - E_b = 2H_{12} = 2 \langle 0; 0, -1 | v_{11}(z) \exp(i\mathbf{G}_{11} \cdot \mathbf{R}) | 0; -1, -2 \rangle \quad (3.44)$$

Thus by transferring the observed  $\gamma$  splitting to an energy splitting the corresponding matrix element may be

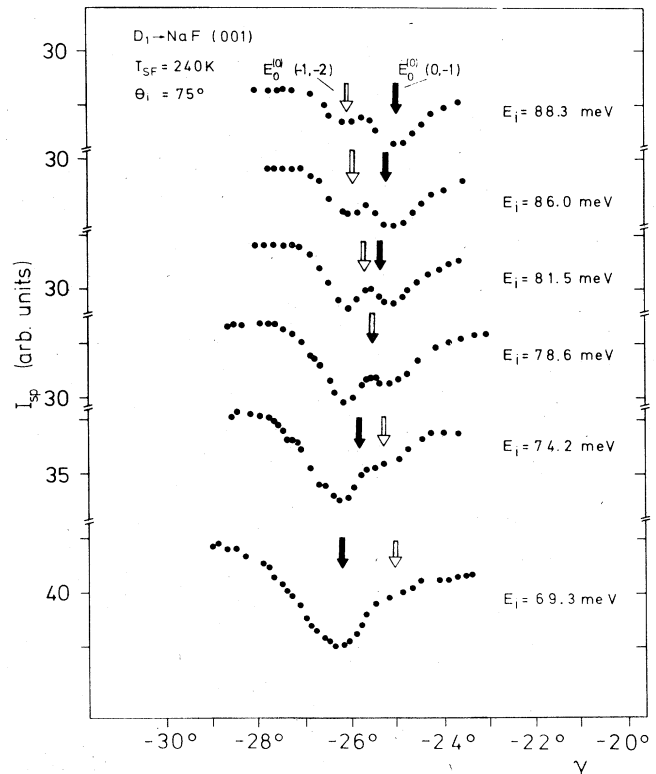


FIG. 20. Splitting of bound-state resonance minima in azimuthal plots of the specular intensity of atomic deuterium scattered from NaF (001), measured at different incident energies  $E_i$ . The contributing bound states are indicated by arrows.

determined from experiment. We find from the minimum splitting shown in Fig. 20:

$$\langle 0; 0, -1 | v_{11}(z) \exp(i\mathbf{G}_{11} \cdot \mathbf{R}) | 0; -1, -2 \rangle_{\text{exp}} = 0.48 \text{ meV}.$$

Further, by comparing this experimental matrix element with the matrix element calculated with the eigenfunctions of  $v_{00}(z)$  and an appropriate form of  $v_{11}(z)$  the strength  $\beta_{11}$  of  $v_{11}(z)$  can be evaluated. We have done this in an approximative way by taking harmonic oscillator wave functions for the  $z$  motion in the  $j=0$  state with  $\omega = 2(D - |E_0|)/\hbar$  and by using for the form of  $v_{11}(z)$  the repulsive part of the known Morse potential multiplied by the strength factor  $\beta_{11}$

$$v_{11}(z) = \beta_{11} D \exp(-2\kappa z).$$

So we get for the matrix element

$$H_{12} = \beta_{11} D \exp(\kappa^2 \hbar / m_g \omega) \quad (3.45)$$

The only unknown parameter is  $\beta_{11}$ , which finally results from comparison with experiment to be

$$\beta_{11}(\text{H-NaF}) = 0.02.$$

Figure 21 demonstrates that the observed splitting is well described by curves of resonance angles calculated with the energy eigenvalues of the mixed states  $E_{a,b}$  as given in Eq. (3.43) using  $\beta_{11} = 0.02$ .

It should be pointed out here also that the resonance minimum produced by the relative high-order G vector

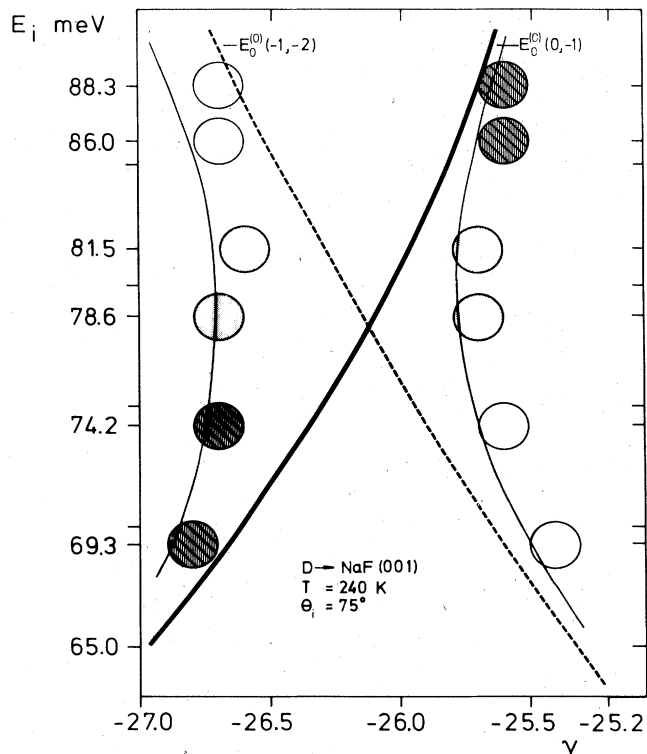


FIG. 21. Calculated dependence of incident energy  $E_i$  on azimuthal angle  $\gamma$  under bound-state resonance conditions for independent bound channels (crossing lines) and for admixed bound channels with  $\beta_{11}=0.02$ . The disks represent the experimentally observed angles of resonance minima (the darkness indicates the depth of the minimum).

$(-1, -2)$  is only observed near the point of degeneracy with the strong resonance produced by  $G = (0, -1)$ . This change in strength of the resonance is demonstrated in Fig. 21 by the varying darkness of the disks.

More detailed theoretical investigations concerning this splitting in D-NaF and also concerning a more complicated structure of interacting bound states observed with D-LiF (see Fig. 22) were carried out recently by Garcia-Sanz and Garcia (1979). In calculations based on the theory of Cabrera *et al.* (1970) with a Morse potential (parameters as given in Table IX) and the two periodic terms  $v_{10}$  and  $v_{11}$  they determined the two-dimensional band structure in the region of degeneracy. The results are given in Fig. 23 for D-NaF and in Fig. 24 for D-LiF. The calculated curves represent the bound-state energy  $E(j, K+G)$  as function of the azimuthal angle  $\gamma$  at constant incident surface vector  $K$ .

Figure 23a shows the degeneracy of the bound states  $(0; 0, -1)$  and  $(0; -1, -2)$  in free band approximation ( $\beta_{10}=\beta_{11}=0$ ) at  $\gamma=26.1^\circ$ , where both states are also in resonance with the incident beam  $E(0; 0, -1)=E(0; -1, -2)=E_i$ . And from Fig. 23(b)–(d) it is clearly seen that only  $\beta_{11}>0$  causes a splitting, whereas  $\beta_{10}$  has practically no influence on the band structure in this region. As a final result a value of  $\beta_{11}=0.03$  may be extracted leading to resonance angles of  $25.5^\circ$  and  $26.7^\circ$  which compare well with the experimental ones.

The more complicated structure observed with D-LiF around the  $(0; 0, 1)$  resonance is shown in Fig. 22. The simple two-band perturbation theory seemed not to be suited to extract  $\beta$  values from the splitting. But the band structure calculations by Garcia-Sanz and Garcia again result in energy splittings which compare well to experiment when reasonable values of  $\beta_{10}$  and  $\beta_{11}$  are used. Figure 24(a)–(c) shows the free bands at three different incident energies  $E_i=21.7, 22.0,$  and  $22.3$  meV, where in case (c) the three bound states  $(0; 0, 1)$ ,  $(3; -1, 1)$ , and  $(3; 0, -2)$  are degenerate and simultaneously in resonance with the incident beam at  $\gamma=27.2^\circ$ . The band structure with  $\beta_{10}=0.055$  and  $\beta_{11}=0.027$  is given in Fig. 24(d)–(f) showing a splitting in the resonance angles of  $\Delta\gamma_{\text{calc}}\approx 0.8^\circ$ , which compares rather well to an experimental value of  $\Delta\gamma_{\text{exp}}\approx 1^\circ$ . So for the gas-surface systems discussed here we get from resonance splitting the following  $\beta_G$  values:

$$\beta_{10}(\text{H-LiF}) = 2\beta_{11}(\text{H-LiF}) \geq 0.055,$$

$$\beta_{11}(\text{H-NaF}) = 0.02-0.03.$$

These values can be compared with approximative  $\beta_G$  values determined previously (Finzel *et al.*, 1975) with different methods:

(i) The interaction potential for H-LiF (001) was calculated by pairwise potential summation (see Sec. II.B.2) and the resulting potential function  $v(r)$  was then fitted by the expansion given in Eq. (2.1) taking  $v_G$  terms up to the order  $(1, 1)$ . For the form of the higher-order terms  $[G \neq (0, 0)]$  again  $v_G(z) = \beta_G D \exp(-2\kappa z)$  was assumed. The  $\beta_G$  values resulting from this procedure were

$$\beta_{10}(\text{H-LiF}) \approx 0.055; \quad \beta_{11}(\text{H-LiF}) \approx 0.027.$$

(ii) A second way to get information on  $\beta_G$  values was comparing experimental diffraction intensities in the  $(1, 0)$  and  $(1, 1)$  beams with intensities calculated in first order distorted wave Born approximation (FODWBA) with formulas given by Cabrera *et al.* (1970). Here we obtained:

$$\beta_{10}(\text{H-LiF}) = 0.017; \quad \beta_{11}(\text{H-LiF}) \approx \beta_{10}/2$$

$$\beta_{10}(\text{H-NaF}) = 0.015; \quad \beta_{11}(\text{H-NaF}) = 0.010.$$

(iii) Finally, we have compared the experimentally observed dependence of the specular intensity on the angle of incidence with calculations according to the theory by Cabrera *et al.* (1970). With the assumption  $\beta_{11}=0$  we have extracted in this case:

$$\beta_{10}(\text{H-LiF}) = 0.035-0.040.$$

In the case (i) the calculated  $\beta_G$  values represent the strength of the periodic terms in the whole  $z$  region and may well be compared with the values obtained from resonance splitting, which represents the periodic structure in the potential well. The situation is different in the cases (ii) and (iii); there the  $\beta_G$  values result from the periodic structure at positive energies normal to the surface. But because of the approximative character of these values no decisive conclusions on the energy dependence of the periodic terms can be drawn from our results. Garcia-Sanz and Garcia (1979) could also explain resonance splittings observed by Liva,

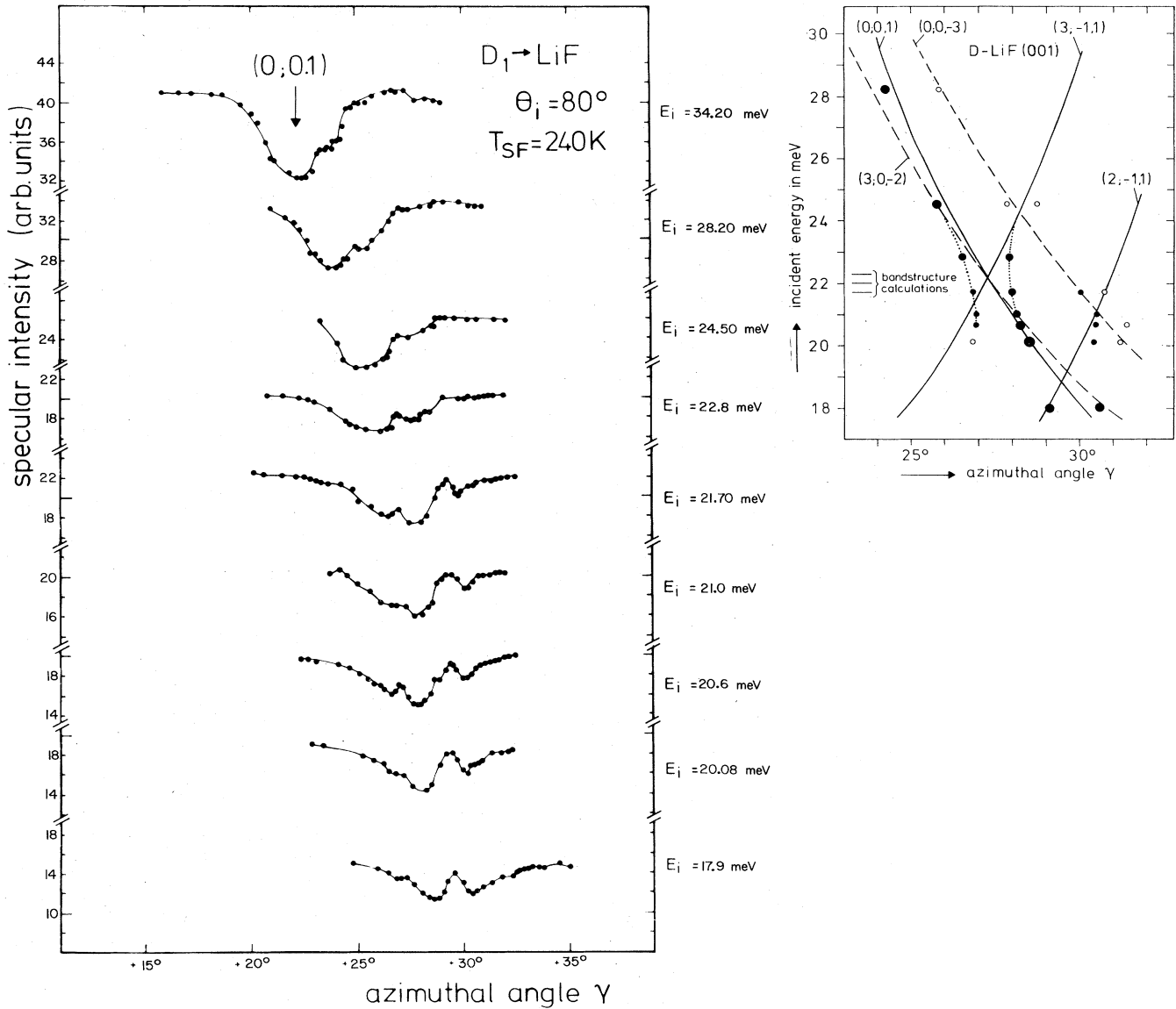


FIG. 22. Splitting of bound-state resonance minima for atomic deuterium scattered from LiF(001). (a) Azimuthal plots of specular intensity measured around the (0; 0,1) resonance at different incident energies  $E_i$ . (b) Calculated dependence of incident energy  $E_i$  on azimuthal angle  $\gamma$  under bound-state resonance conditions for independent resonances  $(j; m, n)$ ; position and increasing strength of observed minima indicated by points with increasing cross section.

Derry, and Frankl (1976) for He-NaF(001). With band structure calculations for this system they got

$$\beta_{10}(\text{He-NaF}) = 0.05; \quad \beta_{11}(\text{He-NaF}) = 0.02.$$

Very recently Boato *et al.* (1979a, 1979b) have done detailed experimental resonance investigations for He on graphite. They observed several crossings of resonances and found out that practically only the first Fourier component  $v_{10}$  is contributing to the periodic part of the potential. Using perturbation calculations of the kind we had shown to work well with D-NaF (Hoinkes, Greiner, and Wilsch, 1977), as discussed above, they determined from the observed splittings matrix elements of the type  $\langle \varphi_j | v_{10} | \varphi_{j'} \rangle$  and used these to get more insight in the complete form of the gas-surface in-

teraction potential for He graphite. Following the variable exponent potential form (see Appendix C.7) for  $v_{00}(z)$ , Boato *et al.* (1979b) chose as a representation of the first Fourier component of the potential

$$v_{10}(z) = -\beta D(1 + \lambda z/p)^{-\alpha p}, \tag{3.46}$$

where the parameters  $D = 15.70$  meV,  $\lambda = 1.413 \text{ \AA}$ , and  $p = 5.3$  are known from fitting experimental binding energies. Calculating the matrix elements  $\langle \varphi_j | v_{10} | \varphi_{j'} \rangle$  with  $\varphi_j$  and  $\varphi_{j'}$  being wave functions evaluated from  $v_{00}^{VE}(z)$  with parameters given above, they got best fits with  $\alpha = 3$  and  $\beta = 0.019$ . The fit is not so good with the less steep repulsion given by  $\alpha = 2$  which would represent the repulsive form of  $v_{00}^{VE}(z)$ ; also, the repulsive term of an appropriate Morse potential is not steep enough to get a

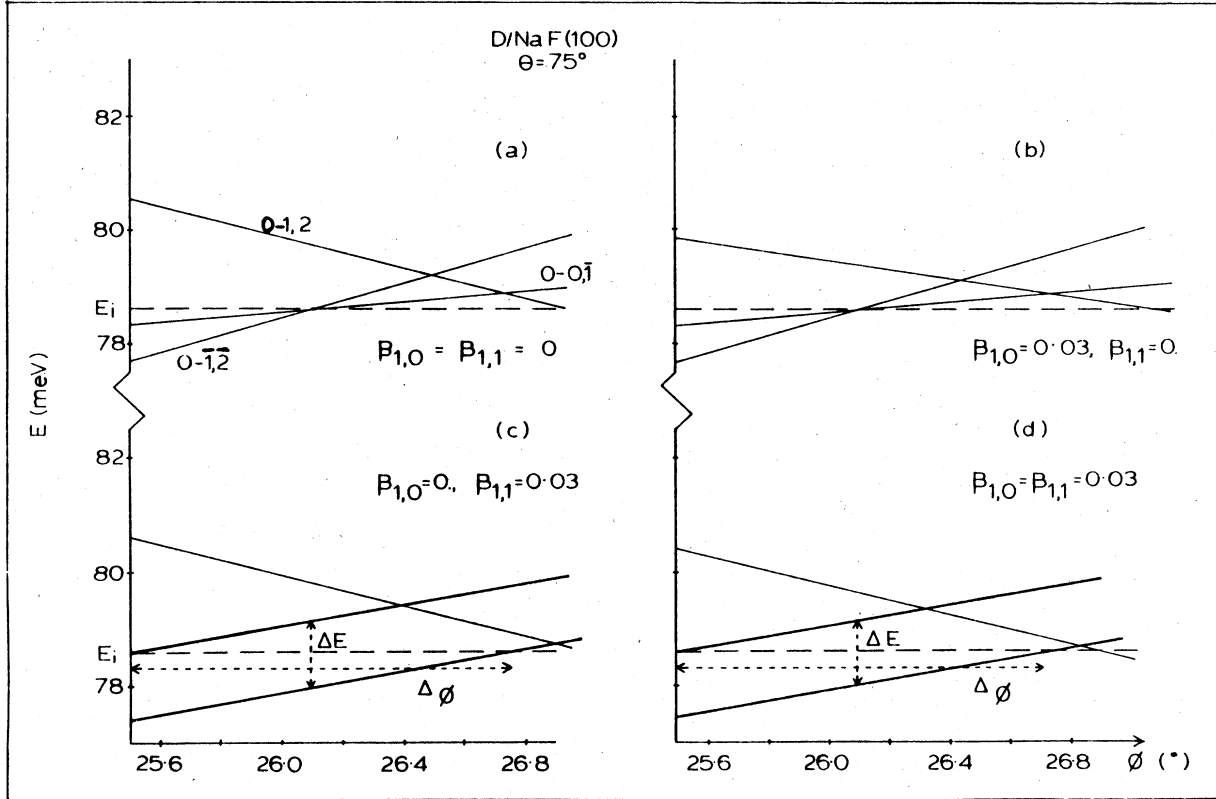


FIG. 23. Calculated band structure for D-NaF(001) representing the bound-state energy  $E(j; m, n)$  as function of the azimuthal angle  $\phi$  at constant incident surface component  $K = k_i \sin \theta_i$  of the wave vector ( $E_i = 78.6$  meV;  $\theta_i = 75^\circ$ ). (a) Free bands; (b) shows that influence of  $v_{10}(z)$  is practically zero; (c) splitting due to  $v_{11}(z)$ , and (d) from  $v_{10}(z)$  and  $v_{11}(z)$  together the same splitting results as from  $v_{11}(z)$  only [from Garcia-Sanz and Garcia (1979)].

good fit of the matrix elements. So resonance splitting delivers not only information on the strength of the periodic potential terms but also on the  $z$  dependence of the periodic terms in the region of the well.

Calculations of band structure effects by Chow (1979) and of matrix elements  $\langle \varphi_j | v_G | \varphi_j \rangle$  by Carlos and Cole (1978) done in advance of these recent experiment by Boato *et al.* (1979b) agree only qualitatively with experiment. This shows that the expressions for the He-graphite potential gained from pairwise summation are only of approximative character. In very recent calculations, however, Carlos and Cole (1979) showed the agreement between calculated and experimentally determined matrix elements is strongly improved if an anisotropic He-C pair interaction is assumed in the pairwise summation. On the other hand, Hutchison and Celli (1980) showed that they get good agreement between theoretical and experimental matrix elements in calculations with the flat-bottom corrugated hard-wall potential (see Appendix C.8) if they include additionally a weak periodic variation of the depth of the flat bottom.

## 2. Results from comparison of calculated and experimental resonance structure in diffracted beams

In the last few years the elastic gas-surface diffraction theory has developed to a state where not only over-all diffracted beam intensities out of resonances can be

described, but where also the experimentally observed resonance structure can be reproduced quite well. This was demonstrated clearly with calculations by Harvie and Weare (1978) and in more detail by Garcia, Celli, and Goodman (1979) for He on LiF(001). Their calculated curves describe almost quantitatively all the features seen in the detailed resonance structure measurements by Frankl *et al.* (1978) at relatively low incident energy ( $k_i \approx 60$  nm<sup>-1</sup>).

Using for the interaction potential the flat-bottom corrugated hard-wall model (FBHW) as described in Appendix C.8, Garcia *et al.* achieved this good agreement between theory and experiment with the following potential parameters:

(a) the well parameters determined from fitting the binding energies  $\{E_j\}$

$$D = 8.0 \text{ meV}, \quad \alpha = 14.1 \text{ nm}^{-1}, \quad \text{and} \quad \beta = 10.4 \text{ nm}^{-1}$$

(b) the corrugation function

$$\xi(\mathbf{R}) = \left(\frac{1}{2}\right) \xi_1 [\cos(2\pi x/l) + \cos(2\pi y/l)] + \xi_2 \cos(2\pi x/l) \cos(2\pi y/l), \quad (3.47)$$

with  $\xi_1 = 0.0307$  nm and  $\xi_2 = 0.0017$  nm, as known from hard corrugated model calculations at higher incident energies ( $k_i \approx 110$  nm<sup>-1</sup>) (Garcia, 1976).

So we see that at least in the case of He-LiF this some-

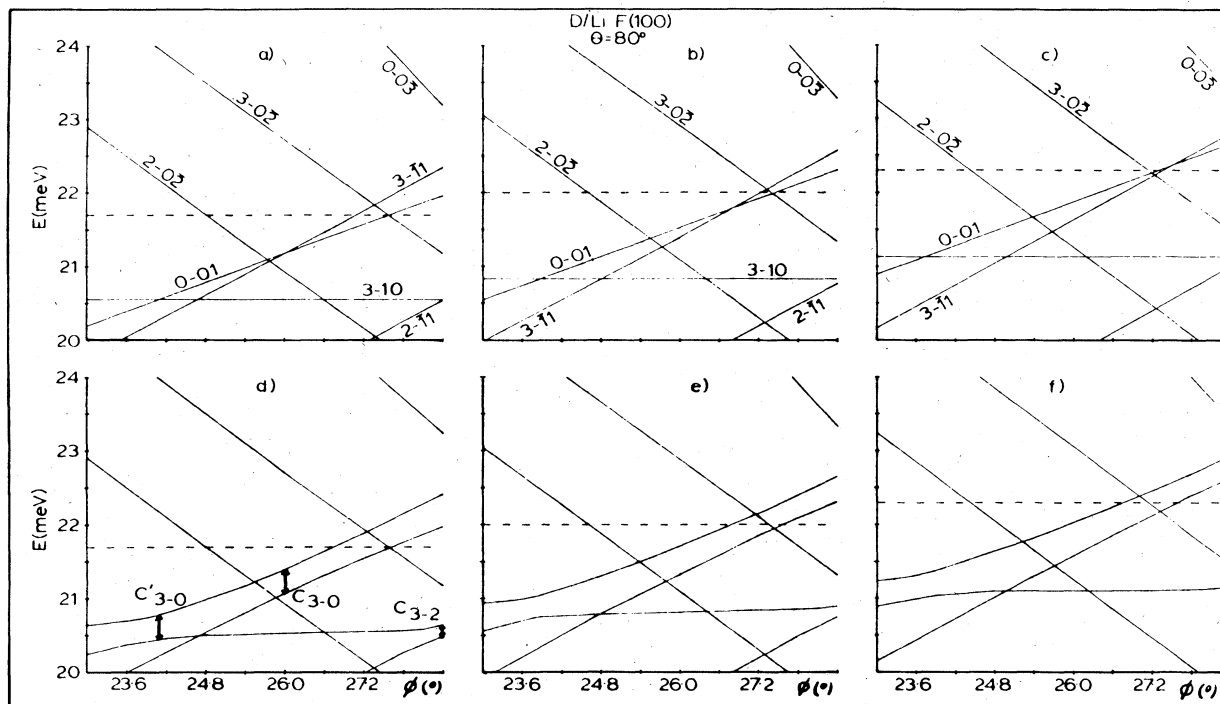


FIG. 24. Calculated band structure for D-LiF(100) representing the bound-state energy  $E(j; m, n)$  as function of the azimuthal angle  $\phi$  at constant angle of incidence ( $\theta_i = 80^\circ$ ) and at three incident energies  $E_i = 21.7; 22.0; 22.3$  meV. (a)–(c) Free bands:  $\beta_{10} = \beta_{11} = 0$ ; (d)–(e) splittings from interacting bands with  $\beta_{10} = 0.055, \beta_{11} = 0.027$  [from Garcia-Sanz and Garcia (1979)].

what approximative model potential with the hard corrugated wall and the flat bottom works quite well to describe the scattering behavior, even if this is strongly controlled by bound state resonances. Concerning the gas-surface potential, however, no further information is achieved from this detailed comparison of experimental and theoretical resonance structure since the parameters of the model potential used were already known from bound-state levels and from diffracted beam intensities observed out of resonance at higher incident energies. Some additional information concerning the question whether the periodic structure near the bottom of the potential well is really well described by the FBHW potential could perhaps be obtained from band structure splittings which seem to exist in the experimental data but are not investigated in detail by Garcia *et al.*

### 3. Relation between the periodic structure parameters $\xi_G$ and $\beta_G$

We have now seen that there are two essentially different methods for studying the periodic structure of the gas-surface interaction potential by atomic beam diffraction experiments. There is first the possibility of describing the experimentally observed distribution of scattered intensity to the different diffracted beams. This is usually done with the corrugated hard-wall model by fitting the corrugation parameters  $\xi_G$  (see Sec. III.B). The second way to get information on the periodic structure of the gas-surface interaction potential is to investigate splittings in the resonance structure of degenerate

bound states. In this case the strength of the periodic terms  $v_G(z)$  of a Fourier expansion [Eq. (2.1)] of the gas-surface potential may be determined. Since these Fourier coefficients are usually represented by

$$v_G(z) = \beta_G D f_r(z), \quad (3.48)$$

where  $f_r(z)$  gives the repulsive form of the assumed model potential the final result of such investigations are certain values of  $\beta_G$  which of course depend on the form of  $f_r(z)$  used.

These two methods mentioned above can be considered to contribute information on the periodic structure of the potential in two different regions; while the observed splitting results from the structure in the region of the well, the distribution of intensity to different diffracted beams is mainly determined by the repulsive part in the region of  $v_{00} > 0$ .

Looking more closely at these two representations of the potential (i.e., the hard wall with the corrugation parameters  $\xi_G$  and the softer potential with Fourier coefficients characterized by  $\beta_G$  values), the problem is how to correlate the parameters  $\xi_G$  with  $\beta_G$ . To get a relation between these two different representations it is reasonable to assume that the form of the hard wall is given by  $z_0(x, y)$ , the  $z$  coordinate at which the incident energy normal to the surface  $E_{i,n}$  equals the potential energy  $v(x, y, z)$ . In other words  $z_0(x, y)$  is given by the turning points of the incident atoms. To give an example of a transformation  $\xi_G \rightarrow \beta_G$  we represent  $v(x, y, z)$  by a Morse potential and corresponding periodic terms up to order (1, 1) and get:

$$v(x, y, z_0) = D \exp[-2\kappa(z_0 - z_m)] \{ [1 - 2 \exp\kappa(z_0 - z_m)] + 2\beta_{10}(\cos gx + \cos gy) + 4\beta_{11} \cos gx \cos gy \} = E_{i,n}, \quad (3.49)$$

and we have to compare it with the corrugation of the hard wall expanded to the same order

$$\xi(x, y) = (\frac{1}{2})\xi_{10}(\cos gx + \cos gy) + \xi_{11} \cos gx \cos gy. \quad (3.50)$$

The parameters  $D$  and  $\kappa$  represent the constant term  $v_{00}(z)$  and are assumed to be known from  $\{E_j\}$ , and  $z_m$  is a free parameter which has to be chosen so that the values of  $\xi$  and  $z_0$  averaged over the surface fall together:

$$\bar{z}_0^{x,y} = \bar{\xi}^{x,y}. \quad (3.51)$$

Equation (3.49) may be transformed to

$$(E_{i,n}/D)[\exp\kappa(z_0 - z_m)]^2 + 2 \exp\kappa(z_0 - z_m) - 1 = 2\beta_{10}(\cos gx + \cos gy) + 4\beta_{11} \cos gx \cos gy = C(x, y), \quad (3.49')$$

and from this  $z_0$  is evaluated to be

$$z_0(x, y) = z_m + (1/\kappa) \ln \{ \{ D/E_{i,n} \} \times \langle [1 + (E_{i,n}/D)(1 + C(x, y))]^{1/2} - 1 \rangle \}. \quad (3.52)$$

Equating this expression of  $z_0(x, y)$  and  $\xi(x, y)$  from Eq. (3.50) for the following three selected pairs of

$$(gx, gy) = (\pi/2, \pi/2); \quad (0, \pi/2); \quad (0, \pi)$$

we finally get the relations

$$z_m = -(1/\kappa) \ln \{ (D/E_{i,n}) ([1 + E_{i,n}/D]^{1/2} - 1) \}, \quad (3.53)$$

and

$$\xi_{10} = (2/\kappa) \ln \left\{ \frac{\langle [1 + (E_{i,n}/D)(1 + 2\beta_{10})]^{1/2} - 1 \rangle}{([1 + E_{i,n}/D]^{1/2} - 1)} \right\}, \quad (3.54)$$

$$\xi_{11} = (1/\kappa) \ln \left\{ \frac{([1 + E_{i,n}/D]^{1/2} - 1)}{\langle [1 + (E_{i,n}/D)(1 - 4\beta_{11})]^{1/2} - 1 \rangle} \right\}. \quad (3.55)$$

The results for the inverse transformation  $\xi \rightarrow \beta$  is given by

$$\beta_{10} = (1/2) [(E_{i,n}/D) U_m^2 \exp \kappa \xi_{10} + 2U_m \exp(\kappa \xi_{10}/2) - 1], \quad (3.56)$$

$$\beta_{11} = (1/4) \{ 1 - (E_{i,n}/D) U_m^2 [\exp(-\kappa \xi_{11})]^2 - 2U_m \exp(-\kappa \xi_{11}) \}, \quad (3.57)$$

with

$$U_m = (D/E_{i,n}) ([1 + E_{i,n}/D]^{1/2} - 1). \quad (3.58)$$

In order to show that this transformation works well we examine as an example the case He-LiF (001) which is the most extensively investigated system. From Goodman and Tan (1973) we get the Morse potential and  $\beta_G$  parameters corresponding to Eq. (3.49),  $D = 7.60$  meV,  $\kappa = 11$  nm<sup>-1</sup>,  $\beta_{10} = 0.10$ , and  $\beta_{11} = 0.007$ , and transforming these by Eqs. (3.54) and (3.55), values of  $\xi_{10}$  and  $\xi_{11}$  are obtained which compare quite well to the corrugated hard-wall parameters given by Garcia (1976, 1977b). The actual values are listed in Table

VIIa. Of course the  $\xi_G$  values achieved from the Morse potential depend somewhat on  $E_{i,n}$ , the energy incident normal to the surface.

It should be mentioned here that both the  $\beta_G$  and the  $\xi_G$  values were obtained by fitting calculated intensity distributions to experimentally observed distributions. In both cases the experimental results were obtained at fixed incident energy  $E_i = 65$  meV and with angles of incidence  $\theta_i$  between 0° and 65°; that means the values of  $E_{i,n} = E_i \cos^2 \theta_i$  lie between 65 meV and 22 meV. So both evaluations give information on the same repulsive part of the potential.

The agreement is not so good if, for the system H-LiF parameters  $\beta_G$  from resonance splittings are transformed to hard-wall parameters and vice versa. As shown in Table VIIb for the example of  $E_{i,n} = 50$  meV, the transformation of the known  $\beta_G$  values yields  $\xi_G$  parameters which are obviously larger than those extracted from comparing experimental intensity distributions to corrugated hard-wall calculations. This result can again be a hint that the corrugated hard-wall model works worse for atomic hydrogen than for helium, an effect which was already discussed in Sec. III.B. However, it should also be mentioned that for the hydrogen results discussed here the  $\beta_G$  values represent the periodic structure in the well, whereas the  $\xi_G$  values are related to the repulsive part of the potential at positive energies. So the results in Table VIIb could also mean that the variation of the  $v_G$  terms as functions of  $z$  is stronger than assumed in Eq. (3.49).

For more decisive results on the periodic structure in different regions of the potential additional experimental investigations are necessary. For instance, resonance splittings with the contribution of different bound levels should be investigated, and also more detailed investigations of intensity distributions at different incident energies should be done.

### E. Complex potential for describing inelastic effects in bound-state resonances

In the previous section we stated that the resonance structure observed in specular intensity for He-LiF(001)

TABLE VIIa. Transformation of Fourier coefficient strength  $\beta_G$  for hard-wall corrugation parameter  $\xi_G$  by Eqs. (3.54), (3.55) for three normal incident energies  $E_{i,n}$ . Example shown here: He-LiF (001) with  $D = 7.6$  meV,  $\kappa = 1.1 \text{ \AA}^{-1}$ ,  $\beta_{10} = 0.1$ ,  $\beta_{11} = 0.007$  [from Goodman and Tan (1973)].

$E_{i,n}/\text{meV}$	10	50	90	Hard wall values (Garcia, 1976)
$\xi_{10}/\text{nm}$	0.0272	0.0224	0.0210	0.0307
$\xi_{11}/\text{nm}$	0.00214	0.00176	0.00165	0.0017

TABLE VIIb. Transformation  $\beta_G \leftrightarrow \xi_G$  for H-LiF (001) at  $E_{i,n} = 50$  meV with  $D = 17.8$  meV and  $\kappa = 10.4 \text{ nm}^{-1}$ ,  $\beta_G$  values from resonance splitting and  $\xi_G$  values from diffracted beam intensity distributions.

$\beta_{10}$	$\beta_{11}$		$\xi_{10}/\text{nm}$	$\xi_{11}/\text{nm}$
0.055	0.027	→	0.015	0.0084
0.032	0.0078	←	0.009	0.0023

measured at relatively low surface temperature  $T_{SF} = 125$  K and small incident wave vector  $k_i = 57.6$   $\text{nm}^{-1}$  can be described almost quantitatively by elastic theory, where resonance-independent inelastic effects are taken into account by an overall Debye-Waller factor.

This simple elastic description turned out to be not possible for the specular bound-state resonance structure observed for H, D on LiF(001) and NaF(001) (Finzel *et al.*, 1975) at a surface temperature of  $T_{SF} = 240$  K and incident wave vectors in the region of  $30 \text{ nm}^{-1} < k_i < 70 \text{ nm}^{-1}$ . Chow and Thompson (1979) investigated these resonances by means of coupled channel calculations and found out that a quantitative fitting of some of the resonance structure is possible if the effects of inelastic scattering are taken into account. This was achieved by a complex interaction potential

$$v(\mathbf{r}) = v_R(\mathbf{r}) - iv_I(\mathbf{r}). \quad (3.59)$$

For the real part of the potential they used two different forms:

(a) Morse potential  $v_{00}^M(z)$  (see Appendix C.1), with

$$v_G(z) = \beta_G D \exp(-2\kappa z) \quad (3.60)$$

(b) exp-3 potential:  $v_{00}^{\text{exp-3}}(z)$  (see Appendix C.6), with

$$v_G(z) = \beta_G [3D/(\kappa z_e - 3)] \exp[-\kappa(z - z_e)], \quad (3.61)$$

with the parameters of  $v_{00}(z)$  as given in Table IX.

Unknown was the form of the imaginary part  $v_I$ , but since it should account here in an empirical way for the inelastic scattering from interaction with phonons,  $v_I$  should be large in the region where inelastic scattering occurs that is near the surface. So  $v_I$  was assumed to be of the form

$$\begin{aligned} v_I(z) &= \gamma D, & z \leq z_e \\ v_I(z) &= 0, & z > z_e \end{aligned} \quad (3.62)$$

with  $D$  = well depth,  $z_e$  = position of potential minimum, and the strength parameter  $\gamma$  to be determined from fitting the shape of resonances.

The imaginary part in the potential attenuates the incoming as well as the outgoing waves so that the overall elastically diffracted intensity will be smaller than the incident intensity. This effect happens on and off any bound-state resonance, but in addition  $v_I$  will cause a decreased lifetime of a bound state of  $v_{00}(z)$  which results in broader intensity structures.

A comparison of calculated and experimental resonance structures is given in Fig. 25 concerning a (0;0,1) resonance in the azimuthal variation of the specular intensity of the system H-NaF. In these calculations a Morse potential with  $D = 18.4$  meV and  $\kappa = 11.8 \text{ nm}^{-1}$ , a Debye-Waller factor with  $\theta_D = 416$  K (Hoinkes *et al.*, 1974a), and a velocity distribution in the beam of 12% FWHM have been used. For the periodic and the imaginary potential parameters three sets were chosen as shown in Fig. 25:

(a) With a real potential only with  $\beta_{10} = \beta_{11} = 0.025$  and  $\gamma = 0$  the calculated intensity curve agrees well with the experimental measurements in the region away from the resonance, but the width of the minimum is too

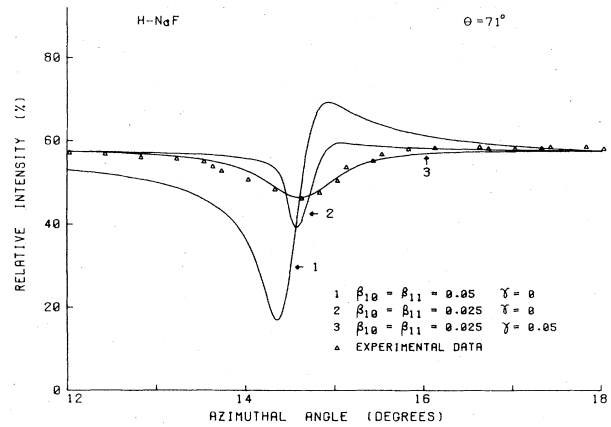


FIG. 25. Calculated and experimental specular intensity for the H-NaF(001) system. The experimental data ( $\Delta$ ) were taken from Finzel *et al.* (1975). The potential parameters are varied as indicated to give a fit to the experimental data. A 12% FWHM velocity distribution has been included in making this fit [from Chow and Thompson (1979)].

small.

(b) Increasing the values of the periodic terms ( $\beta_{10} = \beta_{11} = 0.05$ ,  $\gamma = 0$ ) increases the width of the resonance, but the shape does not fit the experimental one.

(c) Only with a nonzero imaginary potential is a very good fit to the experimental results obtained. The parameters in this case were

$$\beta_{10} = \beta_{11} = 0.025 \quad \text{and} \quad \gamma = 0.05.$$

In a second example, Fig. 26 shows calculations of the specular intensity versus incident energy for atomic deuterium and hydrogen on LiF(001). Here an exp-3 potential was used (Appendix C.6) with the parameters

$$D = 19.7 \text{ meV}, \quad \alpha = 36.7 \text{ nm}^{-1}, \quad z_e = 0.24 \text{ nm}$$

determined from known  $\{E_j\}$  levels. The periodic and imaginary potential parameters were varied in order to get a good fit with the experimental curves. The resulting most appropriate values were:

$$\beta_{10} = 0.06, \quad \beta_{11} = 0.03, \quad \text{and} \quad \gamma = 0.04.$$

For H-LiF the agreement is quite good for incident energies above 25 meV but it is not good with D-LiF. In this case the (2;0,1) minimum is much deeper in the calculated curve on the other hand the pronounced minimum at the (3;0,1) resonance does not appear in the calculations. The question is whether there are other effects beside the (3;0,1) resonance which were not included in these calculations but which contribute to this observed minimum.

A further attempt to include atom-phonon interactions by an optical potential was made by Hamauzu (1976, 1977). He derived an intensity formula for diffracted beams near resonance where the effect of the optical potential finally is given by two empirical parameters: the shift of the resonance energy and a resonance width  $\Gamma$ . Applying this intensity formula to azimuthal resonance measurements of the specular intensity [ $I_{sp} = f(\gamma)$ ] for the system H-NaF(001) by Finzel *et al.* (1975), he showed that this method of calculation works well with reasonable parameters. The resultant value

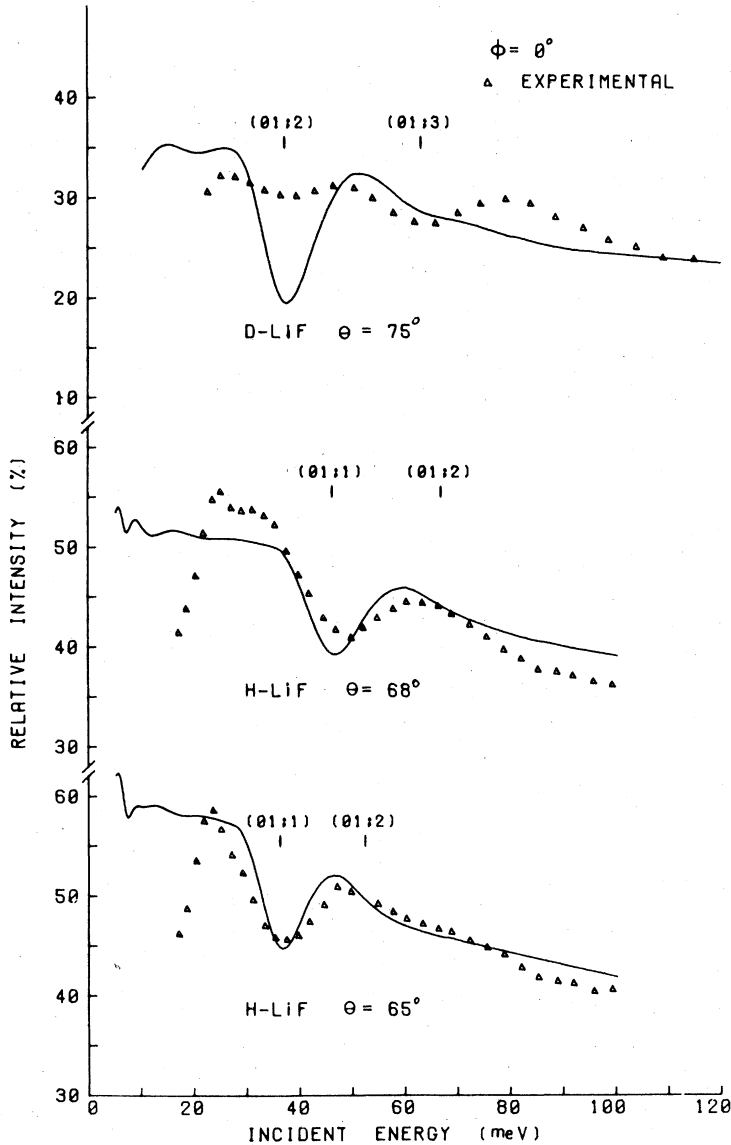


FIG. 26. Calculated and experimental specular intensity for H and D-LiF(001). The experimental data ( $\Delta$ ) were taken from Finzel *et al.* (1975). The calculations were done with  $v_{00}^{\text{exp}3}$  ( $D=19.7$  meV;  $\alpha=36.7$  nm $^{-1}$ ;  $z_e=0.24$  nm) and the strengths of periodic and imaginary terms  $\beta_{10}=0.06$ ;  $\beta_{11}=0.03$ , and  $\gamma=0.04$  resulting from a fit of the experimental data (12% FWHM velocity distribution is included) [from Chow and Thompson (1979)].

of  $\Gamma$  for the  $(0;0,1)$  resonance is  $\Gamma=1.0$  meV, but this is an upper limit since the velocity spread of the beam was not included in the calculations; correspondingly the mean lifetime of  $\tau=0.7 \times 10^{-12}$  sec has to be regarded as a lower limit.

In order to establish more generally an optical potential suitable for describing the effect of phonons on the diffracted intensities, it would be necessary to know how the potential parameters depend on the conditions of incidence and on the thermal properties of the crystal. In the examples discussed here by Chow and Thompson (1979) and by Hamazu (1976, 1977), it was only shown that the model potential works with reasonable values of the potential parameters at the special conditions given in the experiment.

In very recent investigations with atomic deuterium

scattered from LiF (001) (Greiner *et al.*, 1980) it was again shown that purely elastic calculations yield resonances which are too narrow and too deep (or high) as compared to experimental data. Only if the contribution of inelastic scattering is taken into account by a multiple Debye-Waller factor in the resonances is a reasonable description of the resonances obtained.

#### IV. CONCLUDING DISCUSSION

There are two essentially different aspects in the attempt to get information on the physical gas-surface interaction potential from gas-surface diffraction experiments with atomic beams of small mass ( $m_g \leq m_{He}$ ) and energies in the thermal range.

One aspect is getting information on the periodic

structure on the surface of a crystal. In those cases, where atoms with thermal energies interact by van der Waals forces only with the atoms or ions of the top-most surface layer, the results on the surface structure achieved here are really results on the first layer without any influence of deeper layers. Most of the investigations concerning this aspect have been done by diffracting He nozzle beams from crystal surfaces and then comparing the observed diffracted beam intensities with calculations where the interaction potential is approximated by a corrugated hard wall. The applicability of this method has been tested extensively with the system He on LiF (001) as is, for instance, discussed in detail by Garcia (1977b). Garcia (1976) gave also a tentative analysis of the surface crystallography of LiF (001) based on experimental diffraction intensities by Boato, Cantini, and Mattera (1976) showing that the  $\text{Li}^+$  ions appear to be displaced upwards from the crystal surface by  $3.6 \pm 0.6$  pm. Very recent experiments with He diffracted from a stepped metal surface of Cu (117) by Lapujoulade, Lejay, and Papanicolaou (1979), or of Pt (997) by Comsa *et al.* (1979), from clean and hydrogen saturated Ni (110) surfaces by Rieder and Engel (1979), from reconstructed (100) and (111) Si surfaces by Cardillo and Becker (1978, 1979; Cardillo, 1979), and from  $\text{TaS}_2$  corrugated at the surface due to charge-density waves by Boato, Cantini, and Colella (1979) show indeed that thermal energy atom diffraction (TEAD) is further developing as a technique of surface structure analysis. In combination with low-energy electron diffraction (LEED) and low-energy ion scattering the method of TEAD can give a complete instrument with respect to surface structure analysis; the chemical composition of the surface should be checked by additional methods (ESCA, SIMS, AES. . .).

A problem in this context is still whether the hard-wall model, which was shown to work very well in the case of He-LiF (001), is also a good approximation for analyzing the scattering distributions of He observed from silicon, and clean or adsorbate-covered metal surfaces, or whether a softer form like the exponential corrugated potential recently discussed by Armand and Manson (1979) and Armand (1980) should be applied in order to get a realistic description of the periodic structure at the surface. A good test for the applicability of the hard corrugated wall or other models would, for instance, come from an examination of the resulting corrugation parameters as function of the incident energy.

The second main aspect in trying to extract information on the gas-surface interaction potential from diffraction experiments is to find out the form of the attractive potential well; that means its well depth, its range, and in some respect also the periodic variation of the depth. The knowledge of these parameters is important, for instance, in adsorption-desorption calculations or in considerations on surface reactions where precursor states with a certain mobility parallel to the surface have to be regarded.

We have discussed in detail how experimental investigations of bound-state resonances can give binding energies  $\{E_j\}$  and from these detailed information

on the attractive potential well of several gas-surface systems. And we have shown that these experimental results may be used to test general theoretical models for calculating potential forms or parameters, for instance, the constant  $C_3$  of dispersion attraction, or to establish empirical rules which may be used to estimate potential parameters from electrical constants of a certain gas-surface system which possibly is not accessible to experiments. The gas-surface systems most extensively investigated in this respect were H,  $\text{H}_2$ , and He on alkali halides and graphite, but recent diffraction experiments on MgO (001) (Rowe and Ehrlich, 1975) or NiO (001) and on metal surfaces promise more detailed experimental results on the physical gas-surface interaction potential well for these systems also.

#### ACKNOWLEDGMENTS

I would like to thank Professor H. Wilsch for many stimulating discussions during this work and for his comments on the manuscript. I also want to acknowledge helpful discussions with Dr. N. Garcia and the members of our group, especially H. Kaarmann and L. Greiner. Financial support by the Deutsche Forschungsgemeinschaft is greatly appreciated.

#### APPENDIX A: SOME SPECIAL RESULTS CONCERNING GAS-SURFACE POTENTIAL CURVES CALCULATED FROM SUMMATION OF PAIR POTENTIALS

##### 1. Potential formulas obtained from summation or integration of pair potentials

Approximative formulas for gas-surface potentials may be achieved by replacing the summation of pair potentials by an integration. The following formulas have been obtained by Steele (1974) on the basis of a Lennard-Jones (12-6) pair potential:

$$U_{gs}(\rho) = 4\epsilon_{gs} [(\sigma_{gs}/\rho)^{12} - (\sigma_{gs}/\rho)^6]. \quad (\text{A1})$$

Here  $\epsilon_{gs}$  is the well depth and  $\sigma_{gs}$  is the distance at which the potential curve crosses the zero energy line.  $\sigma_{gs}$  is connected to the equilibrium distance  $\rho_0$  between the gas atom and the surface atom by

$$\sigma_{gs} = \rho_0 2^{-1/6}. \quad (\text{A2})$$

Treating a simple cubic lattice, using for  $\sigma_{gs}$  the combination rule (2.4) and assuming  $\sigma_{ss}$  to be equal to the lattice constant of the solid, the following three expressions for the gas atom-solid surface interaction potential may be formulated (with reduced distances  $\rho^* = \rho/\sigma_{gs}$  and  $z^* = z/\sigma_{gs}$ ).

(a) The summed pairwise potential is given by

$$v_{gs}(\mathbf{r}) = 4\epsilon_{gs} \sum_i \left[ \left( \frac{\sigma_{gs}}{\sigma_{ss}} \right)^{12} \left( \frac{1}{\rho_i^*} \right)^{12} - \left( \frac{\sigma_{gs}}{\sigma_{ss}} \right)^6 \left( \frac{1}{\rho_i^*} \right)^6 \right]. \quad (\text{A3})$$

(b) After integration over the (100) planes parallel to the surface the gas atom-solid surface potential, which is now constant parallel to the surface, is represented by

$$v_{gs}(z) = 2\pi\epsilon_{gs} \sum_{k=0}^{\infty} \left[ \frac{2}{5} \left( \frac{\sigma_{gs}}{\sigma_{ss}} \right)^{12} \left( \frac{1}{z^* + k} \right)^{10} - \left( \frac{\sigma_{gs}}{\sigma_{ss}} \right)^6 \left( \frac{1}{z^* + k} \right)^4 \right], \quad (\text{A4})$$

where  $k$  is an integer that indexes the crystal layers.

(c) Full integration finally results in the following potential function, which is again constant parallel to the surface:

$$v_{gs}(z) = \frac{2\pi}{3} \epsilon_{gs} \left[ \frac{2}{15} \left( \frac{\sigma_{gs}}{\sigma_{ss}} \right)^{12} \left( \frac{1}{z^*} \right)^9 - \left( \frac{\sigma_{gs}}{\sigma_{ss}} \right)^6 \left( \frac{1}{z^*} \right)^3 \right]. \quad (A5)$$

A comparison of the results of these three procedures is given in Fig. 27, showing that the fully integrated approximation is a rather poor one in the presented region of  $z$ , whereas the partially summed curve approximates the lateral average of the summed potential rather well.

2. Relations on the potential well depth extracted from pairwise potential summation

Since in the case of physical adsorption the dominant contribution to the total binding energy is given by attractive dispersion forces, Rogowska (1978) calculated by pairwise summation gas-surface potential curves for Ne, Ar and Xe on Na, K, and Rb halides and tried to find out relations between the calculated well depth  $D$  and physical properties of the ionic crystal and of the gas atoms which influence the dispersion forces.

The potential as function of the distance of the gas atom from the surface was calculated at four positions over the unit cell  $A, B, C$ , and  $D$  (see Fig. 1). For the two sites with the deepest well depth ( $A$  and  $C$ ) the following relations could be deduced from the calculated curves. For the  $A$  sites

$$D_A = (A_1\alpha_0 + A_2) [a^2(\epsilon - 1)/(\epsilon + 1) + A_3] + A_4 \quad (A6)$$

and for the  $C$  sites

$$D_C = (B_1\alpha_0 + B_2)(\epsilon + B_3) + B_4, \quad (A7)$$

where  $\alpha_0$  is the polarizability of the gas atom,  $\epsilon$  the optical dielectric constant,  $a$  half the bulk lattice con-

stant, and  $A_1 \dots A_4, B_1 \dots B_4$  parameters derived from fitting the calculated values of  $D_{A,C}$  to the relations (A6) or (A7). For the  $C$  site  $B_1 \dots B_4$  depend somewhat on the kind of the positive ion, but for the  $A$  site all the  $D_A$  values are well approximated by one equation:

$$D_A = \left[ 0.016 - (0.009\alpha_0 + 0.0148) \left( \frac{\epsilon - 1}{\epsilon + 1} \right) a^2 + 2.05 \right] \times 10^{-12}. \quad (A8)$$

(When  $\alpha_0$  and  $a$  are expressed in Å in this relation,  $D_A$  is obtained in ergs per atom.)

APPENDIX B: BINDING ENERGIES FROM EXPERIMENTAL RESONANCE INVESTIGATIONS

The binding energies  $E_j$  determined from resonance investigations of all the systems known to the author are listed in Table VIII. Some of the results in Table VIII are based only on one or a small number of  $I_{sp} = f(\gamma)$  curves and, therefore, are questionable. This is the case with the first  $E_j$  values for  $^4\text{He}$  on NaF calculated by Devonshire (1936) and Tsuchida (1969) from the experimental results of Frisch and Stern (1933b). The correct levels of this system are now well established from the experiments by Derry *et al.* (1977, 1978). Also questionable are the value of the deepest level of He on NaCl estimated by Bledsoe (1972) and the values of the levels for  $\text{H}_2$  and  $\text{D}_2$  on LiF as determined by Tsuchida (1969) from Frisch and Stern's results (1933b) but also as given by O'Keefe *et al.* (1970) from their experiments. In the last case especially, the fact of finding almost identical values of the binding energies for the two isotopes  $\text{H}_2$  and  $\text{D}_2$  casts doubt on these results.

APPENDIX C: REVIEW OF MODEL POTENTIALS USED TO FIT EXPERIMENTAL BINDING ENERGIES  $E_j$

1. Morse potential

$$v_{00}^M(z) = D \{ \exp[-2\kappa(z - z_e)] - 2\exp[-\kappa(z - z_e)] \}, \quad (C1)$$

with  $D$  = well depth,  $\kappa$  = reciprocal range parameter,  $z_e$  = position of minimum, not determined by  $\{E_j\}$ , and spectrum of energy eigenvalues:

$$E_j = -\{D^{1/2} - [\hbar\kappa/(2m_g)^{1/2}](j + 1/2)\}^2; \quad j = 0, 1, 2, \dots, \leq [(2m_g D)^{1/2}/\hbar\kappa - 1/2]. \quad (C2)$$

*Advantages:* simple form representing the general behavior of repulsion and attraction, analytical form of  $\{E_j\}$  spectrum, capability of fitting  $E_j$  of the strongly bound states.

*Disadvantages:* too short ranged in the asymptotic region, not suited to represent the levels near the dissociation limit.

An appropriate test for the applicability of the Morse potential is linear behavior in a plot of  $|E_j|^{1/2} = f(\eta)$  with  $\eta$  as defined in Eq. (3.28). The Morse potential was used by Devonshire (1936) and Lennard-Jones and Devonshire (1937) for He-LiF and after that in many theoretical investigations. It worked also well for de-

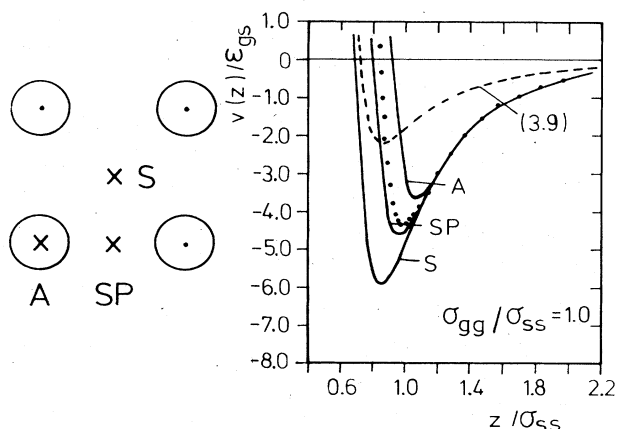


FIG. 27. Example of gas-surface interaction potential curves calculated from pair potentials for an atom over a simple cubic crystal lattice: (a) full curves calculated from direct sums of pair potentials for three different positions ( $A, SP, S$ ) above the unit cell [see Eq. (A3)], (b) black dots give the result from summing after integration over the (001) planes [see Eq. (A4)], (c) dashed curve obtained by replacing the sum by an integral over the solid [see Eq. (A5)] [after Steele (1974)].

TABLE VIII. Binding energies in the gas-surface potential well  $v_0(z)$  as determined from experimental resonance investigations.

Gas	Surface	$E_0$	$E_1$	$E_2$	$E_3$	$E_4$	$E_5$	$E_6$	$E_7$	Ref.	
H	LiF(001)	$-12.3 \pm 0.3^a$	$-3.9 \pm 0.4^a$	$-0.5 \pm 0.5^a$						g, h	
	LiF(001)	$-12.2 \pm 0.2$	$-3.5 \pm 0.3$	$-0.5 \pm 0.3$						i	
	NaF(001)	$-11.8 \pm 0.2$	$-3.0 \pm 0.2$	$-0.4 \pm 0.4$						i, j	
	KCl(001)-H <sub>2</sub> O	$-29.8 \pm 0.7^b$	$-22.5 \pm 0.6^b$	$-15.9 \pm 0.5^b$	$-10.3 \pm 0.3^b$	$-6.0 \pm 0.3^b$					k+1
	Graphite	$-31.6 \pm 0.2$	$-15.3 \pm 0.3$								m
D	LiF(001)	$-13.4 \pm 0.2^a$	$-6.6 \pm 0.2^a$	$-2.4 \pm 0.2^a$	$-0.5 \pm 0.3^a$					h, n	
	LiF(001)	$-14.0 \pm 0.2$	$-6.7 \pm 0.2$	$-2.3 \pm 0.2$	$-0.5 \pm 0.3$					i	
	NaF(001)	$-13.3 \pm 0.2$	$-5.8 \pm 0.2$	$-1.6 \pm 0.3$	$-0.3 \pm 0.3$						i, j
	KCl(001)-H <sub>2</sub> O		$-19.3 \pm 0.5^b$	$-12.0 \pm 0.1$	$-15.6 \pm 0.6^b$	$-11.0 \pm 0.4^b$	$-7.7 \pm 0.4^b$	$-4.6 \pm 0.6^b$			k
	Graphite	$-35.4 \pm 0.2$	$-21.35 \pm 0.1$	$-12.0 \pm 0.1$	$-5.9 \pm 0.3$						m
<sup>3</sup> He	LiF(001)		$-2.3$							o	
	LiF(001)	$-5.59 \pm 0.1$	$-2.00 \pm 0.1$							p	
	NaF(001)	$-4.50 \pm 0.1$	$-1.38 \pm 0.1$							p, q	
	Graphite	$-11.62 \pm 0.12$	$-5.38 \pm 0.12$	$-1.78 \pm 0.12$							r
	LiF(001)	$-5.6$	$-2.5$	$-0.65 \pm 0.2$							exp. s, calc. t
<sup>4</sup> He	LiF(001)	$-5.8 \pm 0.2$	$-2.6 \pm 0.2$							exp. s, calc. u	
	LiF(001)	$-5.8$								v	
	LiF(001)	$\approx -5.1$								o	
	LiF(001)	$-5.8$	$-2.55$	$-0.17$						w	
	LiF(001)	$-5.6$	$-2.25$	$-0.84$						x	
	LiF(001)	$-5.8 \pm 0.1$	$-2.2 \pm 0.1$	$-0.6 \pm 0.1$	$-0.1 \pm 0.1$					y	
	LiF(001)	$-5.9 \pm 0.1$	$-2.46 \pm 0.1$	$-0.78 \pm 0.1$	$-0.21 \pm 0.1$					p	
	NaF(001)	$-8.4^c$	$-3.5^c$								exp. s, calc. t
	NaF(001)	$-8.3^c$	$-4.7 \pm 0.2$	$-1.95 \pm 0.2$							exp. s, calc. u
	NaF(001)	$-4.92 \pm 0.1$	$-1.87 \pm 0.1$	$-0.54 \pm 0.1$							p, q
	NaCl(001)	$-10.4 \pm 0.4^d$	$-3.7 \pm 0.4$								w
	NiO(001)	$-7.9 \pm 0.4$	$-4.0 \pm 0.4$	$-1.6 \pm 0.4$							z, aa
	Graphite	$-11.7 \pm 0.3$	$-6.1 \pm 0.4$	$-2.6 \pm 0.3$	$-0.9 \pm 0.2$						bb
	Graphite	$-11.77 \pm 0.10$	$-6.13 \pm 0.10$	$-2.68 \pm 0.08$	$-0.83 \pm 0.04$						cc
	Graphite	$-12.06 \pm 0.12$	$-6.36 \pm 0.12$	$-2.85 \pm 0.12$	$-1.01 \pm 0.12$	$-0.17 \pm 0.12$					r
Graphite	$-11.98 \pm 0.07$	$-6.33 \pm 0.06$	$-2.85 \pm 0.06$	$-0.99 \pm 0.05$	$-0.17 \pm 0.06$					dd	
Cu(117)	$-5.9 \pm 0.2$	$-4.0 \pm 0.3$	$-2.1 \pm 0.2$							ee	
H <sub>2</sub>	LiF(001)	$-8.7 \pm 0.9^c$	$-4.34 \pm 0.2$	$-1.5 \pm 0.9^c$						exp. s, calc. u	
	LiF(001)	$-30.4^e$	$-19.1^e$	$-10.0^e$						o	
	LiF(001)	$-17.3 \pm 1.0^f$	$-10.0 \pm 1.0^f$	$-4.3 \pm 1.0^f$							exp. s, calc. ff
	NiO(001)	$-48.0 \pm 2.0$	$-24.5 \pm 1.5$	$-14.5 \pm 1.5$	$-7.5 \pm 0.5$	$-3.7 \pm 0.7$					z
	Graphite	$-41.61 \pm 0.25$	$-26.43 \pm 0.25$	$-15.33 \pm 0.25$	$-7.96 \pm 0.25$	$-3.61 \pm 0.25$	$-1.46 \pm 0.25$				gg
D <sub>2</sub>	LiF(001)	$-30.0^e$	$-19.1^e$	$-10.9^e$						o	
	Graphite		$-23.11 \pm 0.25$	$-15.40 \pm 0.25$	$-10.00 \pm 0.25$	$-6.37 \pm 0.25$	$-3.78 \pm 0.25$	$-1.93 \pm 0.25$		gg	

<sup>a</sup> Measured with Maxwellian beam.<sup>b</sup> Made doubtful by new experimental investigations in our group.<sup>c</sup> Estimate from poor experimental information which was not confirmed later.<sup>d</sup> Not strongly supported from experiment.<sup>e</sup> Questionable results since the energy levels do not differ for the two isotopes.

TABLE VIII. (Continued)

- <sup>f</sup> Revised analysis by Tsuchida [private communication cited by Le Roy (1976)].
- <sup>g</sup> Hoinkes, Nahr, and Wilsch (1972a).
- <sup>h</sup> Hoinkes, Nahr, and Wilsch (1972b).
- <sup>i</sup> Finzel *et al.* (1975).
- <sup>j</sup> Wilsch *et al.* (1974).
- <sup>k</sup> Frank, Hoinkes, and Wilsch (1977).
- <sup>l</sup> Hoinkes, Greiner, and Wilsch (1977).
- <sup>m</sup> Tommasini and Valbusa (1979).
- <sup>n</sup> Hoinkes, Nahr, and Wilsch (1974b).
- <sup>o</sup> O'Keefe *et al.* (1970).
- <sup>p</sup> Derry *et al.* (1978).
- <sup>q</sup> Derry *et al.* (1977).
- <sup>r</sup> Derry *et al.* (1979).
- <sup>s</sup> Frisch and Stern (1938b).
- <sup>t</sup> Devonshire (1936).
- <sup>u</sup> Tsuchida (1969).
- <sup>v</sup> Crews (1967).
- <sup>w</sup> Bledsoe (1972).
- <sup>x</sup> Houston and Frankl (1973).
- <sup>y</sup> Meyers and Frankl (1975).
- <sup>z</sup> Cantini, Felcher, and Tatarek (1977).
- <sup>aa</sup> Cantini, Tatarek, and Felcher (1979).
- <sup>bb</sup> Boato, Cantini, Tatarek (1978).
- <sup>cc</sup> Boato, Cantini, Tatarek (1979a).
- <sup>dd</sup> Boato *et al.* (1979b).
- <sup>ee</sup> Lapujoulade, Lejay, and Papanicolaou (1979).
- <sup>ff</sup> Le Roy (1976).
- <sup>gg</sup> Mattera *et al.* (1980a).

scribing the experimental values of  $E_j$  for H, D on LiF and NaF (Finzel *et al.*, 1975); this is clearly demonstrated in Fig. 16.

## 2. (12-3) potential

$$v_{00}^{12-3}(z) = (D/3)[(z_e/z)^{12} - 4(z_e/z)^3] \quad (C3)$$

with  $D$  = well depth and  $z_e$  = position of minimum and range parameter.

*Advantages:* correct asymptotic form of attraction, good fit of the potential form achieved from pairwise summation [see Tsuchida (1969) and Fig. 2].

*Disadvantages:* arbitrary repulsive form, no analytical formula of the  $\{E_j\}$  spectrum,

The (12-3) potential was used by Tsuchida (1969) for calculating diffracted beam intensities for He-LiF.

## 3. (9-3) potential

$$v_{00}^{9-3}(z) = (D/2) \left[ \left( \frac{z_r}{z+z_0} \right)^9 - 3 \left( \frac{z_r}{z+z_0} \right)^3 \right] \quad (C4)$$

$$= (3^{3/2}D/2) \left[ \left( \frac{\sigma}{z+z_0} \right)^9 - \left( \frac{\sigma}{z+z_0} \right)^3 \right], \quad (C5)$$

with  $D$  = well depth,  $z_r, \sigma$  = range parameter,  $z_m = z_r - z_0 = 3^{1/6}\sigma - z_0$  = position of minimum,  $z = \sigma - z_0$  = point of vanishing  $v_{00}$ ,  $z_0$  shifts the potential in  $z$  direction but is not determined by  $\{E_j\}$ . Spectrum of energy eigenvalues derived in WKB approximation (Cole and Tsong, 1977)

$$E_j = -D[1 - (j+1/2)/L]^6 \quad (C6)$$

with

$$L = (3.07/\pi)(2m_e D \sigma^2 / \hbar^2)^{1/2},$$

and  $j = 0, 1, 2, \dots$ ;  $j_{\max}$  = next integer to  $(L - 1/2)$ .

*Advantages:* (9-3) form results from pairwise summation of Lennard-Jones (12-6) potential in the continuum limit of the solid (Steele, 1974), correct asymptotic form of attractive part with  $C_3 = 3^{3/2}D\sigma^3/2$ .

*Disadvantages:*  $z^{-9}$  repulsion as arbitrary as the  $r^{-12}$  repulsion in interatomic interaction.

A test for the applicability of this form is the linear variation of  $E_j^{1/6}$  with  $\eta$ . For a detailed discussion of this potential form see Cole and Tsong (1977) and also Schwartz, Cole, and Pliva (1978) who constructed (9-3) potentials for the systems H, D on LiF and NaF (see Figs. 14, 15) and also  $^3\text{He}$ ,  $^4\text{He}$  on LiF and NaF.

## 4. Shifted Morse potential

$$v_{00}^{\text{SM}}(z) = D' \{ \exp[-2\kappa(z - z_e)] - 2 \exp[-\kappa(z - z_e)] - \Delta \} \quad (C7)$$

with  $D = D'(1 + \Delta)$  = well depth,  $\kappa$  = reciprocal range parameter,  $\Delta$  = shift parameter,  $z_e$  = position of minimum, not determined by  $\{E_j\}$ . Spectrum of energy eigenvalues

$$E_j = -D'(1 + \Delta) + \hbar\kappa(2D'/m_e)^{1/2}(j+1/2) - (\hbar^2\kappa^2/2m_e)(j+1/2)^2. \quad (C8)$$

*Advantages:* analytical formula for  $\{E_j\}$ , small shift

$-D\Delta$  results in strong improvements in the fit of observed  $\{E_j\}$  as compared to normal Morse potential.

*Disadvantages:* long-range attraction still incorrect. The shifted Morse potential was used by Schwartz, Cole, and Pliva (1978) to construct a hybrid potential (see next subsection).

## 5. Shifted Morse hybrid potential

$$v_{00}^{\text{SMH}}(z) = v^{\text{SM}}(z); \quad z \leq z_p, \quad (C9)$$

$$v_{00}^{\text{SMH}}(z) = -C_3 z^{-3}; \quad z \geq z_p,$$

with  $D', \kappa$ , and  $\Delta$  (see Sec. C.4) determined from fit of the observed levels, but without highest levels which lie in the asymptotic region.  $z_e$  = position of minimum varied so that the SM potential matches value and slope of the asymptotic potential form  $-C_3 z^{-3}$  at a point of contact  $z_p$ .

For more details see Schwartz, Cole, and Pliva (1978), who constructed SMH potentials for H, D-LiF, and NaF (see Figs. 14, 15) and also  $^3\text{He}$ ,  $^4\text{He}$ -LiF, and NaF using for  $C_3$  the values calculated by Bruch and Watanabe (1977).

## 6. Exponential-3 potential

$$v_{00}^{\text{exp-3}}(z) = \frac{\kappa z_e}{\kappa z_e - 3} D \left\{ \frac{3}{\kappa z_e} \exp[-\kappa(z - z_e)] - \left( \frac{z_e}{z} \right)^3 \right\}, \quad (C10)$$

with  $D$  = well depth,  $\kappa$  = reciprocal range of repulsion,  $z_e$  = position of minimum.

*Advantages:* form of repulsive and attractive part as expected from theoretical considerations.

*Disadvantages:* no analytical formula for energy eigenvalues.

The exp-3 potential was used for calculating diffracted beam intensities for the systems He-LiF (Chow, 1977), He-Ag (111) (Chow and Thompson, 1978), and H, D-LiF, and NaF (Chow and Thompson, 1979).

## 7. Variable exponent potential

$$v_{00}^{\text{VE}}(z) = D \left[ \left( 1 + \frac{\lambda z}{p} \right)^{-2p} - 2 \left( 1 + \frac{\lambda z}{p} \right)^{-p} \right], \quad (C11)$$

with  $D$  = well depth,  $\lambda$  = reciprocal range parameter,  $p$  = variable exponent,  $z_e = 0$  = position of minimum, and spectrum of energy eigenvalues (accuracy better than 1%):

$$E_j = -D \left[ 1 - \frac{(j+1/2)2\hbar\lambda}{(2mD)^{1/2}N(p)} \right]^{S(p)} \quad (C12)$$

with  $N(p)$  and  $S(p)$  functions calculated by Mattera *et al.* (1980b).

*Advantages:* flexible analytical form, analytical formula for eigenvalue spectrum.

*Disadvantages:* deficiencies of the general form are compensated by using the exponent as fit parameter, the resultant exponents have in general no theoretical justification.

A detailed discussion of this potential form is given by Mattera *et al.* (1980a). It was used to fit the  $E_j$  spectra of H (Tommasini and Valbusa, 1979), He

(Boato *et al.*, 1979b), and H<sub>2</sub>, D<sub>2</sub> (Mattera *et al.*, 1980a) on graphite.

8. Flat-bottom hard-wall potential (includes surface corrugation)

$$v^{\text{FBHW}}(\mathbf{r}) = \infty; \quad z < \xi(\mathbf{R}),$$

$$v^{\text{FBHW}}(\mathbf{r}) = v_a(z); \quad z > \xi(\mathbf{R}), \tag{C13}$$

with  $\xi(\mathbf{R})$  = surface corrugation profile,  $v_a(z)$  = attrac-

tive part approximated by:

$$v_a(z) = -D; \quad z < \beta$$

$$v_a(z) = -D \left( \frac{\alpha + \beta}{\alpha + z} \right)^3; \quad z > \beta \tag{C14}$$

with  $D$  = well depth,  $\alpha, \beta$  = position and range parameters with  $\beta \geq \xi_{\text{max}}$ .

*Advantages:* correct long-range asymptotic form with  $C_3 = (\alpha + \beta)^3 D$ , suited for theoretical calculations.

TABLE IX. Gas-surface potential parameters determined from fitting experimental binding energies.

Surface	Model potential	D/meV	Range	3rd Parameter	C <sub>3</sub> /meV nm <sup>3</sup>	Ref.
A. Atomic hydrogen and deuterium						
LiF (001)	Morse	17.8	$\kappa = 10.4 \text{ nm}^{-1}$	...	...	a
	RKR method	18.4	...	...	...	b
	SMH	18.77	$\kappa = 12.0 \text{ nm}^{-1}$	$\Delta = 0.048$	0.170	b
	9-3	20.73	$\sigma = 0.194 \text{ nm}$	...	0.393	b
	exp-3	19.7	$\alpha = 36.7 \text{ nm}^{-1}$	$z_e = 0.24 \text{ nm}$	...	c
NaF (001)	FBHW	17.8	$\alpha = 0.104 \text{ nm}$	$\beta = 0.123 \text{ nm}$	0.208	d
	Morse	17.9	$\kappa = 11.5 \text{ nm}^{-1}$	...	...	a
	RKR method	17.6	...	...	...	b
	SMH	18.36	$\kappa = 12.4 \text{ nm}^{-1}$	$\Delta = 0.028$	0.135	b
	9-3	20.62	$\sigma = 0.18 \text{ nm}$	...	0.312	b
Graphite	FBHW	17.6	$\alpha = 0.096 \text{ nm}$	$\beta = 0.115 \text{ nm}$	0.165	d
	VE	43.2	$\lambda = 13.5 \text{ nm}^{-1}$	$p = 5.1 + 0.9$	...	e
B. <sup>3</sup> He, <sup>4</sup> He						
LiF (001)	9-3	9.20	$\sigma = 0.185 \text{ nm}$	...	0.139	f
	RKR method	7.5	...	...	...	b
	SMH	8.32	$\kappa = 12.9 \text{ nm}^{-1}$	$\Delta = 0.075$	0.0817	b
	9-3	8.92	$\sigma = 0.194 \text{ nm}$	...	0.1692	b
	Morse	8.03	$\kappa = 12 \text{ nm}^{-1}$	...	...	g
	12-3	9.34	$z_e = 0.23 \text{ nm}$	...	...	g
	Zeta potential	8.90	...	...	...	g
	FBHW	7.98	$\alpha = 0.141 \text{ nm}$	$\beta = 0.104 \text{ nm}$	0.117	d
	exp-3	8.8	$\kappa = 47.8 \text{ nm}^{-1}$	$z_e = 0.23 \text{ nm}$	...	h
	$\Sigma$ Yukawa-6	9.20	...	...	...	i
NaF (001)	9-3	7.72	$\sigma = 0.189 \text{ nm}$	...	0.124	f
	SMH	6.91	$\kappa = 12.3 \text{ nm}^{-1}$	$\Delta = 0.059$	0.0725	b
	9-3	7.64	$\sigma = 0.191 \text{ nm}$	...	0.138	b
	FBHW	6.72	$\alpha = 0.137 \text{ nm}$	$\beta = 0.109 \text{ nm}$	0.100	d
NiO (001)	Morse	10.1	$\kappa = 10.7 \text{ nm}^{-1}$	...	...	j
Graphite	$\Sigma$ Yukawa-6	15.75	...	...	...	k
	$\Sigma$ 12-6	16.25	...	...	...	k
	VE	15.70	$\lambda = 14.13 \text{ nm}^{-1}$	$p = 5.3$	...	l
	SM	14.59	$\kappa = 13.5 \text{ nm}^{-1}$	$\Delta = 0.058$	...	l
	FBHW	14.4	$\alpha = 0.133 \text{ nm}$	$\beta = 0.093 \text{ nm}$	0.165	d
C. H <sub>2</sub> , D <sub>2</sub>						
Graphite	VE	51.5	$\lambda = 14.5 \text{ nm}^{-1}$	$p = 4.03$	...	m

<sup>a</sup> Finzel *et al.* (1975).  
<sup>b</sup> Schwartz, Cole, and Pliva (1978).  
<sup>c</sup> Chow and Thompson (1979).  
<sup>d</sup> Goodman, Garcia, and Celli (1979).  
<sup>e</sup> Tommasini and Valbusa (1979).  
<sup>f</sup> Derrý *et al.* (1978).  
<sup>g</sup> Tsuchida (1975).  
<sup>h</sup> Chow (1977).  
<sup>i</sup> Chow and Thompson (1976).  
<sup>j</sup> Cantini, Tatarek, and Felcher (1979).  
<sup>k</sup> Derrý *et al.* (1979).  
<sup>l</sup> Boato *et al.* (1979b).  
<sup>m</sup> Mattera *et al.* (1980a).

*Disadvantages:* approximate character of hard wall and flat bottom with discontinuities, no analytical formula for  $\{E_j\}$  spectrum.

This potential was used in theoretical investigations of the diffraction behavior at resonances, with the parameters  $D$ ,  $\alpha$ , and  $\beta$  determined from fitting the energy eigenvalues to the experimental  $\{E_j\}$  spectrum [see, for instance, Garcia, Celli, and Goodman (1979); Garcia, Goodman, Celli, and Hill (1979)]. Very recently Goodman, Garcia, and Celli (1979) gave a detailed discussion of this potential and showed that it is well suited to reproduce the experimental  $\{E_j\}$  spectra of H, D on LiF, NaF, and  $^3\text{He}$ ,  $^4\text{He}$  on LiF, NaF, and graphite.

### 9. Potential forms produced by pairwise summation

$$v(\mathbf{r}) = \sum_N u_N(|\mathbf{r} - \mathbf{r}_N|) \quad (\text{C15})$$

summation over all solid atoms or ions located at  $\mathbf{r}_N$ , with different forms used for the pair potential  $u_N$ .

#### a. $u_N = (12-6)$ Lennard-Jones potential

This results in  $\zeta$  potential

$$v_{00}^{\zeta}(z) = A_+ \zeta(10, z/d) - 2B_+ \zeta(4, z/d) \quad (\text{C16})$$

with  $\zeta =$  Riemann  $\zeta$  function,  $d =$  lattice layer spacing,  $A_+, B_+ =$  energy parameters, which may be calculated from pair parameters or used as fitting parameters in order to reproduce the experimental  $\{E_j\}$  spectrum,  $z_e =$  position of minimum given by  $\zeta(11, z_e/d)/\zeta(5, z_e/d) = 4B_+/5A_+$ .

For more details of this form see Tsuchida (1974), who used this potential to calculate diffracted beam intensities for He on LiF. Another form resulting from summing the 12-6 potentials [see also Eq. (A4)] (Steele, 1974; Carlos and Cole, 1978) is

$$v_{00}^{\Sigma 12-6}(z) = \frac{4\pi\epsilon}{A_c} \sum_{n=0}^{\infty} \left[ \frac{2}{5} \frac{\sigma^{12}}{z_n^{10}} - \frac{\sigma^6}{z_n^4} \right] \quad (\text{C17})$$

with  $z_n = z + nd$ ;  $d =$  lattice layer spacing,  $A_c =$  area of unit cell,  $\epsilon =$  well depth parameter of pair potential,  $\sigma =$  range parameter of pair potential.  $\epsilon$  and  $\sigma$  may be used for fitting the experimental  $\{E_j\}$  spectrum.

#### b. $u_N =$ Yukawa-6 potential

$$u_N(r) = \frac{\epsilon(1 + \alpha r_m)}{\alpha r_m - 5} \left\{ \frac{6r_m}{(1 + \alpha r_m)r} \exp[\alpha(r_m - r)] - (r_m/r)^6 \right\} \quad (\text{C18})$$

where  $\epsilon$ ,  $r_m$ , and  $\alpha$  are well depth, separation at minimum and range of repulsion of the pair potential.

This potential was used by Chow and Thompson (1976) for calculating diffracted beam intensities at bound-state resonances for He on LiF. For the two kinds of ions in an alkali halide crystal the values of  $\epsilon_{1,2}$  and  $r_{m1,2}$  were estimated from combination rules and the values of  $\alpha_{1,2}$  were determined from fitting the experimental binding energies  $\{E_j\}$ .

The potential parameters obtained for the different potential forms from fitting experimental  $\{E_j\}$  spectra are gathered in Table IX.

## APPENDIX D: TABLE WITH POTENTIAL WELL DEPTHS CALCULATED WITH THE SEMIEMPIRICAL RULE GIVEN IN SEC. III.C.4

TABLE X. Well depth  $D$  in meV of physical gas-surface interaction potentials, calculated from  $D = K_D \alpha(\epsilon - 1)/(\epsilon + 1)$ , with  $\bar{K}_D = 12 \text{ meV}/10^{-25} \text{ cm}^3$  and  $\alpha(\epsilon - 1)/(\epsilon + 1)$  given in Table IV.

Surface \ Gas	H	He	H <sub>2</sub>	Ne	Ar	Kr	Xe
LiF	25.3	7.9	30.6	15.0	62.4	94.2	153
NaF	21.7	6.8	26.3	12.8	53.5	80.6	132
NaCl	31.0	9.7	37.4	18.2	76.2	115	187
KCl	29.0	9.1	35.0	17.2	71.5	108	176
RbCl	30.0	9.4	36.2	17.8	73.9	111	182
NiO	52.2	16.3	63.1	30.8	128.5	194	316
MnO	52.2	16.3	63.1	30.8	128.4	194	316
MgO	39.7	12.5	48.0	23.4	97.8	147	240
Graphite	47.6	14.9	57.5	29.2	117.2	177	288

## REFERENCES

- Armand, G., J. Lapujoulade, and Y. Lejay, 1976, *J. Phys. (Paris) Lett.* **37**, L187.
- Armand, G., J. Lapujoulade, and Y. Lejay, 1977, *Surf. Sci.* **63**, 143.
- Armand, G., and J. R. Manson, 1978, *Phys. Rev. B* **18**, 6510.
- Armand, G., and J. R. Manson, 1979, *Phys. Rev. Lett.* **43**, 1839.
- Armand, G., 1980, *J. Phys. (Paris)* (to be published).
- Beder, E. C., 1967, *Adv. At. Mol. Phys.* **3**, 205.
- Bledsoe, J. R., 1972, Ph.D. thesis, University of Virginia.
- Bledsoe, J. R., and S. S. Fisher, 1976, *Surf. Sci.* **55**, 141.
- Boato, G., P. Cantini, and R. Colella, 1979, *Phys. Rev. Lett.* **42**, 1635.
- Boato, G., P. Cantini, and L. Mattera, 1976, *Surf. Sci.* **55**, 141.
- Boato, G., P. Cantini, and R. Tatarek, 1976, *J. Phys. F* **6**, L237.
- Boato, G., P. Cantini, and R. Tatarek, 1978, *Phys. Rev. Lett.* **40**, 887.
- Boato, G., P. Cantini, and R. Tatarek, 1979a, *Surf. Sci.* **80**, 518.
- Boato, G., P. Cantini, C. Guidi, R. Tatarek, and G. P. Felcher, 1979b, *Phys. Rev. B* **20**, 3957.
- Bruch, L. W., and Th. W. Ruijgrok, 1979, *Surf. Sci.* **79**, 509.
- Bruch, L. W., and H. Watanabe, 1977, *Surf. Sci.* **65**, 619.
- Cabrera, N., V. Celli, F. O. Goodman, and J. R. Manson, 1970, *Surf. Sci.* **19**, 67.
- Cabrera, N., and F. O. Goodman, 1972, *J. Chem. Phys.* **56**, 4899.
- Cantini, P., G. P. Felcher, and R. Tatarek, 1977, in *Proceedings of the Seventh International Vacuum Congress and the Third International Conference on Solid Surfaces*, edited by R. Dobrozemsky *et al.* (Berger, Vienna), p. 1357.
- Cantini, P., R. Tatarek, and G. P. Felcher, 1979, *Phys. Rev. B* **19**, 1161.
- Cardillo, M. J., 1979, *Book of Abstracts, Seventh International Symposium on Molecular Beams*, Riva del Garda, p. 250.
- Cardillo, M. J., and G. E. Becker, 1978, *Phys. Rev. Lett.* **40**, 1148.
- Cardillo, M. J., and G. E. Becker, 1979, *Phys. Rev. Lett.* **42**, 508.
- Carlos, W. E., and M. W. Cole, 1978, *Surf. Sci.* **77**, L173.
- Carlos, W. E., and M. W. Cole, 1979, *Phys. Rev. Lett.* **43**, 697.
- Celli, V., N. Garcia, and J. Hutchison, 1979, *Surf. Sci.* **87**, 112.

- Chiroli, C., and A. C. Levi, 1976, *Surf. Sci.* **59**, 325.
- Chow, H., 1977, *Surf. Sci.* **66**, 221.
- Chow, H., 1979, *Surf. Sci.* **79**, 157.
- Chow, H., and E. D. Thompson, 1976, *Surf. Sci.* **59**, 225.
- Chow, H., and E. D. Thompson, 1978, *Surf. Sci.* **71**, 731.
- Chow, H., and E. D. Thompson, 1979, *Surf. Sci.* **82**, 1.
- Cole, M. W., and D. R. Frankl, 1978, *Surf. Sci.* **70**, 585.
- Cole, M. W., and T. T. Tsong, 1977, *Surf. Sci.* **69**, 325.
- Comsa, G., G. Mechttersheimer, B. Poelsema, and S. Tomoda, 1979, *Surf. Sci.* **89**, 123.
- Crews, J. C., 1967, in *Fundamentals of Gas-Surface Interaction*, edited by H. Saltsburg, J. N. Smith, Jr., and M. Rogers (Academic, New York), p. 480.
- Davies, R. O., and L. S. Ullermayer, 1973, *Surf. Sci.* **39**, 61.
- Derry, G., D. Wesner, W. Carlos, and D. R. Frankl, 1979, *Surf. Sci.* **87**, 629.
- Derry, G., D. Wesner, S. V. Krishnaswamy, M. W. Cole, and D. R. Frankl, 1977, in *Proceedings of the Seventh International Vacuum Congress and the Third International Conference on Solid Surfaces*, Vienna, edited by R. Dobrozemsky *et al.* (Berger, Vienna), p. 1353.
- Derry, G., D. Wesner, S. V. Krishnaswamy, and D. R. Frankl, 1978, *Surf. Sci.* **74**, 245.
- Devonshire, A. F., 1936, *Proc. R. Soc. London A* **156**, 37.
- Estel, J., H. Hoinkes, H. Kaarmann, H. Nahr, and H. Wilsch, 1976, *Surf. Sci.* **54**, 393.
- Estermann, I., R. Frisch, and O. Stern, 1931, *Z. Phys.* **73**, 348.
- Estermann, I., and O. Stern, 1930, *Z. Phys.* **61**, 95.
- Finzel, H.-U., H. Frank, H. Hoinkes, M. Luschka, H. Nahr, H. Wilsch, and U. Wonka, 1975, *Surf. Sci.* **49**, 577.
- Frank, H., 1973, *Diplom-Thesis*, Universität Erlangen-Nürnberg.
- Frank, H., H. Hoinkes, and H. Wilsch, 1977, *Surf. Sci.* **63**, 121.
- Frankl, D. R., D. Wesner, S. V. Krishnaswamy, G. Derry, and T. O'Gorman, 1978, *Phys. Rev. Lett.* **41**, 60.
- Freeman, D. L., 1975, *J. Chem. Phys.* **62**, 941.
- Frisch, R., 1933, *Z. Phys.* **84**, 443.
- Frisch, R., and O. Stern, 1932, *Naturwissenschaften* **20**, 721.
- Frisch, R., and O. Stern, 1933a, *Handbuch der Physik* **XXII/2**, 337.
- Frisch, R., and O. Stern, 1933b, *Z. Phys.* **84**, 430.
- Garcia, N., 1976, *Phys. Rev. Lett.* **37**, 912.
- Garcia, N., 1977a, *Surf. Sci.* **63**, 113.
- Garcia, N., 1977b, *J. Chem. Phys.* **67**, 897.
- Garcia, N., G. Armand, and J. Lapujoulade, 1977, *Surf. Sci.* **68**, 399.
- Garcia, N., and N. Cabrera, 1977, in *Proceedings of the Seventh International Vacuum Congress and the Third International Conference on Solid Surfaces*, Vienna, edited by R. Dobrozemsky *et al.* (Berger, Vienna), p. 379.
- Garcia, N., and N. Cabrera, 1978, *Phys. Rev. B* **18**, 576.
- Garcia, N., V. Celli, and F. O. Goodman, 1979, *Phys. Rev. B* **19**, 634.
- Garcia, N., F. O. Goodman, V. Celli, and N. R. Hill, 1979, *Phys. Rev. B* **19**, 1808.
- Garcia-Sanz, J., and N. Garcia, 1979, *Surf. Sci.* **79**, 125.
- Garibaldi, U., A. C. Levi, R. Spadacini, and G. E. Tommei, 1975, *Surf. Sci.* **48**, 649.
- Goodman, F. O., 1967, *Phys. Rev.* **164**, 1113.
- Goodman, F. O., 1971, *Surf. Sci.* **26**, 327.
- Goodman, F. O., 1973, *J. Chem. Phys.* **58**, 5530.
- Goodman, F. O., 1976, *J. Chem. Phys.* **65**, 1561.
- Goodman, F. O., 1977a, *CRC Crit. Rev. Solid State Sci.* **7**, 33.
- Goodman, F. O., 1977b, *J. Chem. Phys.* **66**, 976.
- Goodman, F. O., 1978, *Surf. Sci.* **70**, 578.
- Goodman, F. O., N. Garcia, and V. Celli, 1979, *Surf. Sci.* **85**, 317.
- Goodman, F. O., and W.-K. Tan, 1973, *J. Chem. Phys.* **59**, 1805.
- Goodman, F. O., and H. Y. Wachman, 1976, *Dynamics of Gas-Surface Scattering* (Academic, New York).
- Gordon, R. G., and Y. S. Kim, 1972, *J. Chem. Phys.* **56**, 3122.
- Greenaway, D. L., G. Harbeke, F. Bassani, and E. Tosatti, 1969, *Phys. Rev.* **178**, 1340.
- Greiner, L., H. Hoinkes, H. Kaarmann, H. Wilsch, and N. Garcia, 1980, *Surf. Sci.* **94**, L195.
- Hall, P. G., and M. A. Rose, 1978, *Surf. Sci.* **74**, 644.
- Hamazu, Y., 1976, *Phys. Lett. A* **57**, 275.
- Hamazu, Y., 1977, *J. Phys. Soc. Jpn.* **42**, 961.
- Harvie, C. E., and J. H. Weare, 1978, *Phys. Rev. Lett.* **40**, 187.
- Hill, N. R., and V. Celli, 1978, *Surf. Sci.* **75**, 577.
- Hoinkes, H., H. Finzel, H. Frank, H. Nahr, and H. Wilsch, 1974a, in *Proceedings of the 9th International Symposium on Rarefied Gas Dynamics*, Göttingen, edited by M. Becker and M. Fiebig (DFVLR, Porz-Wahn), Vol. II, p. E.7-1.
- Hoinkes, H., L. Greiner, and H. Wilsch, 1977, in *Proceedings of the Seventh International Vacuum Congress and the Third International Conference on Solid Surfaces*, Vienna, edited by R. Dobrozemsky *et al.* (Berger, Vienna), p. 349.
- Hoinkes, H., H. Nahr, and H. Wilsch, 1972a, *Surf. Sci.* **30**, 363.
- Hoinkes, H., H. Nahr, and H. Wilsch, 1972b, *J. Phys. C* **5**, L143.
- Hoinkes, H., H. Nahr, and H. Wilsch, 1974b, *Rarefied Gas Dynamics* (Academic, New York), p. 421.
- Horne, J. M., and D. R. Miller, 1977, *Surf. Sci.* **66**, 365.
- Houston, D. E., and D. R. Frankl, 1973, *Phys. Rev. Lett.* **31**, 298.
- Hutchison, J., and V. Celli, 1980, *Surf. Sci.* **93**, 263.
- Johnson, T. H., 1930, *Phys. Rev.* **35**, 1299.
- Johnson, T. H., 1931, *Phys. Rev.* **37**, 847.
- Kittel, C., 1969, *Einführung in die Festkörperphysik*, 2nd edition (Oldenburg, München-Wien).
- Kleinman, G. G., and U. Landman, 1973, *Phys. Rev. B* **8**, 5484.
- Kleinman, G. G., and U. Landman, 1974, *Phys. Rev. Lett.* **33**, 524.
- Landman, U., and G. G. Kleinman, 1975, *J. Vac. Sci. Technol.* **12**, 206.
- Landolt, H. H., and R. Börnstein, 1951a, *Zahlenwerte und Funktionen* (Springer, Berlin), Vol. 1, pt. 3, pp. 509.
- Landolt, H. H., and R. Börnstein, 1951b, *Zahlenwerte und Funktionen* (Springer, Berlin), Vol. 2, pt. 6, pp. 449.
- Lapujoulade, J., and Y. Lejay, 1977, *Surf. Sci.* **69**, 354.
- Lapujoulade, J., Y. Lejay, and N. Papanicolaou, 1979, *Surf. Sci.* **90**, 133.
- Lennard-Jones, J. E., and A. F. Devonshire, 1936, *Nature (London)* **137**, 1069.
- Lennard-Jones, J. E., and A. F. Devonshire, 1937, *Proc. R. Soc. London A* **158**, 253.
- Le Roy, R. J., 1976, *Surf. Sci.* **59**, 541.
- Lifshitz, E. M., 1956, *Sov. Phys.-JETP* **2**, 73.
- Liva, M. P., G. Derry, and D. R. Frankl, 1976, *Phys. Rev. Lett.* **37**, 1413.
- Logan, R. M., 1973, *Solid State Surf. Sci.* **3**, 1.
- Masel, R. I., R. P. Merrill, and W. H. Miller, 1975, *Phys. Rev. B* **12**, 5545.
- Mason, B. F., and B. R. Williams, 1978, *Surf. Sci.* **75**, L786.
- Mattera, L., F. Rosatelli, C. Salvo, F. Tommasini, U. Valbusa, G. Vidali, 1980a, *Surf. Sci.* **93**, 515.
- Mattera, L., C. Salvo, S. Terreni, F. Tommasini, 1980b, *Surf. Sci.*, **97**, 158.
- Meyers, J. A., and D. R. Frankl, 1975, *Surf. Sci.* **51**, 61.
- O'Keefe, D. R., J. N. Smith, Jr., R. L. Palmer, and H. Saltsburg, 1970, *J. Chem. Phys.* **52**, 4447.
- Pitzer, K. S., 1959, *Adv. Chem. Phys.* **2**, 59.
- Rieder, K. H., and T. Engel, 1979, *Phys. Rev. Lett.* **43**, 373.
- Rogowska, J. M., 1978, *J. Chem. Phys.* **68**, 3910.
- Rowe, R. G., and G. Ehrlich, 1975, *J. Chem. Phys.* **63**, 4648.
- Schwartz, C., M. W. Cole, and J. Pliva, 1978, *Surf. Sci.* **75**, 1.
- Smith, J. N., Jr., 1973, *Surf. Sci.* **34**, 613.

- Somorjai, G. A., and S. B. Brumbach, 1974, *CRC Crit. Rev. Solid State Sci.* **4**, 429.
- Steele, W. A., 1973, *Surf. Sci.* **36**, 317.
- Steele, W. A., 1974, *The Interaction of Gases with Solid Surfaces* (Pergamon, Oxford).
- Stern, O., 1929, *Naturwissenschaften* **17**, 391.
- Stickney, R. E., 1967, *Adv. At. Mol. Phys.* **3**, 143.
- Stoll, A. G., Jr., J.-J. Ehrhardt, and R. P. Merrill, 1976, *J. Chem. Phys.* **64**, 34.
- Stoll, A. G., and R. P. Merrill, 1973, *Surf. Sci.* **40**, 405.
- Tang, K. T., J. M. Norbeck, and P. R. Certain, 1976, *J. Chem. Phys.* **64**, 3063.
- Tendulkar, D. V., and R. E. Stickney, 1971, *Surf. Sci.* **27**, 516.
- Toennies, J. P., 1974, *Appl. Phys.* **3**, 91.
- Tommasini, F., and U. Valbusa, 1979, *Book of Abstracts, Seventh International Symposium on Molecular Beams, Riva del Garda*, p. 155.
- Tsuchida, A., 1969, *Surf. Sci.* **14**, 375.
- Tsuchida, A., 1970, *Sci. Pap. Inst. Phys. Chem. Res. (Jpn.)* **64**, 75.
- Tsuchida, A., 1974, *Surf. Sci.* **46**, 611.
- Tsuchida, A., 1975, *Surf. Sci.* **52**, 685.
- Vidali, G., M. W. Cole, and C. Schwartz, 1979, *Surf. Sci.* **87**, L273.
- Weast, R. C., 1974, *CRC Handbook of Chemistry and Physics*, 55th edition (CRC, Cleveland).
- Wilsch, H., H.-U. Finzel, H. Frank, H. Hoinkes, and H. Nahr, 1974, *Proceedings of the 2nd International Conference on Solid Surfaces*, Kyoto, (Japan. *J. Appl. Phys. Suppl.* **2**, Pt. 2, 567).
- Wilsch, H., 1978, in *Topics in Surface Chemistry*, edited by Eric Kay and Paul S. Bagus (Plenum, New York), p. 135.
- Wonka, U., 1973, *Zulassungsarbeit, Universität Erlangen-Nürnberg*.
- Wood, J. C., 1978, *Surf. Sci.* **71**, 548.
- Zaremba, E., and W. Kohn, 1976, *Phys. Rev. B* **13**, 2270.
- Zaremba, E., and W. Kohn, 1977, *Phys. Rev. B* **15**, 1769.